

Semileptonic Meson Decays in the Quark Model: An Update

Daryl Scora

Department of Applied Mathematics

York University, 4700 Keele Street

North York, Ontario M3J 1P3

Nathan Isgur

Continuous Electron Beam Accelerator Facility

12000 Jefferson Avenue, Newport News, Virginia 23606

We present the predictions of ISGW2, an update of the ISGW quark model for semileptonic meson decays. The updated model incorporates a number of features which should make it more reliable, including the constraints imposed by Heavy Quark Symmetry, hyperfine distortions of wavefunctions, and form factors with more realistic high recoil behaviors.

I. OVERVIEW

It has been nearly ten years since the ISGW model [1] was introduced [2,3] so it is not surprising that the heavy quark semileptonic landscape now looks very different. At that time, for both theoretical and experimental reasons, inclusive decays were the main focus of attention, and the ISGW model, which studied exclusive decays and approximated the inclusive semileptonic spectra by summing over resonant channels, was considered quite eccentric. Today, improvements in both theory and experiment have made exclusive semileptonic decays a main focus of attention. Such decays seem very likely to provide the most accurate determinations of the weak mixing angles V_{cb} and V_{ub} . They also provide excellent probes of hadronic structure via precision tests of Heavy Quark Symmetry (HQS) [4-7].

The ISGW model was in many respects a stepping-stone to Heavy Quark Symmetry: it is a model which respects the symmetry in the heavy quark limit near zero recoil. It also played a role in the discussion of the reliability of the free quark decay model (and its derivatives) for the endpoint region in $b \rightarrow u$ semileptonic decay. Indeed, the model had its origin in that discussion, and was *designed* to provide the minimum reasonable prediction for the decay rate in this region for a fixed V_{ub} . In this paper we present an updated version of ISGW, which (with the permission of the ISGW authors) we call ISGW2 to emphasize that it is *not* a new model but rather an improved version of an old one [8]. The new features are described in detail in Section III, but briefly they are:

1. Heavy Quark Symmetry constraints on the relations between form factors away from zero recoil are respected,
2. Heavy Quark Symmetry constraints on the slopes of form factors near zero recoil are built in [9],
3. the naive currents of the quark model are related to the full weak currents *via* the matching conditions of Heavy Quark Effective Theory (HQET) [6],

4. Heavy-Quark-Symmetry-breaking color magnetic interactions are included, whereas ISGW only included the symmetry-breaking due to the heavy quark kinetic energy,
5. the ISGW prescription for connecting its quark model form factors to physical form factors is modified to be consistent with the constraints of Heavy Quark Symmetry breaking at order $1/m_Q$,
6. relativistic corrections to the axial coupling constants (known to be important in the analogous coupling g_A in neutron beta decay) are taken into account, and
7. more realistic form factor shapes, based on the measured pion form factor, are employed.

The discovery of Heavy Quark Symmetry has not eliminated the need for models; it has rather provided a solid foundation for model-building and redefined the role that models should play. Consequently, an updated version of the ISGW model that incorporates the lessons of Heavy Quark Symmetry, and is designed with current usage in mind, seems very worthwhile. Among other roles, models should:

1. provide predictions for the various universal form factors (“Isgur-Wise functions”) of Heavy Quark Symmetry,
2. provide predictions for the form factors governing $b \rightarrow u$, $c \rightarrow s$, $c \rightarrow d$, and $s \rightarrow u$ transitions not directly governed by Heavy Quark Symmetry, and
3. give estimates for the sizes of Heavy-Quark-Symmetry-breaking effects in the $b \rightarrow c$ decays determining V_{cb} , in the relations between $b \rightarrow u$ and $c \rightarrow d$ matrix elements which can be used to determine V_{ub} from exclusive semileptonic decays [4,10], and in the relation between $c \rightarrow s$ and $b \rightarrow s$ matrix elements which enter into the prediction of exclusive $b \rightarrow s\gamma$ decays [10].

In the next section we will give some of the background to ISGW and to the events leading up to ISGW2, as well as a quick review of the basic elements of the ISGW approach.

As already mentioned, Section III describes the new features of ISGW2 in detail. In Section IV we present our results. Section V discusses their implications for Heavy Quark Symmetry, while Section VI compares our results to experiment. Section VII closes with a few comments.

II. BACKGROUND

A. Some History

In 1985, when the model that was eventually published as the ISGW model [1] was introduced [2,3], its intended use was very different from its present use. Moreover, much less was known about semileptonic b and c quark decays, both theoretically and experimentally. The ISGW2 model presented here is designed to update the earlier version to address both of these shortcomings. Ten years ago, the experimental study of the semileptonic decays of b and c quarks was in its infancy. In particular, for b quarks the main available data was on the inclusive lepton energy spectra for $\bar{B} \rightarrow X \ell \bar{\nu}_\ell$, generated by the quark level $b \rightarrow c \ell \bar{\nu}_\ell$ and $b \rightarrow u \ell \bar{\nu}_\ell$ transitions. At that time the principal theoretical tool being used to analyze these spectra was the QCD-corrected parton model of ACCMM [11] and its relatives [12], with particular emphasis on extracting the Cabibbo-Kobayashi-Maskawa (CKM) [13] matrix elements V_{cb} and V_{ub} from inclusive lepton spectra. Early fits to these spectra [14] near the $b \rightarrow c \ell \bar{\nu}_\ell$ endpoint were leading to alarmingly small upper limits for the ratio $|V_{ub}/V_{cb}|^2$. Such results could of course simply be attributed to errors in the data. Alternatively, they could be taken as serious limits on V_{ub} which would indicate a failure of the Standard Model scenario for CP violation. The ISGW model was introduced to explore a third possibility: that a partonic description of the $b \rightarrow c \ell \bar{\nu}_\ell$ and $b \rightarrow u \ell \bar{\nu}_\ell$ transitions in the endpoint region, where the lepton energy is near its maximum, might be deficient. The basic motivation for this concern arises from the observation that the highest energy leptons in these decays are associated with the production of the lowest-mass hadronic final states X in $\bar{B} \rightarrow X_c \ell \bar{\nu}_\ell$ and $\bar{B} \rightarrow X_u \ell \bar{\nu}_\ell$ respectively; the partonic description would only be expected to apply once the states X_c and X_u had masses above their respective resonance regions.

We will discuss this issue in more detail below. We raise it at this point to recall that one of the main goals of the ISGW model was the production of an alternative description of the endpoint region which intentionally represented an *extreme* example of how little

$b \rightarrow u\ell\bar{\nu}_\ell$ could show up in the endpoint region. The motivation was to illustrate the theoretical uncertainty which should be reflected in upper limits on $|V_{ub}/V_{cb}|^2$ extracted from inclusive endpoint spectra and to thereby place more realistic constraints on Standard Model CP-violation scenarios. Along the path to this primary goal, the ISGW model produced a number of other results. In retrospect, the most important of these were probably conceptual: much of the framework for Heavy Quark Symmetry [4-7] was presented in these early papers [1-3], including the vital role of the zero recoil point (where $t = (p_\ell + p_{\bar{\nu}_\ell})^2$ is at its maximum value t_m), the insensitivity of $\bar{B} \rightarrow D\ell\bar{\nu}_\ell$ and $\bar{B} \rightarrow D^*\ell\bar{\nu}_\ell$ transitions to m_b/m_c , and the role of $D \rightarrow \bar{K}\ell^+\nu_\ell$ and $D \rightarrow \bar{K}^*\ell^+\nu_\ell$ measurements in “tuning” exclusive models to be used for the extraction of V_{cb} and V_{ub} . ISGW also made a number of predictions. For example, ISGW was the first exclusive model to calculate rates to channels other than the pseudoscalar and vector ground states and consequently to predict that in both $b \rightarrow c\ell\bar{\nu}_\ell$ and $c \rightarrow s\ell^+\nu_\ell$ decays the exclusive transitions $\bar{B} \rightarrow D, D^*$ and $D \rightarrow \bar{K}, \bar{K}^*$ would dominate. This prediction (which is surprising since kinematically masses up to m_B and m_D , respectively, are allowed), now has a firm basis in theory [15,16, 4-7]. They also pointed out that in the nonrelativistic limit (applicable to such exotic processes as $\bar{B}_c \rightarrow \psi\ell\bar{\nu}_\ell$), the weak transition form factors would be controlled by a set of universal functions given by the Fourier transforms of wave function overlaps and not by t -channel meson masses. This point has since been explored by many authors [17].

As mentioned in Section I, this update of ISGW has been prompted by a number of developments. The most fundamental of these is the discovery and development of Heavy Quark Symmetry [4-7]. In particular, the development of Heavy Quark Effective Theory [6] as a tool for systematically treating both the $1/m_Q$ and perturbative QCD corrections to the extreme Heavy Quark Symmetry limit has helped place models like ISGW in clear focus. HQET divides the calculation of current matrix elements into two steps: matching the currents of the full theory onto those of a low energy effective theory associated with some relatively light renormalization scale μ , and then calculating matrix elements in the low energy effective theory. From this perspective, a quark model like ISGW or ISGW2

is presumed to be associated with a quark model scale $\mu_{qm} \sim \mathcal{O}(1 \text{ GeV})$ where a valence constituent quark structure of hadrons dominates the physics.

Since the constraints of Heavy Quark Symmetry for current matrix elements of the low energy effective theory are consequences of QCD, every model should display these results (including an allowed symmetry-breaking pattern) in the appropriate limit. In fact, in the low-recoil region where nonrelativistic dynamics apply, the ISGW model was already totally consistent with the Heavy Quark Symmetry limit. Adding the constraints of Heavy Quark Symmetry in ISGW2 nevertheless has significant impact. In high recoil $b \rightarrow c\ell\bar{\nu}_\ell$ transitions, some ISGW form factors have missing functions of $w \equiv v \cdot v'$ (v and v' are the four-velocities of the initial and final hadronic systems; this variable is called w after the origin of the name of this letter in, *e.g.*, French) which are unity at zero recoil, *e.g.*, the f form factor in $\bar{B} \rightarrow D^*\ell\bar{\nu}_\ell$ is missing a factor of $\frac{1}{2}(1+w)$ which goes to unity at $w = 1$. A related issue is embedded in the recoil dependence of the ISGW form factors. As discussed in ISGW, the slope of a quark model form factor consists of two terms: a normal “transition charge radius” term and a relativistic correction (of order $1/m_j m_i$ in a $Q_i \rightarrow Q_j$ current matrix element) which is outside of the scope of a nonrelativistic quark model. ISGW posited that such relativistic effects could be taken into account in an approximate way by replacing all factors of $(t_m - t)$ appearing in their nonrelativistic formulas for form factors by $\kappa^{-2}(t_m - t)$, where κ is the ratio of the nonrelativistic charge radius to the true charge radius. Heavy Quark Symmetry [9] tells us that this prescription (while fortuitously close numerically in the cases to which it was applied) is incorrect; the symmetry moreover dictates the correct result in the heavy quark limit. This result, to be described below, is adopted in ISGW2. Consideration of the allowed pattern of HQS-breaking at order $1/m_Q$ also has an impact. Among other effects, it requires a change in the ISGW prescription for relating the form factors of the weak binding limit calculated here to physical form factors. Although such modifications to ISGW are only strictly required near the heavy quark limit, ISGW2 adopts the usual constituent quark model stance of treating all constituent quarks like heavy quarks, so the same changes are made, *e.g.*, to $c \rightarrow s$ transitions.

QCD also demands that the matrix elements of a low energy effective theory like the quark model be corrected by the matching conditions which map them onto the matrix elements of the full theory. At the level of the currents of the two theories, these matching conditions take the generic form

$$J_{ji}^\mu = \mathbf{C}_{ji} \mathbf{J}_{ji}^\mu + \frac{\alpha_s}{\pi} \Delta \mathbf{J}_{ji}^\mu + \frac{1}{m_{Q_j}} \delta_j \mathbf{J}_{ji}^\mu + \frac{1}{m_{Q_i}} \delta_i \mathbf{J}_{ji}^\mu. \quad (1)$$

In ISGW2, we explicitly calculate the $1/m_{Q_j}$ and $1/m_{Q_i}$ corrections in the quark model, so only the factor \mathbf{C}_{ji} mapping the naive vector $(\bar{\mathbf{Q}}_j \gamma^\mu \mathbf{Q}_i)$ and axial vector $(\bar{\mathbf{Q}}_j \gamma^\mu \gamma_5 \mathbf{Q}_i)$ currents of the quark model onto the true currents $(\bar{Q}_j \gamma^\mu Q_i)$ and $(\bar{Q}_j \gamma^\mu \gamma_5 Q_i)$ and the expansion in terms of the new naive currents appearing in $\Delta \mathbf{J}_{ji}^\mu$ in order α_s/π are needed. We will give these matching factors in Section III.A below.

There are other reasons why an update of the ISGW model is warranted. In the period since the publication of ISGW, its role in providing a very conservative upper limit on $|V_{ub}/V_{cb}|^2$ has become antiquated; ISGW2 attempts to modernize ISGW so that its predictions become *best* estimates rather than *most conservative* estimates. Consider, for example, the curve in Figure 1 showing the ISGW form factor $F_\pi(Q^2)$ with Gaussian wavefunctions. The charge radius of the pion was used to determine the value of the parameter κ which in turn determines the rate of decrease of $F_\pi(Q^2)$ shown. Thus, instead of choosing a value that provided a best global fit to the data over the whole kinematic range applicable to the $b \rightarrow u \ell \bar{\nu}_\ell$ transition, ISGW chose a value that fits at low Q^2 but, as a result of its unrealistic Gaussian form, underestimates $F_\pi(Q^2)$ at high Q^2 . This choice was driven by the ISGW goal of providing a minimum rate for $\bar{B} \rightarrow X_u \ell \bar{\nu}_\ell$ in the endpoint region. In ISGW2 we attempt a more realistic description of the recoil dependence of all form factors.

There have also been important experimental developments since 1985! In \bar{B} decays [19], the inclusive spectra near the endpoint region show a definite $\bar{B} \rightarrow X_u \ell \bar{\nu}_\ell$ excess [20], although, for the reasons already mentioned, the resulting value of V_{ub} is unclear. The decays $\bar{B} \rightarrow D \ell \bar{\nu}_\ell$ and $\bar{B} \rightarrow D^* \ell \bar{\nu}_\ell$ have both been measured [21] in sufficient detail to extract the CKM matrix element V_{cb} with some confidence since the observed features of these decays

are consistent with the expectations of Heavy Quark Symmetry. Preliminary evidence for $\bar{B} \rightarrow D^{**} \ell \bar{\nu}_\ell$ decays (here D^{**} represents non- D or D^* decays) has been reported and searches have begun for the exclusive $b \rightarrow u \ell \bar{\nu}_\ell$ processes $\bar{B} \rightarrow \rho \ell \bar{\nu}_\ell$ and $\bar{B} \rightarrow \omega \ell \bar{\nu}_\ell$ [22]. In D decays [23], where V_{sc} is known, $D \rightarrow \bar{K} \ell^+ \nu_\ell$ and $D \rightarrow \bar{K}^* \ell^+ \nu_\ell$ decays have been measured [24] in sufficient detail to extract the four $c \rightarrow s$ form factors contributing in the limit $m_\ell \rightarrow 0$, and rather tight limits on $D \rightarrow \bar{K}^{**} \ell^+ \nu_\ell$ have been set. In all cases the experimental results are qualitatively consistent with the predictions of ISGW (despite some initial indications to the contrary [25]); indeed, all results to date are consistent with ISGW within its anticipated “quark model accuracy” of predicting matrix elements to $\pm 25\%$. However, in the spirit of “tuning” the quark model to higher accuracy, in ISGW2 we have taken note of a substantial failure of ISGW to predict the magnitude of the S-wave axial vector form factor f in $D \rightarrow \bar{K}^* \ell^+ \nu_\ell$ decay. In the quark model, this form factor is analogous to g_A in neutron beta decay, where experiment is about 25% below the quark model prediction of 5/3; the data on f indicate that it is also smaller than the quark model prediction. There is a very natural explanation for the g_A discrepancy within the quark model [26,27]: the matrix elements of the space components of the axial current in a relativistic S-wave spinor are reduced in proportion to the probability of lower components in that spinor. We accordingly build this relativistic correction factor into ISGW2.

With the predictions of Heavy Quark Symmetry to facilitate the extraction of V_{cb} and V_{ub} from the data, one of the main uses of models has shifted from predicting form factors to predicting the *deviations* of form factors, or relations between form factors, from the predictions of Heavy Quark Symmetry. In view of this changing role, we implement one further elaboration of ISGW in ISGW2: we consider the effects of hyperfine interactions on meson wavefunctions. ISGW already naturally took into account the other $1/m_Q$ effect in HQET [6], the heavy quark kinetic energy, so this addition to the model completes the parallel with the most general symmetry-breaking effects allowed. As we will see, the “ g_A effect” and these hyperfine interactions, in concert with matching corrections, eliminate the problem with the $D \rightarrow \bar{K}^* \ell^+ \nu_\ell$ form factor f .

To summarize: ISGW2 is an updated version of ISGW designed to make “best estimates” within the context of a constituent quark model that fully respects Heavy Quark Symmetry.

B. A Review of the Foundations of the ISGW Model

In Section III we will describe in detail the new features which we incorporate in ISGW2. Here, we review the basic ideas and methods of the ISGW model.

ISGW breaks the problem of computing a current matrix element of a transition from a state H of mass, momentum, and spin m, p, s to H' with m', p', s' into kinematical and dynamical parts. It first makes the usual mechanical Lorentz-invariant decomposition of the matrix element into Lorentz tensors and invariant form factors f_i ($i = 1, 2, \dots, N$) which depend only on the four momentum transfer variable $(t_m - t)$ where $t = (p' - p)^2$ and where $t_m = (m' - m)^2$ is the maximum momentum transfer. The variable $(t_m - t)$ is used since it is zero at the “zero recoil point” where H' is left at rest in the rest frame of H ; the importance of momentum transfers near t_m will be made clear below.

It should be noted that *any* specification of the functions $f_i(t_m - t)$ leads to a Lorentz invariant description of these weak decay processes. In this sense ISGW *is not* a nonrelativistic approximation. It is, however, a nonrelativistic estimate of the intercepts $f_i(0)$ and “charge radii” $r_i \equiv [6 \frac{df_i(0)}{d(t_m - t)}]^{1/2}$ (or more generally the shapes) of the Lorentz invariant form factors $f_i(t_m - t)$. These estimates are made by noting that there is a one-to-one correspondence between the f_i and a partial wave expansion of the $\langle H' | j^\mu(0) | H \rangle$ matrix elements. For example, if H and H' are pseudoscalars P and P' , then

$$\langle P'(p') | V^\nu(0) | P(p) \rangle = f_+^{P'P} (p + p')^\nu + f_-^{P'P} (p - p')^\nu \quad . \quad (2)$$

This decay also has two partial wave amplitudes. In the rest frame of P , $V^0(0) | P(0) \rangle$ is still a pseudoscalar, and so creates P' in an S-wave; $\vec{V}(0) | P(0) \rangle$ is an axial vector and so must create P' in a P-wave. Thus $m(f_+^{P'P} + f_-^{P'P}) + E'(f_+^{P'P} - f_-^{P'P})$ and $\vec{p}'(f_+^{P'P} - f_-^{P'P})$ are proportional to the rest frame S-wave and P-wave amplitudes, respectively.

A vital element of the ISGW model is that each partial wave amplitude is calculable in the nonrelativistic limit; the one-to-one correspondence with the f_i then allows a calculation of each in this limit (*i.e.*, none of the f_i are intrinsically relativistic in character). The ISGW model therefore calculates the f_i in a limit in which the model would in principle be exact, and then extrapolates these exact formulas to the physical regime. It should be noted that the nonrelativistic limit requires more than \vec{p}/m and \vec{p}'/m' being small. It also requires that the internal motion of the constituents of H and H' be nonrelativistic. One of the essential assumptions of the ISGW model is that such “mock meson” form factors \tilde{f}_i which are derived in the approximation that m_u , m_d , and m_s are large compared to Λ_{QCD} can be extrapolated down to their actual constituent quark masses to estimate the f_i .

In the heavy quark world in which the ISGW formulas would be exact in principle, the low-lying mesons would all be simple quarkonia. ISGW is therefore necessarily a model for matrix elements between resonances, *i.e.*, it does not directly address the issue of whether semileptonic meson decays are resonance dominated. The original ISGW paper argues that nonresonant contributions are likely to be small (their absence is correlated with the known success of the narrow resonance approximation), and there is some evidence from the data for this prediction. Nevertheless, the issue remains a hotly debated one. Note that this debate is relevant to our updating of the resonant matrix elements only once we use them to estimate the *inclusive* rates, *e.g.*, those in the $\bar{B} \rightarrow X_u \ell \bar{\nu}_\ell$ endpoint region. At that point we will discuss this issue in more depth.

The semileptonic decays of the $b\bar{c}$ meson \bar{B}_c via the $\bar{c}\gamma^\mu(1 - \gamma_5)b$ current provide a good illustration of a system in which the ISGW model would in principle be an excellent approximation. Both \bar{B}_c and the low-lying states of the $c\bar{c}$ system can be reasonably well-described as nonrelativistic, and matrix elements like $\langle\psi(p's')|A^\nu|\bar{B}_c(p)\rangle$ can be accurately calculated in the frame where $\vec{p} = 0$ for small \vec{p}' as atomic-physics-type wavefunction overlap integrals. This is the essence of the ISGW method. However, serious model dependence can occur when these matrix elements are extrapolated to large recoils; moreover, it occurs even at small recoil when any quark mass is extrapolated down to the constituent masses of the

u , d , or s quarks. Amongst the issues which must be addressed when a light quark plays a role are:

1. *the quarkonium approximation*: It is a fundamental tenet of the constituent quark model that, up to “small” corrections which arise from pair creation leading to resonance widths, systems containing a light quark can still be treated as quarkonia. *I.e.*, extra $q\bar{q}$ pairs and the gluonic degrees of freedom do not have to be introduced explicitly. ISGW adopts this approximation. In addition, for simplicity it uses harmonic oscillator wavefunctions to approximate the true quarkonium wavefunctions.
2. *the weak binding approximation*: For heavy quarkonia, the quark masses and energies are approximately equal and as a result the hadron mass is approximately the sum of the constituent quark masses. Once a quark becomes light, the failure of this approximation and other associated complexities make even a low velocity boost of the wavefunction problematic. Moreover, when both constituents are light, there can be a great discrepancy between the mass of a hadron and the sum of the masses of its constituents; this in turn leads to ambiguities in the extrapolation of the nonrelativistic formulas. ISGW adopts a specific prescription for dealing with such ambiguities.
3. *relativistic corrections*: Even if the extrapolation of the nonrelativistic ISGW formulas were straightforward, they would still suffer from their failure to incorporate important relativistic physics. A simple example is the charge radius r_i : in general such a radius will receive both nonrelativistic contributions with a scale controlled by the radius of the quarkonium wavefunctions and relativistic contributions controlled by the Compton wavelengths of the participating quarks. (The latter contributions are themselves of several types: relativistic corrections from the quarkonium wave equation, field-theory-induced pair creation effects, *etc.* Such effects are simply lost in the nonrelativistic limit since $r \sim 1/p \gg 1/m$.) Of course the form factor intercepts will also receive relativistic corrections: generically, we can write $f_i(0) = f_i^{nr}(0)[1 + \mathcal{O}(p/m)]$. ISGW invokes the empirical success of the nonrelativistic quark model in assuming

that $f_i^{nr}(0)$ will be a reasonable approximation to $f_i(0)$. Finally, there is of course no guarantee that $f_i(t_m - t)$ won't contain $(t_m - t)$ dependence that is intrinsically relativistic. For example, an additional “kinematic” factor of $[1 + \frac{t_m - t}{4mm'v}]$ would be “seen” as unity by a nonrelativistic calculation.

All of these shortcomings, and others left unmentioned, make it surprising that the nonrelativistic constituent quark model works as well as it does. It may be that its successes are based on one crucial fact: that “it is better to have the right degrees of freedom moving at the wrong speed than the wrong degrees of freedom moving at the right speed” [28]. Given that the quark model would be correct if all the quarks were heavy quarks, its utility may reside in its ability to *parameterize* the evolution of the properties of these correct degrees of freedom from heavy to light systems.

III. ISGW2: THE NEW FEATURES

As already repeatedly emphasized, ISGW2 is *not* a new model: it is a slightly improved version of ISGW [1]. In this section we describe one by one the differences between ISGW and ISGW2. For closely related studies of the marriage of the quark model with the physics of Heavy Quark Symmetry, see the work cited in Ref. [7].

A. the constraints of Heavy Quark Symmetry

Although ISGW is completely consistent with the constraints of Heavy Quark Symmetry at maximum recoil t_m (or $w = 1$) in the symmetry limit, HQS also determines various aspects of the behavior of the form factors at finite recoil and at nonleading order in the $1/m_Q$ expansion. For example, the six form factors of $\bar{B} \rightarrow D\ell\bar{\nu}_\ell$ and $\bar{B} \rightarrow D^*\ell\bar{\nu}_\ell$ are required by Heavy Quark Symmetry to have, in the low energy effective theory, the form [4-7]

$$\tilde{f}_+ + \tilde{f}_- = \tilde{f}_+ - \tilde{f}_- = \tilde{g} = \tilde{f} = \tilde{a}_- - \tilde{a}_+ = \xi(w) \quad (3)$$

$$\tilde{a}_+ + \tilde{a}_- = 0 \quad (4)$$

where $\xi(w)$ is the Isgur-Wise function (we have adopted conventions for defining the HQS form factors which lead to these simple forms; see Section V for explicit formulas relating these $\tilde{f}^{(\alpha)}$ to the usual ISGW form factors). In the heavy quark limit, the ISGW model respects all of these constraints at all w except for that on \tilde{f} : it gives $\tilde{f} = (\frac{2}{1+w})\xi(w)$, corresponding to the nonrelativistic approximation $1+w \simeq 2$. Such effects, which correspond to v^2/c^2 corrections to a leading nonrelativistic prediction, lie outside of the dynamical framework of ISGW, but are easily appended to the model (see, e.g., the second of Refs. [7]). Using eq. (3) and the corresponding results of Ref. [29] on the $\bar{B} \rightarrow D_2^*\ell\bar{\nu}_\ell$, $\bar{B} \rightarrow D_1^{3/2}\ell\bar{\nu}_\ell$, $\bar{B} \rightarrow D_1^{1/2}\ell\bar{\nu}_\ell$, and $\bar{B} \rightarrow D_0^*\ell\bar{\nu}_\ell$ decays, the required modifications to be incorporated into

ISGW2 are easily enumerated. They are all listed explicitly in Appendix C. The simplest example is the axial vector form factor f of eq. (B15) of ISGW, which, as the form factor corresponding to \tilde{f} in eq. (3), picks up an additional factor of $\frac{1}{2}(1+w)$ in the HQS limit (additional nonleading effects in the $1/m_Q$ expansion will be described below). In addition to these modifications, Heavy Quark Symmetry tells us that in heavy quark systems the eigenstates with $J^P = 1^+$ are *not* the $L-S$ coupled states 3P_1 and 1P_1 , but rather the $j-j$ coupled states $P_1^{3/2}$ and $P_1^{1/2}$ with $s_\ell^{\pi_\ell} = \frac{3}{2}^+$ and $\frac{1}{2}^+$, respectively [30,29]. We therefore also list the new form factors appropriate to semileptonic decays to such excited P -wave mesons in Appendix C.

In addition to these constraints of Heavy Quark Symmetry on the matrix elements of the low energy effective theory, HQET prescribes how to match these matrix elements onto matrix elements of the full theory, as already mentioned above. The matching of a generic form factor $f_{ji}^{(\alpha)}$ of type α associated with the underlying $Q_i \rightarrow Q_j$ transition can be written in the form [31]

$$f_{ji}^{(\alpha)} = \mathbf{C}_{ji}(w) \left[f^{(\alpha)} + \tilde{\beta}_{ji}^{(\alpha)}(w) \frac{\alpha_s(\mu_{ji})}{\pi} \right] \xi(w) \quad (5)$$

where the $f^{(\alpha)}$ are unity for $\tilde{f}_+ + \tilde{f}_-$, $\tilde{f}_+ - \tilde{f}_-$, \tilde{g} , \tilde{f} , and $\tilde{a}_+ - \tilde{a}_-$, and zero for $\tilde{a}_+ + \tilde{a}_-$. Here

$$\mathbf{C}_{ji} = \left[\frac{\alpha_s(m_i)}{\alpha_s(m_j)} \right]^{a_I} \left[\frac{\alpha_s(m_j)}{\alpha_s(\mu_{qm})} \right]^{a_L(w)} \quad (6)$$

is independent of α and has

$$a_I = - \frac{6}{33 - 2N_f} \quad (7)$$

and

$$a_L(w) = \frac{8}{33 - 2N_f} [wr(w) - 1] \quad (8)$$

with

$$r \equiv \frac{1}{\sqrt{w^2 - 1}} \ln \left(w + \sqrt{w^2 - 1} \right), \quad (9)$$

N_f the number of active flavors below the scale m_i (four for $i = b$) and N'_f the number below m_j (three for $j = c$). In contrast, the radiative correction functions $\tilde{\beta}_{ji}^{(\alpha)}(w)$ multiplying α_s/π (evaluated at a scale μ_{ji} intermediate between m_i and m_j which we take to be the geometric mean $\mu_{ji} = (m_j m_i)^{\frac{1}{2}}$) are α -dependent.

The $\tilde{\beta}_{ji}^{(\alpha)}(w)$ associated with each of six form factors \tilde{f}_+ , \tilde{f}_- , \tilde{g} , \tilde{f} , $\tilde{a}_+ - \tilde{a}_-$, and $\tilde{a}_+ + \tilde{a}_-$ are known. At $w = 1$ they are simply

$$\tilde{\beta}_{ji}^{(f_++f_-)}(1) = \gamma_{ji} - \frac{2}{3}\chi_{ji} \quad (10)$$

$$\tilde{\beta}_{ji}^{(f_+-f_-)}(1) = \gamma_{ji} + \frac{2}{3}\chi_{ji} \quad (11)$$

$$\tilde{\beta}_{ji}^{(g)}(1) = \frac{2}{3} + \gamma_{ji} \quad (12)$$

$$\tilde{\beta}_{ji}^{(f)}(1) = -\frac{2}{3} + \gamma_{ji} \quad (13)$$

$$\tilde{\beta}_{ji}^{(a_++a_-)}(1) = -1 - \chi_{ji} + \frac{4}{3} \frac{1}{(1-z_{ji})} + \frac{2}{3} \frac{1+z_{ji}}{(1-z_{ji})^2} \gamma_{ji} \quad (14)$$

$$\tilde{\beta}_{ji}^{(a_+-a_-)}(1) = -\frac{4}{3} \frac{1}{(1-z_{ji})} - \chi_{ji} + \frac{1}{3} + \left[1 - \frac{2}{3} \frac{1+z_{ji}}{(1-z_{ji})^2} \right] \gamma_{ji} \quad (15)$$

where

$$\gamma_{ji} \equiv \frac{2z_{ji}}{1-z_{ji}} \ln \frac{1}{z_{ji}} - 2 \quad (16)$$

and

$$\chi_{ji} \equiv -1 - \frac{\gamma_{ji}}{1-z_{ji}} \quad (17)$$

with

$$z_{ji} \equiv \frac{m_j}{m_i}. \quad (18)$$

We deviate from the use of these matching conditions only in case of transitions between light (u , d , and s) quarks. Since, as described in Appendix A, we assume that α_s “freezes out” at the quark model scale μ_{qm} , the “renormalization group improved” matching conditions, as embodied in the $\mathbf{C}_{\mathbf{j}\mathbf{i}}$ factor, are inappropriate for such transitions. For them we use the expansion of $\mathbf{C}_{\mathbf{j}\mathbf{i}}$ to lowest order in α_s , *i.e.* we resort to “lowest order matching”.

In principle the $\tilde{\beta}_{ji}^{(\alpha)}$ are functions of w , but this w -dependence is predicted [31] to be so weak relative to uncertainties in the w -dependence associated with nonperturbative effects that we ignore it here. (This dependence would, for example, correspond to a change in the predicted rates for the exclusive $b \rightarrow c$ decays of the order 1% *if* it could be distinguished from the w -dependence in the preasymptotic nonperturbative Isgur-Wise functions.) On the other hand, there is nontrivial w -dependence contained in the factor $\left[\frac{\alpha_s(m_j)}{\alpha_s(\mu_{qm})}\right]^{a_L(w)}$: for w near 1,

$$\left[\frac{\alpha_s(m_j)}{\alpha_s(\mu_{qm})}\right]^{a_L(w)} \simeq 1 - \frac{2}{3} \left(\frac{8}{33 - 2N_f'} \right) \ln \left[\frac{\alpha_s(\mu_{qm})}{\alpha_s(m_j)} \right] (w - 1) \quad (19)$$

We will make use of this factor below.

The preceding HQS- and HQET-induced modifications to ISGW are consequences which emerge from considerations of the heavy quark limit. There are additional modifications which arise from restrictions on the form of $1/m_Q$ corrections to this limit. From the most general form of $1/m_b$ and $1/m_c$ corrections to the $\bar{B} \rightarrow D\ell\bar{\nu}_\ell$ and $\bar{B} \rightarrow D^*\ell\bar{\nu}_\ell$ form factors (see Section V), it is possible to resolve an ambiguity in the procedure for relating the form factors of the ISGW weak binding nonrelativistic calculation to physical form factors. Such a calculation in principle only determines form factors up to factors like $(m_H/\tilde{m}_H)^n$ where m_H is a physical hadron mass and \tilde{m}_H is the sum of its constituent quarks’ masses. HQET resolves this ambiguity in a pleasing way: it specifies that the form factors \tilde{f}_i^{qm} being calculated in such a quark model are (up to order $1/m_Q$) the dimensionless form factors \tilde{f}_i of the heavy quark limit which expand matrix elements in Lorentz invariants using the heavy quark four velocities v^μ , v'^μ and *not* the f_i which expand them in terms of their momenta. (As far as we can determine, it is purely by accident that the ISGW

notation \tilde{f}_i for the weak binding form factors coincides with the notation for the HQS form factors). Such considerations in addition demand that the conventional form factors f_i be obtained from the f_i^{qm} by mass scaling factors which differ from the physical masses by at most $1/m_Q$ effects. In ISGW2 we choose to resolve this residual ambiguity by using the hyperfine-averaged physical masses $\bar{m}_{H_1 H_2} \equiv \bar{m}_{H_1} \equiv \bar{m}_{H_2}$ of a HQS spin doublet of hadrons H_1 and H_2 to relate the \tilde{f}_i^{qm} to the f_i . (For the $s_\ell = \frac{1}{2}$ ground state doublet this mass is just $\bar{m}_{VP} = \frac{3}{4}m_V + \frac{1}{4}m_P$; in general $\bar{m}_{s_\ell} = \left(\frac{s_\ell+1}{2s_\ell+1}\right)m_{j=s_\ell+\frac{1}{2}} + \left(\frac{s_\ell}{2s_\ell+1}\right)m_{j=s_\ell-\frac{1}{2}}$ for an HQS multiplet with light degrees of freedom having spin s_ℓ). As in ISGW, we use the f_i to compute all rates; this may be viewed as a residual model-dependent choice of certain $1/m_Q^2$ terms, and illustrates very clearly how HQS and HQET have reduced the model-dependence of the results of ISGW2 relative to ISGW.

There are two additional but clearly related elements to the correspondence between the \tilde{f}_i^{qm} and the f_i . The \tilde{f}_i^{qm} are functions of \tilde{w} which is the weak-binding variable analogous to the physical variable w . In passing to the physical form factors f_i which depend on $t_m - t$ we identify

$$\tilde{w} - 1 = \frac{t_m - t}{2\bar{m}_{PQ}\bar{m}_{XQ}} \quad (20)$$

for a transition $P_Q \rightarrow X_q \ell \bar{\nu}_\ell$ induced by an underlying $Q \rightarrow q \ell \bar{\nu}_\ell$ transition. In addition, we correct all form factors for relativistic terms proportional to $t_m - t$ that are required by the form of $1/m_Q$ corrections: see Section V and Appendix C for details.

We next note that consideration of sum rules for the $Q_i \rightarrow Q_j \ell \bar{\nu}_\ell$ transition in the heavy quark limit provides a constraint on the slope of the Isgur-Wise function $\xi(w)$. If we define ρ^2 by the expansion

$$\xi(w) = 1 - \rho^2(w - 1) + \dots \quad (21)$$

about $w = 1$, then [9] in the heavy quark limit

$$\rho^2 = \frac{1}{4} + \rho_{sd}^2 + \Delta\rho_{pert}^2. \quad (22)$$

As will be seen below, the structure-dependent term ρ_{sd}^2 dominates for a weakly bound system. The $\Delta\rho_{pert}^2$ term is that appearing in eq. (19) from the w -dependence of the matching factors. The $\frac{1}{4}$ represents a relativistic correction to the nonrelativistic limit. It corresponds to the relativistic correction found in Ref. [27]; its generalization to systems with different spins is discussed in Ref. [32]. The results of Ref. [27] actually dictate the subleading (order $1/m_Q$ and $1/m_q$) corrections to the $\frac{1}{4}$ of the heavy quark limit. In terms of a conventional charge radius r^2 defined by

$$f(t) = f(t_m)[1 - \frac{1}{6}r^2(t_m - t) + \dots] \quad (23)$$

in an expansion of the generic $P_Q \rightarrow X_q$ form factor f around $t = t_m$, the relation corresponding to eq. (22) with subleading terms from Ref. [27] included is

$$r^2 = \frac{3}{4m_Q m_q} + r_{wf}^2 + \frac{1}{\bar{m}_{P_Q} \bar{m}_{X_q}} \left(\frac{16}{33 - 2N'_f} \right) \ln \left[\frac{\alpha_s(\mu_{qm})}{\alpha_s(m_q)} \right] \quad (24)$$

where, for a ground state harmonic oscillator wavefunction (see Appendix A),

$$r_{wf}^2 = \frac{3m_{sp}^2}{2\bar{m}_{P_Q} \bar{m}_{X_q} \beta_{PX}^2} . \quad (25)$$

The terms of eq. (24) are associated in order with the terms of eq. (22). Indeed, r_{wf}^2 in eq. (25) is the transition matrix element of the square of the interquark separation between P_Q and X_q ; it would be *four* times the squared charge radius of the pion in the case where $P_Q = X_q = \pi$. Since $m_{sp}/\beta_{PX} \sim m_{sp}/p_{wf} \gg 1$ in the nonrelativistic limit, the $\frac{1}{4}$ is indeed a “relativistic correction”, as stated earlier. However, in the constituent quark model $m_{sp}/p_{wf} \sim 1$, so it could be a very significant “correction”! ISGW recognized the *generic* possibility of $1/m_Q m_q$ corrections to r^2 and accordingly introduced a “relativistic correction factor” κ to compensate for them: they took $f(t_m - t) \rightarrow f(\frac{t_m - t}{\kappa^2})$, corresponding to enlarging r by a factor κ^{-1} . It is now clear that the $\frac{3}{4m_Q m_q}$ term in eq. (24) is a well-defined and necessary relativistic kinematic correction which should be added to the r_{wf}^2 term of a nonrelativistic model. In ISGW2 we note that this required correction is actually sufficient to achieve the same empirical effect as the multiplicative factor κ of ISGW, which

was fit to the low t pion charge form factor. While relativistic dynamics missing from the constituent quark model might in principle still affect r_{wf}^2 , we assume that such effects were on the whole subsumed into the quark model once its parameters were chosen to give a good description of the meson spectra. Thus, in ISGW2 we drop the *ad hoc* κ factor in favor of the use of eq. (24). This has the additional bonus of making ISGW2 consistent with the dynamical constraints of the Bjorken sum rule [9]: in the heavy quark limit, the “structure-dependent terms” in eq. (22) are determined by the amplitudes to excite final states X_q with $s_\ell^{\pi\ell} = \frac{3}{2}^+$ and $\frac{1}{2}^+$. Finally, we note that the $\Delta\rho_{pert}^2$ term vanishes for decays to s , d , and u quarks since their masses are already below the quark model scale μ_{qm} where the running coupling constant has been assumed to saturate (see Appendix A). As a result, it only comes into play for $b \rightarrow c$ transitions.

In addition to this improvement in the way we deal with the slopes of the form factors, in ISGW2 we also abandon the gaussian form factors of ISGW, which are unrealistic at large recoils. This modification is described in Section III.C below.

B. some relativistic corrections to the quark model

As stressed in Section II, the ISGW model was introduced to illuminate some basic issues surrounding semileptonic decays. It therefore used the simplest possible version of the quark model capable of addressing these issues. It is, however, known that the predictive accuracy of the naive nonrelativistic quark model can be substantially improved by considering various relativistic corrections to that model. One of the simplest such corrections occurs in the matrix elements of the axial current. The naive nonrelativistic quark model predicts that $g_A = \frac{5}{3}$ in neutron beta decay. However, it has been known for twenty years that when the constituent quarks are given realistic momenta, g_A is reduced by a factor of $1 - \frac{4}{3}P_{lower}$, where P_{lower} is the probability of lower components in the quark spinors [26]. By taking this effect into account, most models [26,27] obtain values of g_A about 25% smaller than $\frac{5}{3}$, close to its observed value of 1.257 ± 0.003 [33]. For the $P_Q \rightarrow V_q$ axial vector S-wave form factor

(called f in ISGW) the correction factor is

$$C_f = J_{V_q P_Q}^{-1} \int d^3 p \phi_{V_q}^*(p) \left[\frac{E_q + m_q}{2E_q} \right]^{1/2} \left[1 - \frac{p^2}{3(E_q + m_q)(E_Q + m_Q)} \right] \left[\frac{E_Q + m_Q}{2E_Q} \right]^{1/2} \phi_{P_Q}(p) \quad (26)$$

where the ϕ 's are S-wave momentum space wavefunctions, $E_i = (p^2 + m_i^2)^{1/2}$, and $J_{V_q P_Q} = \int d^3 p \phi_{V_q}^*(p) \phi_{P_Q}(p)$. For a heavy quark transition in the heavy quark limit $C_f = 1$, but for a light quark transition, the analog of eq. (26) for $n \rightarrow p$ would give roughly the required reduction of g_A . In ISGW2 we adopt this correction factor as being at the least a reasonable interpolation between these two extremes. The correction factors resulting from eq.(26) using the masses and wavefunctions of Appendix A are given in Table I.

Two potential deficiencies of this approach should be noted. There is in the first place no reason to suppose that there are not other more dynamical effects which renormalize the matrix elements of the light axial quark currents: the effect taken into account by eq. (26) should be only part of the story [34]. In addition, it is not clear that only the S-wave form factor f will be affected by relativistic corrections. We nevertheless take this as the simplest working hypothesis, and assume that the effective constituent quark mass subsumes other relativistic corrections as it does for quark model magnetic moments [27].

A second class of relativistic corrections to the quark model appears in the wavefunctions themselves. For simplicity, ISGW ignored the effect of relativistic corrections to the effective interquark potential. In particular, although quark model hyperfine interactions are responsible for the $\bar{B}^* - \bar{B}$, $D^* - D$, $\bar{K}^* - \bar{K}$, and $\rho - \pi$ splittings, their effects on the wavefunctions were not taken into account. (In HQET [6], this origin of the $\bar{B}^* - \bar{B}$ and $D^* - D$ splittings can be given a firm foundation *via* the $\sigma_{\mu\nu} G^{\mu\nu}/2m_Q$ operator appearing at order $1/m_Q$ in the heavy quark expansion. The quark model assumes the continuing relevance of this mechanism for light quarks as well). For our purposes, the net effect is that pseudoscalar and vector particles of a given flavor are no longer characterized by the same wavefunction parameter β_S (see Table II of ISGW). An update of this Table which takes into account this splitting is given in Appendix A. Given that both hyperfine and spin-orbit

effects in P-wave mesons are empirically very weak, we ignore such effects.

C. more realistic form factors

As mentioned above, ISGW used the gaussian form factors generated by their highly truncated harmonic oscillator basis; moreover, they used them out to relativistic recoils. Here we attempt a more accurate parameterization of the form factors which will have a more realistic behaviour at large $(t_m - t)$ by making the replacement

$$\exp\left[-\frac{1}{6}r_{wf}^2(t_m - t)\right] \rightarrow \left[1 + \frac{1}{6N}r^2(t_m - t)\right]^{-N} \quad (27)$$

where r^2 is given by eq. (24). In eq. (27), $N = 2 + n + n'$ where n and n' are the harmonic oscillator quantum numbers of the initial and final wavefunctions (*i.e.*, $N = 2$ for S -wave to S -wave, $N = 3$ for S -wave to P -wave, $N = 4$ for S -wave to S' -wave, *etc.*). These form factors all have the charge radii dictated by the quark model in the nonrelativistic limit, approach the gaussian form factors of the harmonic oscillator model as $N \rightarrow \infty$, but provide a much better global fit to the pion form factor (see Fig. 1). In fact, with eq. (24) we predict $\langle r_\pi^2 \rangle^{\frac{1}{2}} = 0.61$ fm, in satisfactory agreement with the observed [18] value of 0.71 ± 0.02 fm. Since the Q^2 range covered by this figure corresponds to a $(t_m - t)$ range that covers the recoils available in the semileptonic decays we treat here, we adopt the substitution of eq. (27) for all our decays. We emphasize that these substitutions should be viewed as low energy parameterizations of the form factors and *not* as appropriate descriptions of their analytic or high $(t_m - t)$ forms.

IV. RESULTS AND DISCUSSION

The formulas we require to predict semileptonic form factors and rates may all be obtained from ISGW [1] (supplemented by formulas given in refs. [25] and [29] for decays in which the lepton mass is not negligible) by making the few simple modifications described in the text. The required changes are described explicitly in Appendix C. To calculate rates we insert into these formulas the constituent quark masses and β -values from Tables A1 and A2 of Appendix A.

We now present our results, organized by the underlying quark decay and arranged in order of increasing spectator quark mass. We will compare these results to the predictions of Heavy Quark Symmetry in Section V and to experiment in Section VI.

A. $\underline{b \rightarrow c\ell\bar{\nu}_\ell}$

These decays are generally the most stable predictions of our model, and those that are underwritten by Heavy Quark Symmetry are the most reliable. All states contain a heavy quark and the available recoil is limited, reducing the sensitivity to form factor slopes. Since the b and c quarks are not only heavy but also have a modest mass difference, the Shifman-Voloshin limit [15,16] is also relevant to the decays with a light spectator and thus provides a simple explanation for why the electron spectral shape is very similar to that of the free quark decay model despite dominance by the ground state pseudoscalar and vector final states.

1. $\bar{B} \rightarrow X_{c\bar{d}}\ell\bar{\nu}_\ell$

Our results for $\bar{B} \rightarrow X_{c\bar{d}}e\bar{\nu}_e$ are shown in Figure 2; the partial widths are given in Table II. This decay is dominated by the pseudoscalar and vector meson final states, which contribute 29% and 61% of the total semileptonic rate respectively. Our absolute prediction for the inclusive decay rate for $\bar{B} \rightarrow X_{c\bar{d}}e\bar{\nu}_e$ is $\Gamma = 4.06 \times 10^{13} |V_{cb}|^2 \text{sec}^{-1}$, about the same as the ISGW result. The approximate validity of the SV limit gives an electron spectral shape

very similar to the free quark model despite the dominance by the ground states of X_c . Our predicted form factors are also close to those of the heavy quark limit; a detailed discussion of this limit will be given in Section V.

2. $\bar{B}_s \rightarrow X_{c\bar{s}} \ell \bar{\nu}_\ell$

The small difference in the m_d and m_s constituent quark masses on the m_b or m_c scale results in $\bar{B}_s \rightarrow X_{c\bar{s}} e \bar{\nu}_e$ decays behaving in a very similar fashion to the previous case. This may be seen in both Figure 3 and Table II where our results are displayed. As expected, there is a small increase ($\sim 5\%$) in the total fraction of the 1P and 2S states compared to \bar{B} decay since the SV limit holds here to a slightly reduced degree. Our absolute prediction for the inclusive decay $\bar{B}_s \rightarrow X_{cs} e \bar{\nu}_e$ is $\Gamma = 3.90 \times 10^{13} |V_{cb}|^2 \text{sec}^{-1}$, slightly smaller than the previous case.

3. $\bar{B}_c \rightarrow X_{c\bar{c}} \ell \bar{\nu}_\ell$

This decay is different from the preceding two cases in several ways. As the spectator quark is no longer light, both the parent and daughter mesons are approximately non-relativistic and are thus appropriately described by our model. The results, which should therefore be quite reliable, are shown in Figure 4 and Table II. They are still reminiscent of the previous results with lighter spectators even though the spectator approximation prediction that the inclusive semileptonic decay rates should be equal fails by about 25% in going from \bar{B}_d to \bar{B}_s to \bar{B}_c decays. The contributions from the pseudoscalar and vector final states are, however, reduced (to 29% and 47%, respectively) as expected from the spectator arguments given in the ISGW papers and from the inapplicability of the SV limit.

The measurement of the slopes of the form factors for these decays would provide an interesting test of the arguments made in Refs. [1,2,17] that naive dispersion relations for these slopes will fail. These systems are predicted to have charge radii determined by their Bohr radii $\sim [\frac{4(m_b+m_c)}{3m_b m_c \alpha_s}]^{-1}$ while dispersion relations would lead one to believe (unless one were *very* careful [17]) that the charge radii will be of order $(m_b + m_c)^{-1}$. Discussing the possibility of studying these states may not be completely far-fetched: there are suggestions

[37,38] for experiments to observe them.

B. $c \rightarrow s \ell^+ \nu_\ell$

The decays induced by the quark level process $c \rightarrow s \ell^+ \nu_\ell$ are dominated by the ground state pseudoscalar and vector daughter mesons. This is a consequence of the low available recoil momentum which has little probability of producing excited states. These decays are nevertheless not expected to be as accurately described as the $b \rightarrow c$ case since the s quark is too light for Heavy Quark Symmetry to apply.

1. $D \rightarrow X_{s\bar{u}} \ell^+ \nu_\ell$

Our results for $D \rightarrow X_{s\bar{u}} e^+ \nu_e$ are shown in Figure 5; the partial widths are given in Table III. This decay is predicted to be almost totally dominated by the pseudoscalar and vector meson final states, which contribute 63% and 34% of the total semileptonic rate respectively. Our absolute prediction for the rate of the inclusive decay $D \rightarrow X_{s\bar{u}} e^+ \nu_e$ is $\Gamma = 0.17 \times 10^{12} |V_{sc}|^2 \text{sec}^{-1}$, down about 10% from ISGW. This decrease arises from an increase of the K rate of 18% and a decrease in the K^* rate of 41% which dramatically alter the ISGW K^*/K ratio; for details, see Section VI below. Our total predicted width is about one half that of a simple free quark model using our constituent quark masses.

It is amusing to note that while neither the heavy quark nor SV limits should be applicable here, they both seem to have strong residual influences on this decay. The comparison of our predicted form factors with those of Heavy Quark Symmetry assuming that s is a heavy quark will be given below.

2. $D_s \rightarrow X_{s\bar{s}} \ell^+ \nu_\ell$

While m_u and m_s are very similar on the scale of the charm quark mass, they are noticeably different on the scale of the daughter quark mass m_s . As a result we do not expect as strong a similarity between D and D_s decays as that which existed between \bar{B} and \bar{B}_s decays. In addition, non-ideal mixing in the pseudoscalar sector of D_s decays leads to

a very different spectral shape due to the comparatively low mass of the η . This low mass gives a much higher electron endpoint than the corresponding free quark decay endpoint, as may be seen in Figure 6. The fractions of the semileptonic rate going to η , η' , and ϕ are 31%, 26%, and 40%, respectively, with the distribution of rate to the η and η' sensitive to the assumed pseudoscalar mixing angle of -20° , but with the sum relatively insensitive (see Table III). The 1P and 2S contributions are once again predicted to be small: only 3% of the semileptonic width. The ratio of rates for $D \rightarrow K^* e^+ \nu_e$ and $D_s \rightarrow \phi e^+ \nu_e$ is

$$\frac{\Gamma(D_s \rightarrow \phi e^+ \nu_e)}{\Gamma(D \rightarrow K^* e^+ \nu_e)} = 0.84, \quad (28)$$

down about 20% from the ISGW value [39] of 1.02. This decrease is mainly due to hyperfine interaction effects and the new \bar{m} prescription of Section III.A. We note before leaving these decays that the D_s inclusive semileptonic decay rate is itself down by more than 25% from D decay. This substantial failure of the spectator approximation will be discussed in Section VI.

3. $B_c \rightarrow X_{s\bar{b}} \ell^+ \nu_\ell$

Our results for $B_c \rightarrow X_{s\bar{b}} e^+ \nu_e$ are shown in Figure 7. The explicit partial widths are given in Table III. Not surprisingly, the extreme mass of the spectator in this case results in a spectrum that is very different from the naive free quark spectrum. It is dominated by decays to the pseudoscalar (43%) and vector (55%), as the available energy is small. Recoil effects are very small due to the large daughter mass. The softening of the lepton spectra expected due to the high spectator mass is pronounced as is the reduction of the inclusive rate. Our absolute rate $\Gamma(B_c \rightarrow X_{s\bar{b}} e^+ \nu_e) = 0.50 \times 10^{11} |V_{sc}|^2 \text{ sec}^{-1}$ is less than a third that of $D \rightarrow X_{s\bar{u}} e^+ \nu_e$, corresponding to an even more dramatic failure of the spectator approximation.

The ratio of B_c decay via $b \rightarrow c$ to $c \rightarrow s$ decay is

$$\frac{\Gamma(B_c \rightarrow X_{s\bar{b}} e^+ \nu_e)}{\Gamma(B_c \rightarrow X_{c\bar{c}} e^+ \nu_e)} = 0.0014 \left| \frac{V_{sc}}{V_{cb}} \right|^2 \sim 1 \quad (29)$$

for $|V_{cb}| \simeq 0.04$ and $|V_{sc}| \simeq 1$. Thus, amusingly, B_c semileptonic decays will be roughly evenly split between the two very different quark level processes $b \rightarrow c$ and $c \rightarrow s$.

C. $\underline{c \rightarrow d\ell^+\nu_\ell}$

We now consider the Cabibbo-suppressed decays involving the quark level process $c \rightarrow d\ell^+\nu_\ell$ which are also predicted to be dominated by the ground state pseudoscalar and vector final states. These decays have taken on a new importance since the realization that their measured form factors can be related to the form factors of $b \rightarrow u$ via Heavy Quark Symmetry. As indicated in Section V below, these relations should eventually lead to accurate model-independent determinations of $|V_{ub}|$.

1. $D^0 \rightarrow X_{d\bar{u}}\ell^+\nu_\ell$ and $D^+ \rightarrow X_{d\bar{d}}\ell^+\nu_\ell$

Our results for $D^0 \rightarrow X_{d\bar{u}}e^+\nu_e$ and $D^+ \rightarrow X_{d\bar{d}}e^+\nu_e$ are shown in Figures 8a) and b) respectively. The partial widths are given in Tables IV and V, respectively. $D^0 \rightarrow X_{d\bar{u}}e^+\nu_e$ is dominated by π and ρ final states which contribute 63% and 31% of the total respectively, compared to 43% and 52% in ISGW. This shift in relative probability comes mainly from a substantial decrease in the ρ rate. However, there is also a sizeable 5% rate predicted to the $J^P = 1^+$ P -wave states. The longitudinal to transverse ratio for the ρ is 0.67. The D^+ decays look somewhat different as the final states now include both the $I = 0$ and $I = 1$ neutral states. Note that $\Gamma(D^+ \rightarrow X_{d\bar{d}}e^+\nu_e)/\Gamma(D^0 \rightarrow X_{d\bar{u}}e^+\nu_e) = 0.92$, which is mostly due to the effects of the η and η' channels. We also note in passing that Cabibbo-forbidden decays are predicted to represent approximately 5% of D^0 decays and 4% of D^+ decays.

2. $D_s^+ \rightarrow X_{d\bar{s}}\ell^+\nu_\ell$

$D_s \rightarrow X_{d\bar{s}}e^+\nu_e$ decays of Figure 9 and Table IV are again dominated by the pseudoscalar and vector ground states which contribute 60% and 29% of the total resonant semileptonic rate with a 10% contribution from the $J^P = 1^+$ P -wave states. The absolute rate is almost a factor of three times smaller than the free quark decay rate, and the lepton spectrum is much

softer. Note that these Cabibbo-forbidden decays are predicted to contribute approximately 6% of the inclusive D_s decay rate.

D. $\underline{b \rightarrow u \ell \bar{\nu}_\ell}$

We now consider the decays corresponding to the quark level process $b \rightarrow u \ell \bar{\nu}_\ell$. These decays are very important in the determination of the $|V_{ub}|$ matrix element, which is itself important for CP violation in the Standard Model. Here large recoils are available; as a result we are not surprised to find large contributions from the 1P and 2S states in our lepton spectra. In ISGW the decays to the radially excited pseudoscalars n^1S_0 were explicitly checked to confirm that the calculation would converge to the inclusive rate in the appropriate limit. As in ISGW, however, ISGW2 only sums over the low-lying resonances and so for $b \rightarrow u$ decays it can be used as a model for the inclusive spectrum only in the endpoint region. This point is discussed at greater length in Section VI.

1. $\bar{B}^0 \rightarrow X_{u\bar{d}} \ell \bar{\nu}_\ell$ and $\bar{B}^- \rightarrow X_{u\bar{u}} \ell \bar{\nu}_\ell$

We consider both the decays $\bar{B}^0 \rightarrow X_{u\bar{d}} \ell \bar{\nu}_\ell$ and $B^- \rightarrow X_{u\bar{u}} \ell \bar{\nu}_\ell$ which are shown in Figure 10a) and b), respectively. Detailed partial widths are given in Table VI. As in ISGW, there are large contributions from the 1P and 2S states. On comparing with the results of ISGW, one sees that our more realistic form factors have increased the rate to the sum of the rates to the 1S, 1P, and 2S states by about 25% and transferred some of the rate from the heavier to the lighter states. ISGW2 therefore predicts a somewhat hardened endpoint spectrum relative to ISGW. The change in individual exclusive rates is most pronounced for the pion, which has increased by about a factor of four over the ISGW result. As discussed above, and as is apparent from Fig. 1, ISGW was designed to produce a conservative estimate of the endpoint rate. The effect on the π rate is uncharacteristic since it vanishes for kinematic reasons at zero recoil where the ISGW form factor is nearly equal to ours, and grows into the high recoil region where their form factor is far below ours and the measured pion form

factor. The consequent large uncertainty in the π rate is compounded by the potential effect (to be discussed below) of the nearby \bar{B}^* pole. In contrast, the ISGW2 rate to the ρ is only about 70% larger than that of ISGW. A similar increase is obtained for the total rate to the $1P$ states, while the rate to the radial excitations of the π and the ρ decreased by almost a factor of three. We also note that the ratio Γ_L/Γ_T for $\bar{B}\rightarrow\rho e\bar{\nu}_e$ has remained equal to the ISGW value of 0.30, even though this value is sensitive to the method used to treat large recoils and the axial current form factors.

As in ISGW, we have included all resonance states with masses ≤ 1.7 GeV, which implies that our lepton spectra are complete for lepton energies greater than about 2.4 GeV. In this region our spectra are considerably softer than that of the free quark decay. Since our sum over exclusive channels is incomplete, we cannot quote a total rate, although the treatment of the pion radial excitations described in ISGW suggests that it will be within a factor of two of our free quark rate of $1.28 \times 10^{14} |V_{ub}|^2 \text{sec}^{-1}$.

2. $\bar{B}_s \rightarrow X_{u\bar{s}} \ell \bar{\nu}_\ell$

Our results for $\bar{B}_s \rightarrow X_{u\bar{s}} e \bar{\nu}_e$ are shown in Figure 11, with the explicit partial widths in Table VII. As expected, this decay is very similar to that of the \bar{B} -meson. There is, however, a noticeable softening of the spectrum due to the heavier spectator.

3. $\bar{B}_c \rightarrow X_{u\bar{c}} \ell \bar{\nu}_\ell$

Our results for $\bar{B}_c \rightarrow X_{u\bar{c}} e \bar{\nu}_e$ are shown in Figure 12. The explicit partial widths are given in Table VII. This decay is similar to the other $b \rightarrow ue\bar{\nu}_e$ decays. However, the softening of the spectrum due to increased spectator mass is much more pronounced, as is the shifting of probability to states with masses above those of our calculation.

V. COMPARISON TO HEAVY QUARK SYMMETRY

In this section we compare our results to those of Heavy Quark Symmetry, which provides model-independent predictions for some aspects of the weak hadronic matrix elements presented here. While these model-independent predictions are very interesting theoretically, the sizes of the corrections to this limit may restrict its validity to a limited number of processes, or to a small region of phase space. One way to estimate the effects of such Λ_{QCD}/m_q corrections to these limiting predictions is to compute these corrections in a model such as ISGW2. ISGW2 is in fact most reliable precisely at the key zero-recoil point of Heavy Quark Symmetry, and indeed our form factors reduce to those required when taken to the symmetry limit. Away from this limit our results constitute model-dependent predictions for the effects of the finite quark masses. Estimates of such corrections from other hadronic models and from quenched lattice QCD have also been made [40].

The predictions of Heavy Quark Symmetry for the decays $P_Q \rightarrow P_q \ell \bar{\nu}_\ell$ and $P_Q \rightarrow V_q \ell \bar{\nu}_\ell$ were first worked out in Refs. [4]. The relationship between our form factors and those of Heavy Quark Symmetry described by eqs. (3) and (4) which are defined in terms of four-velocity variables is

$$\tilde{f}_+ = \frac{1}{2} \left(\sqrt{\frac{m_{P_Q}}{m_{P_q}}} + \sqrt{\frac{m_{P_q}}{m_{P_Q}}} \right) f_+ + \frac{1}{2} \left(\sqrt{\frac{m_{P_Q}}{m_{P_q}}} - \sqrt{\frac{m_{P_q}}{m_{P_Q}}} \right) f_- \quad (30)$$

$$\tilde{f}_- = \frac{1}{2} \left(\sqrt{\frac{m_{P_Q}}{m_{P_q}}} - \sqrt{\frac{m_{P_q}}{m_{P_Q}}} \right) f_+ + \frac{1}{2} \left(\sqrt{\frac{m_{P_Q}}{m_{P_q}}} + \sqrt{\frac{m_{P_q}}{m_{P_Q}}} \right) f_- \quad (31)$$

$$\tilde{g} = 2\sqrt{m_{P_Q} m_{V_q}} g \quad (32)$$

$$\tilde{f} = \frac{f(1+w)^{-1}}{\sqrt{m_{P_Q} m_{V_q}}} \quad (33)$$

$$\tilde{a}_+ + \tilde{a}_- = - \frac{m_{P_Q}^2}{\sqrt{m_{P_Q} m_{V_q}}} (a_+ + a_-) \quad (34)$$

$$\tilde{a}_+ - \tilde{a}_- = - \sqrt{m_{P_Q} m_{V_q}} (a_+ - a_-). \quad (35)$$

Recall from Section III.A that since these relations involve the physical hadron masses m_H , and not the hyperfine-averaged masses \bar{m}_H , these \tilde{f}_i differ from the \tilde{f}_i^{qm} calculated directly at the quark model level by $1/m_Q^2$ terms.

The $1/m_q$ and $1/m_Q$ corrections to these predictions have been considered by various authors [41-45]. In particular, the first of Refs. [45] gives a general form for such corrections which is, as we will see, particularly suited to our quark model, namely

$$\frac{\tilde{f}_+}{\xi(w)} = 1 + \frac{\rho_1(w)}{\mu_+} \quad (36)$$

$$\frac{\tilde{f}_-}{\xi(w)} = \frac{1}{\mu_-} \left(-\frac{\bar{\Lambda}}{2} + \rho_4(w) \right) \quad (37)$$

$$\frac{\tilde{g}}{\xi(w)} = 1 + \frac{\bar{\Lambda}}{2\mu_+} + \frac{1}{m_q} \rho_2(w) + \frac{1}{m_Q} (\rho_1(w) - \rho_4(w)) \quad (38)$$

$$\frac{\tilde{f}}{\xi(w)} = 1 + \frac{\bar{\Lambda}}{2\mu_+} \left(\frac{w-1}{w+1} \right) + \frac{1}{m_q} \rho_2(w) + \frac{1}{m_Q} \left(\rho_1(w) - \frac{w-1}{w+1} \rho_4(w) \right) \quad (39)$$

$$\frac{(\tilde{a}_+ + \tilde{a}_-)}{\xi(w)} = -\frac{1}{(w+1)m_q} \left(\bar{\Lambda} - (w+1)\rho_3(w) + \rho_4(w) \right) \quad (40)$$

$$\begin{aligned} \frac{(\tilde{a}_+ - \tilde{a}_-)}{\xi(w)} &= 1 + \frac{\bar{\Lambda}}{2} \left(\frac{w-1}{w+1} \frac{1}{m_q} + \frac{1}{m_Q} \right) + \frac{1}{m_q} \left(\rho_2(w) - \rho_3(w) - \frac{1}{w+1} \rho_4(w) \right) \\ &\quad + \frac{1}{m_Q} (\rho_1(w) - \rho_4(w)) \end{aligned} \quad (41)$$

where $\bar{\Lambda}$ is a constant and $1/\mu_{\pm} \equiv 1/m_q \pm 1/m_Q$. The inclusion of these effects thus results in the appearance of four additional unknown functions $\rho_n(w)$ with unknown normalizations (although it can be shown that $\rho_1(1) = \rho_2(1) = 0$). Alternative parameterizations have also been given; we will comment on one of these below.

We can map onto our results by expanding them to leading order in $1/m_q$ and $1/m_Q$; we find

$$\frac{\tilde{f}_+^{\text{qm}}}{\xi} = 1 - \frac{R_P(w)}{\mu_+} \quad (42)$$

$$\frac{\tilde{f}_-^{\text{qm}}}{\xi} = -\frac{m_{sp}}{2\mu_-} \quad (43)$$

$$\frac{\tilde{g}^{\text{qm}}}{\xi} = 1 + \frac{m_{sp}}{2\mu_+} - \frac{R_V(w)}{m_q} - \frac{R_P(w)}{m_Q} \quad (44)$$

$$\frac{\tilde{f}^{\text{qm}}}{\xi} = 1 - \frac{R_V(w)}{m_q} - \frac{R_P(w)}{m_Q} + \left(\frac{w-1}{w+1} \right) \frac{m_{sp}}{2\mu_+} \quad (45)$$

$$\frac{\tilde{a}_+^{\text{qm}} + \tilde{a}_-^{\text{qm}}}{\xi} = -\frac{m_{sp}}{m_q(1+w)} \quad (46)$$

and

$$\frac{\tilde{a}_+^{\text{qm}} - \tilde{a}_-^{\text{qm}}}{\xi} = 1 + \frac{m_{sp}}{2\mu_+} - \frac{m_{sp}}{m_q(1+w)} - \frac{R_V(w)}{m_q} - \frac{R_P(w)}{m_Q} . \quad (47)$$

Here

$$R_{P(V)}(w) \equiv \frac{(w-1)\left[\frac{1}{4}\delta_{sp} + \frac{m_{sp}^2}{2\beta_{sp}^2}\lambda_{Psp(Vsp)}\right]}{1 + \frac{1}{2}\rho^2(w-1)} \quad (48)$$

with $\delta_{sp} \equiv \bar{m}_{P_{Qsp}V_{Qsp}} - m_Q$ as $m_Q \rightarrow \infty$ and with the λ 's parameterizing the approach of the β 's to the heavy quark limit *via*

$$\beta_{P(V)_{Qsp}}^2 \equiv \beta_{sp}^2 \left(1 - \frac{2\lambda_{Psp(Vsp)}}{\tilde{m}_{Qsp}}\right) , \quad (49)$$

with $\lambda_{Psp} = k_{sp} - \frac{3}{4}h_{sp}$ and $\lambda_{Vsp} = k_{sp} + \frac{1}{4}h_{sp}$. Here k_{sp} describes the perturbation of β_{Qsp}^2 in a heavy quark meson with heavy quark Q and a spectator sp due to the heavy quark kinetic energy (which is spin-independent) and h_{sp} is the analogous perturbation due to the residual hyperfine interaction of Q and sp . From Table A2 one can see that $k_d \simeq +0.14$ GeV, $h_d \simeq +0.36$ GeV, $k_s \simeq +0.26$ GeV, and $h_s \simeq +0.50$ GeV. Using the measured masses and the constituent quark masses of Table A1, and correcting for the residual heavy quark kinetic energy, one can estimate that $\delta_d \simeq 0.09$ GeV, and $\delta_s \simeq 0.17$ GeV.

This decomposition allows us to identify

$$\bar{\Lambda} = m_{sp} \quad (50)$$

$$\rho_1(w) = -R_P(w) \quad (51)$$

$$\rho_2(w) = -R_V(w) \quad (52)$$

$$\rho_3(w) = 0 \quad (53)$$

$$\rho_4(w) = 0 \quad , \quad (54)$$

from which one can easily see that the predicted corrections to the Heavy Quark Symmetry limit are all of modest size. This assessment is made quantitative by Table VIII for $b \rightarrow c$ and $c \rightarrow s$ decays with an up or down spectator. In terms of the common $\psi_1, \psi_2, \psi_3, \psi_+$ parameterization [44] of $1/m_Q$ and $1/m_q$ corrections, these results are $\psi_1 = -(R_P + 3R_V/2\bar{\Lambda})\xi$, $\psi_2 = 0$, $\psi_3 = -(R_V - R_P/4\bar{\Lambda})\xi$, and $\psi_+ = -(w - 1/w + 1)\xi$. Note that, as required, ψ_1

respects heavy quark spin symmetry, while ψ_3 is responsible for breaking it. Conclusions similar to ours (couched in terms of the ψ -parameterization) have been reached previously in the quark model [7].

As an aside, let us note that if we focus on $\bar{B} \rightarrow D^* \ell \bar{\nu}_\ell$ transitions alone, and assume *only* that $\rho_3(w) = \rho_4(w) = 0$, we may define a “preasymptotic Isgur-Wise function” $\xi_{D^*\bar{B}}(w)$ such that

$$\frac{\tilde{g}}{\xi_{D^*\bar{B}}(w)} = 1 + \frac{\bar{\Lambda}}{2\mu_+} \quad (55)$$

$$\frac{\tilde{f}}{\xi_{D^*\bar{B}}(w)} = 1 + \frac{\bar{\Lambda}}{2\mu_+} \left(\frac{w-1}{w+1} \right) \quad (56)$$

$$\frac{(\tilde{a}_+ + \tilde{a}_-)}{\xi_{D^*\bar{B}}(w)} = - \frac{\bar{\Lambda}}{m_q(w+1)} \quad (57)$$

$$\frac{(\tilde{a}_+ - \tilde{a}_-)}{\xi_{D^*\bar{B}}(w)} = 1 + \frac{\bar{\Lambda}}{2\mu_+} - \frac{\bar{\Lambda}}{m_q(w+1)} \quad (58)$$

Under this assumption, therefore, the predictions of Heavy Quark Symmetry to order $1/m_Q$ and $1/m_q$ can be described by *one* unknown parameter $\bar{\Lambda}$ known to be approximately m_{sp} and the unknown shape of the “preasymptotic Isgur-Wise function” $\xi_{D^*\bar{B}}(w)$ which retains its normalization to unity at $w = 1$. We also note that the measured slope of this function is predicted by our model to be

$$\rho_{D^*\bar{B}}^2 \simeq 0.74 \quad (59)$$

which value includes a contribution

$$\Delta\rho_{pert}^2 \simeq \frac{16}{81} \ln \left[\frac{\alpha_s(\mu_{qm})}{\alpha_s(m_c)} \right] \simeq 0.13 \quad (60)$$

(The numerical value of $\Delta\rho_{pert}^2$ is quite uncertain: it depends on the leading logarithmic expansion in m_c/μ_{qm} and on the assumption that $\alpha_s(\mu_{qm})$, where μ_{qm} is the “quark model scale”, is the “frozen-out” value $\alpha_s = 0.6$ from Appendix A. We accordingly assign a theoretical error of ± 0.05 to it.)

Another important set of predictions [10] of Heavy Quark Symmetry are those which relate, e.g., the form factors of $\bar{B} \rightarrow \rho \ell \bar{\nu}_\ell$ to those of $D \rightarrow \rho \ell^+ \nu_\ell$. These predictions could

play a vital role in determining V_{ub} if corrections to the symmetry limit are not too severe. With ISGW2 we can check these relations. For example, in the ideal symmetry limit one should have

$$\alpha_s(m_b)^{-a_I(m_b)} \frac{f^{\bar{B} \rightarrow \rho}(p_\rho \cdot v_B)}{2\sqrt{m_\rho m_B}} = \alpha_s(m_c)^{-a_I(m_c)} \frac{f^{D \rightarrow \rho}(p_\rho \cdot v_D)}{2\sqrt{m_\rho m_D}} \quad (61)$$

where p_ρ and v_P are the four momentum of the ρ and the four velocity of the decaying meson P and $a_I(m_Q)$ is given by eq. (7) with N_f appropriate to m_Q . (Note that m_ρ has no special significance in these formulas: we are simply using it to create dimensionless quantities. Also note that we have removed the known quark mass dependence of the leading logarithmic matching condition, but not attempted to remove the mass dependence contained in the α_s/π corrections since, while relatively weak given that $\alpha_s(\mu_{ub}) \simeq \alpha_s(\mu_{dc})$, it is model-dependent.) We find, *e.g.*, that at zero recoil

$$\alpha_s(m_b)^{-a_I(m_b)} \frac{f^{B \rightarrow \rho}(m_\rho)}{2\sqrt{m_\rho m_B}} = 0.49 \quad (62)$$

$$\alpha_s(m_c)^{-a_I(m_c)} \frac{f^{D \rightarrow \rho}(m_\rho)}{2\sqrt{m_\rho m_D}} = 0.45. \quad (63)$$

One also expects

$$2\alpha_s(m_b)^{-a_I(m_b)} \sqrt{m_\rho m_B} g^{B \rightarrow \rho} = 2\alpha_s(m_c)^{-a_I(m_c)} \sqrt{m_\rho m_D} g^{D \rightarrow \rho} \quad (64)$$

while our model predicts (once again at zero recoil)

$$2\alpha_s(m_b)^{-a_I(m_b)} \sqrt{m_\rho m_B} g^{B \rightarrow \rho}(m_\rho) = 1.16 \quad (65)$$

$$2\alpha_s(m_c)^{-a_I(m_c)} \sqrt{m_\rho m_D} g^{D \rightarrow \rho}(m_\rho) = 1.15. \quad (66)$$

The form factors f_+ and a_+ are more complex since it is the combinations $f_+ \pm f_-$ and $a_+ \pm a_-$ which obey simple scaling relations. However, since the objects which scale are $\sqrt{\frac{m_B}{m_\rho}}(f_+ + f_-)$, $\sqrt{\frac{m_\rho}{m_B}}(f_+ - f_-)$, $m_B \sqrt{\frac{m_B}{m_\rho}}(a_+ + a_-)$, and $\sqrt{m_B m_\rho}(a_+ - a_-)$, in the heavy quark limit $f_- = -f_+$ and $a_- = -a_+$ so that in fact the simple scaling laws

$$\alpha_s(m_b)^{-a_I(m_b)} \sqrt{\frac{m_\rho}{m_B}} f_+^{B \rightarrow \pi} = \alpha_s(m_c)^{-a_I(m_c)} \sqrt{\frac{m_\rho}{m_D}} f_+^{D \rightarrow \pi} \quad (67)$$

and

$$2\alpha_s(m_b)^{-a_I(m_b)} \sqrt{m_\rho m_B} a_+^{B \rightarrow \rho} = 2\alpha_s(m_c)^{-a_I(m_c)} \sqrt{m_\rho m_D} a_+^{D \rightarrow \rho} \quad (68)$$

emerge. Our model in fact gives

$$\alpha_s(m_b)^{-a_I(m_b)} \sqrt{\frac{m_\rho}{m_B}} f_+^{B \rightarrow \pi}(m_\pi) = 0.68 \quad (69)$$

$$\alpha_s(m_c)^{-a_I(m_c)} \sqrt{\frac{m_\rho}{m_D}} f_+^{D \rightarrow \pi}(m_\pi) = 0.66 \quad (70)$$

and

$$2\alpha_s(m_b)^{-a_I(m_b)} \sqrt{m_\rho m_B} a_+^{B \rightarrow \rho}(m_\rho) = -0.66 \quad (71)$$

$$2\alpha_s(m_c)^{-a_I(m_c)} \sqrt{m_\rho m_D} a_+^{D \rightarrow \rho}(m_\rho) = -0.60. \quad (72)$$

We conclude that our model strongly supports the conclusion that $1/m_Q$ effects will not obscure the extraction of V_{ub} for exclusive B decays via the scaling relations of Heavy Quark Symmetry so that the proposal [10] to do so appears to be sound. (It should be noted that in the case of $f_+^{B \rightarrow \pi}$ and $f_+^{D \rightarrow \pi}$, our quark model contributions at zero recoil must be supplemented by the B^* and D^* pole terms [46], respectively, before they may be compared to experiment. These pole terms carry with them large but known $1/m_Q$ effects related to the smallness of m_π relative to the $B^* - B$ and $D^* - D$ hyperfine splittings.)

Similar conclusions follow for the validity of relations between $c \rightarrow s$ and $b \rightarrow s$ matrix elements which enter into the prediction of exclusive $b \rightarrow s\gamma$ decays.

VI. COMPARISON TO EXPERIMENT

A. Magnetic Dipole Decays

Magnetic dipole decays of mesons like $\omega \rightarrow \pi\gamma$, $K^* \rightarrow K\gamma$, and $\psi \rightarrow \eta_c\gamma$ proceed through a transition magnetic dipole moment form factor which is precisely analogous to the vector current form factor g in weak decays of ground state pseudoscalar mesons to ground state vector mesons. The ability of our model to describe such decays is therefore relevant to the reliability of the model for the weak decays which are the focus of this paper. For the transition magnetic dipole moment $\mu_{PV} = \mu_{VP}$ underlying the transition $V \rightarrow P\gamma$ (or $P \rightarrow V\gamma$ when it is energetically allowed), theory (experiment [33]) gives, in units of the nucleon magneton, $\mu_{\pi\rho} = 0.52$ (0.69 ± 0.04), $\mu_{\pi\omega} = 1.56$ (2.19 ± 0.09), $\mu_{\pi\phi} = 0.07$ (0.13 ± 0.01), $\mu_{\eta\rho} = 2.16$ (1.77 ± 0.17), $\mu_{\eta\omega} = 0.68$ (0.57 ± 0.07), $\mu_{\eta\phi} = 0.61$ (0.66 ± 0.02), $\mu_{\rho\eta'} = 1.53$ (1.20 ± 0.08), $\mu_{\omega\eta'} = 0.58$ (0.42 ± 0.04), $\mu_{\eta'\phi} = -0.94$ ($|\mu_{\eta'\phi}| < 1.8$), $\mu_{K+K^{*+}} = 0.95$ (0.79 ± 0.03), $\mu_{K^0K^{*0}} = -1.27$ (-0.98 ± 0.26), and $\mu_{\eta_c\psi} = 0.76$ (0.55 ± 0.12). As in the main calculations we have taken the pseudoscalar mixing angle here to be -20° ; we have also assumed that the vector mixing angle is 39° .

We conclude from this comparison that the quark model will probably be able to predict the form factor g with the typical quark model accuracy of $\pm 25\%$ for transitions involving light quarks. Since Heavy Quark Symmetry guarantees that our formulas for g will be correct in the heavy quark limit, this should be an upper bound to the probable error in such predictions.

B. $K \rightarrow \pi \ell \bar{\nu}_\ell$

Although the form factors for these decays are usually referred to the $SU(3)$ symmetry normalization point $t = 0$, we prefer to refer them to the point $t = t_m$ where Heavy Quark Symmetry will develop. We find that $f_+(t_m) = 1.04$ and $f_-/f_+ = -0.28$. The latter is in reasonable agreement with the measured value [33] though there is a substantial uncertainty

since K^\pm decay gives $f_-/f_+ = -0.35 \pm 0.15$ while K_L^0 decay gives -0.11 ± 0.09 . Our equation for f_+ is consistent with the Ademollo-Gatto theorem [47] which protects f_+ from substantial deviations from unity. Our prediction for $f_+(t)$ can be compared with the “standard” [48,49] used to extract V_{us} from these decays. If we convert to the linearized form $f_+(t) = f_+(0)[1 + \frac{1}{6}r_{\pi K}^2 t]$, then we predict $f_+(0) = 0.93$ and $r_{\pi K} = 0.48 \text{ fm}$ versus the “standard” [49] $f_+(0) = 0.97 \pm 0.01$ and $r_{\pi K} = 0.53 \text{ fm}$ corresponding to K^* pole dominance. The best current fit value to this transition radius gives [33] $r_{\pi K} = 0.59 \pm 0.02 \text{ fm}$.

C. Meson Decays through $b \rightarrow c\ell\bar{\nu}_\ell$

Our results for semileptonic meson decays involving the quark level decay $b \rightarrow c\ell\bar{\nu}_\ell$ were given in Section IV.A. Their relatively low recoil and heavy quark masses provide a theoretical stability that makes them our most reliable predictions.

Reviews of the experimental status of semileptonic B meson decays can be found in Refs. [19]. From the measured rate (here we use the latest CLEO result [21])

$$\Gamma(B \rightarrow D^* \ell \bar{\nu}_\ell) = 2.99 \pm 0.39 \times 10^{10} \text{ sec}^{-1}, \quad (73)$$

and our prediction $\Gamma(B \rightarrow D^* \ell \bar{\nu}_\ell) = 2.48 \times 10^{13} |V_{cb}|^2 \text{ sec}^{-1}$ we obtain

$$|V_{cb}| = 0.035 \pm 0.002. \quad (74)$$

The measured rate for $\bar{B} \rightarrow D \ell \bar{\nu}_\ell$ is

$$\Gamma(\bar{B} \rightarrow D \ell \bar{\nu}_\ell) = 1.3 \pm 0.3 \times 10^{10} \text{ sec}^{-1}. \quad (75)$$

Using our predicted rate of $\Gamma(\bar{B} \rightarrow D \ell \bar{\nu}_\ell) = 1.19 \times 10^{13} |V_{cb}|^2 \text{ sec}^{-1}$ implies that

$$|V_{cb}| = 0.033 \pm 0.004. \quad (76)$$

The consistency between eqs. (74) and (76) of course means that the model correctly predicts the ratio of the rates to D and D^* . However, these determinations of $|V_{cb}|$ depend on the prediction of the recoil dependence of the relevant form factors and so have a theoretical

error of order 10%. A comparison with data near zero recoil using Heavy Quark Symmetry, as has become standard, remains the reliable way to determine $|V_{cb}|$.

The measurements of Γ_L/Γ_T for $B \rightarrow D^* e \bar{\nu}_e$ are quite sensitive to the relative importance of the f , g , and a_+ form factors. Experiment gives

$$\frac{\Gamma_L}{\Gamma_T} = \begin{cases} 0.85 \pm 0.45 \text{ (ARGUS [21])} \\ 0.83 \pm 0.33 \pm 0.13 \text{ (CLEO [21])} \\ 1.24 \pm 0.16 \text{ (CLEO [50])} \end{cases} \quad (77)$$

consistent with our prediction of 1.04 (versus 0.97 for ISGW). Furthermore, the predictions of both ISGW and ISGW2 for the q^2 dependence of $\bar{B}^0 \rightarrow D^{*+} \ell \bar{\nu}_\ell$ agrees reasonably well with the measured results: see Refs. [19]. In particular, we predict that the slope of the preasymptotic Isgur-Wise function $\xi_{D^*\bar{B}}(w)$ will be $\rho_{D^*\bar{B}}^2 = 0.74 \pm 0.05$ (see the text below eq. (60) for an explanation of the theoretical error), while the latest fits to the data (see the last of Refs. [21]) give for the closely related quantity $\hat{\rho}^2$ the value 0.84 ± 0.14 . (The ISGW prediction was 0.69.) Table IX shows our predictions for the individual form factors in terms of the HQS form factors defined in Section V. It also compares them with the predictions of ISGW, Heavy Quark Symmetry, and HQET (with matching but no $1/m_Q$ corrections). This comparison illustrates the relatively model-independent nature of these predictions. A recent measurement [50] gives for $\bar{B} \rightarrow D^* \ell \bar{\nu}_\ell$ decay

$$\frac{g}{f} = 0.031 \pm 0.009(stat) \pm 0.004(syst) \text{ GeV}^{-2} \quad (78)$$

$$\frac{a_+}{f} = -0.015 \pm 0.006(stat) \pm 0.003(syst) \text{ GeV}^{-2} \quad (79)$$

in reasonable agreement with our predictions of 0.030 GeV^{-2} and -0.024 GeV^{-2} , respectively.

Both CLEO and ARGUS currently find indications that the D and D^* final states account for much less than all of the semileptonic decay width of the \bar{B} meson. We predict that these final states account for $\simeq 90\%$ of the total rate to the states included in our

calculation. If confirmed, these experimental results may indicate that non-resonant processes are important, or, perhaps, that we have underestimated the effects of the 1P and 2S states. Note that the Bjorken sum rule [9] requires that the rate missing from the D and D^* channels be approximately proportional to ρ^2 . Thus doubling the missing rate would require doubling ρ^2 , in apparent contradiction to the existing agreement between theory and experiment described above.

Finally we note that the decays of the \bar{B}_d , \bar{B}_s , and \bar{B}_c sequence show a marked departure from the spectator approximation in which their inclusive semileptonic decay rates would all be equal. This phenomenon, which is more pronounced in the $c \rightarrow s$ decays, is addressed in the next subsection.

D. Meson Decays through $c \rightarrow s\ell^+\nu_\ell$

The quark level decays $c \rightarrow s\ell^+\nu_\ell$ are at this time better measured than the $b \rightarrow c\ell\bar{\nu}_\ell$ decays. They also provide a greater challenge for our model since in these decays Heavy Quark Symmetry does not guarantee the success of the leading approximation to their form factors: strange quarks do not qualify as heavy quarks! Note that since the CKM matrix element $|V_{sc}|$ may be related to $|V_{ud}|$ *via* the unitarity of the CKM matrix, direct measurements of the form factors can be made. The experimental status of weak charmed meson decays was recently reviewed in Refs. [23].

Averaging over measurements [24] and using isospin gives [23]

$$\Gamma(D \rightarrow \bar{K}\ell\nu_\ell) = 9.0 \pm 0.5 \times 10^{10} \text{ sec}^{-1} \quad (80)$$

which compares reasonably well to our prediction of

$$\Gamma(D \rightarrow K\ell^+\nu_\ell) = 10.0 \times 10^{10} \text{ sec}^{-1}. \quad (81)$$

In this decay one can also measure the pole mass for the f_+ form factor assuming a monopole shape. CLEO obtains $M_{\text{pole}}^{f_+} = 2.00 \pm 0.12 \pm 0.18 \text{ GeV}$, consistent with earlier experiments but

with smaller errors. This mass corresponds to a transition radius $r_{KD} = \frac{\sqrt{6}}{M_{\text{pole}}^{f_+}} = 0.24 \pm 0.03$ fm compared to our prediction of 0.22 fm . The data cannot currently distinguish between the common choices (monopole, dipole, exponential) for the shape of this form factor as the available range of $t_m - t$ is limited and all these shapes give an approximately linear dependence over this range.

Assuming the measured form factor, the rate may be transformed [23] into a measurement of

$$f_+(t_m) = 1.42 \pm 0.25 \tag{82}$$

(or equivalently $f_+(0) = 0.75 \pm 0.03$). We predict $f_+(t_m) = 1.23$ (or equivalently $f_+(0) = 0.85$ using our predicted t dependence and 0.80 using our form factor with the central experimental value of r_{KD}).

As an aside, we would like to explain why such form factor measurements should be referred to $t = t_m$ and not $t = 0$. Heavy Quark Symmetry establishes that heavy to light transition form factors are all related in the region of t_m [4,10], *i.e.*, are independent of the heavy quark mass m_Q as $m_Q \rightarrow \infty$ when scaled by an appropriate power of m_Q . Measurements near t_m are therefore determinations of universal transition form factors (up to $1/m_Q$ corrections). Form factors at $t = 0$ are, in contrast, “random numbers” since they are the product of the universal transition amplitudes relevant at t_m and a complicated dynamical function which depends on the microscopic details of the high momentum tails of the initial and final state wavefunctions. This is because $t = 0$ corresponds to a final state X recoiling with *maximum* three momentum $|\vec{p}_X| = \frac{m_{P_Q}^2 - m_X^2}{2m_{P_Q}}$ in the rest frame of P_Q . This momentum increases with m_Q so that $t = 0$ form factors are ever-decreasing functions of m_Q .

The D meson semileptonic decay to the K^* final state has been the subject of much interest. An early measurement found a value for Γ_L/Γ_T approximately two times larger than expected while the ratio of vector to pseudoscalar branching ratios was about one half what was expected from many models. Attempts were made [25] to accommodate these results

within the ISGW model by allowing for the theoretical uncertainties inherent to the quark model ($\pm 20\%$). It was found that the model could accommodate the vector to pseudoscalar ratio but not the Γ_L/Γ_T ratio with such variations. The current experimental situation is more precise with at least two independent measurements of each quantity. In addition to the above quantities, measurements of the form factors themselves have now been made.

The averaged experimental measurements of Mark III, CLEO, E691, ARGUS, E653, and WA82 are [23]

$$\frac{\Gamma(D \rightarrow K^* e^+ \nu_e)}{\Gamma(D \rightarrow K e^+ \nu_e)} = 0.57 \pm 0.08 , \quad (83)$$

$$\Gamma(D \rightarrow K^* e^+ \nu_e) = 5.1 \pm 0.5 \times 10^{10} \text{ sec}^{-1} \quad (84)$$

and

$$\frac{\Gamma_L}{\Gamma_T} = 1.15 \pm 0.17 . \quad (85)$$

This compares reasonably well with our model values of

$$\frac{\Gamma(D \rightarrow K^* e^+ \nu_e)}{\Gamma(D \rightarrow K e^+ \nu_e)} = 0.54 \quad (86)$$

$$\Gamma(D \rightarrow K^* e^+ \nu_e) = 5.4 \times 10^{10} \text{ sec}^{-1} \quad (87)$$

and

$$\frac{\Gamma_L}{\Gamma_T} = 0.94 . \quad (88)$$

As anticipated in Ref. [25], agreement with the data relative to ISGW has come about *via* a modest shift in the form factor f . In fact, *four* different effects contribute: the matching conditions lower $f(t_m)$ by 11%, C_f from Table I lowers it by about 7%, the wavefunction mismatch induced by hyperfine effects (see Table A2) decreases $f(t_m)$ by another 7%, while the new factor of $\frac{1}{2}(1+w)$ raises the average of the amplitude over the Dalitz plot by about 7%. For this decay the form factors themselves have been determined. The comparison

of our predictions to the measured results [23] are given in Table X. Before leaving these decays, we note that (if we subtract our predicted Cabibbo-suppressed rate) the inclusive Cabibbo-allowed D semileptonic decay rate is measured [33] to be $(16.2 \pm 1.5) \times 10^{10} \text{sec}^{-1}$. This compares favorably with our prediction of $15.8 \times 10^{10} \text{sec}^{-1}$.

Our predictions for the analogous form factors for $D_s \rightarrow \phi e^+ \nu_e$ are

$$\begin{aligned} f(t_m) &= +2.03 \text{ GeV} \\ g(t_m) &= +0.52 \text{ GeV}^{-1} \\ a_+(t_m) &= -0.29 \text{ GeV}^{-1}. \end{aligned} \tag{89}$$

These results are in reasonably good agreement with recent measurements [51] which give (see Ref. [50]) $g(t_m)/f(t_m) = (+0.20 \pm 0.07) \text{ GeV}^{-2}$ and $a_+(t_m)/f(t_m) = (-0.21 \pm 0.05) \text{ GeV}^{-2}$ to be compared with our predictions for these ratios of $+0.26 \text{ GeV}^{-2}$ and -0.14 GeV^{-2} , respectively. CLEO [51] also quotes $\Gamma(D_s \rightarrow \eta e^+ \nu_e)/\Gamma(D_s \rightarrow \phi e^+ \nu_e) = 1.7 \pm 0.4$ and $\Gamma(D_s \rightarrow \eta' e^+ \nu_e)/\Gamma(D_s \rightarrow \phi e^+ \nu_e) = 0.7 \pm 0.2$ to be compared with our predictions of 0.8 and 0.7, respectively, for a pseudoscalar mixing angle of -20° , and 1.2 and 0.5, respectively, for -10° .

Ref. [51] also presents an extraction of the rate $\Gamma(D_s \rightarrow \phi e^+ \nu_e)$ based, among other things, on the assumption that the *inclusive* semileptonic decay rates of the D and D_s are equal. This assumption would appear to be justified on the basis of recent work on the $1/m_Q$ expansion of inclusive heavy quark semileptonic decays [52-55]. However, it is inconsistent with the results quoted here, which predict that $\Gamma(D_s \rightarrow X e^+ \nu_e)$ is 27% smaller than $\Gamma(D \rightarrow X e^+ \nu_e)$, largely as a consequence of the restricted phase space in the η' decay of the D_s . We speculate that the unexpectedly [55] large corrections we predict arise from an inapplicability of the assumptions under which the strong version of the results of Ref. [52] were derived: since these decays (along with those induced by the $b \rightarrow c$ transition) are dominated by the lowest few resonances, the spectral decomposition of the decay is imperfectly described by the smooth partonic spectral function. (As explained by the authors of Ref. [52], this is analogous to R in e^+e^- annihilation being smooth and well-approximated by its partonic value only well above a threshold. We note that heavy quark semileptonic decays can be

deceptive in regard to when they are “well above a threshold” because, while the recoil mass can kinematically run up to the mass of the decaying quark, the hadronic spectrum in $Q \rightarrow q\ell\bar{\nu}_\ell$ in fact cuts off at a recoil mass-squared only of order $\Lambda_{QCD}(m_Q - m_q)^2/m_Q \ll m_Q^2$ above threshold in the decay of a $Q\bar{d}$ meson.) With the assumptions made, Ref. [51] obtains $\Gamma(D_s \rightarrow \phi e^+\nu_e) = (4.4 \pm 0.7) \times 10^{10} \text{ sec}^{-1}$; if their assumptions are modified to correspond to our predictions from Table III for the ratio of inclusive rates and for the degree to which $\Gamma(D_s \rightarrow (\eta + \eta' + \phi)e^+\nu_e)$ saturates $\Gamma(D_s \rightarrow X e^+\nu_e)$, this extracted rate would be changed to $(3.5 \pm 0.5) \times 10^{10} \text{ sec}^{-1}$. These results are both roughly consistent with our prediction that $\Gamma(D_s \rightarrow \phi e^+\nu_e) = 4.6 \times 10^{10} \text{ sec}^{-1}$.

E. Meson Decays through $c \rightarrow d\ell^+\nu_\ell$

The Cabibbo-suppressed charmed meson decays via the quark-level process $c \rightarrow d\ell^+\nu_\ell$ have taken on an enhanced importance recently. As described in Section V, Heavy Quark Symmetry relates the form factors for such decays near $t = t_m$ to their analogues induced by the crucial $b \rightarrow u\ell\bar{\nu}_\ell$ processes. In the short term the better measured $c \rightarrow s\ell^+\nu_\ell$ processes, combined with $SU(3)$ flavor symmetry, can substitute for these decays, but precision determinations of $|V_{ub}|$ will probably require accurate determinations of the Cabibbo-suppressed form factors.

Experimental studies of such decays have begun. The decays $D^0 \rightarrow \pi^- e^+\nu_e$ and $D^+ \rightarrow \pi^0 e^+\nu_e$ have been measured by Mark III and CLEO II, respectively [24]. Using the value of $|V_{cd}/V_{sc}| \simeq 0.227 \pm 0.003$ which follows from CKM unitarity [33], their quoted results can be translated into the form

$$\frac{f_+^{D \rightarrow \pi}(0)}{f_+^{D \rightarrow \bar{K}}(0)} = 1.17 \pm 0.19 \quad (90)$$

where a pole model for the t -dependence of the form factors has been assumed in the determination of the numerical factor, and we have averaged the results of the two experiments. Our model predicts the value 0.71 for this ratio.

F. Meson Decays through $b \rightarrow ul\bar{\nu}_\ell$

Our results for semileptonic meson decays involving the quark level decay process $b \rightarrow ul\bar{\nu}_\ell$ were presented above. Only the decays with a light spectator have been observed. Both CLEO [20] and ARGUS [20] have observed leptons in the 2.4–2.6 GeV energy range that can be populated only by leptons from a $b \rightarrow ul\bar{\nu}_\ell$ process. In addition, searches for exclusive modes like $\bar{B} \rightarrow \pi l\bar{\nu}_\ell$, $\bar{B} \rightarrow \omega l\bar{\nu}_\ell$, and $\bar{B} \rightarrow \rho l\bar{\nu}_\ell$ have begun.

The extraction of $|V_{ub}|$ from these data is based on kinematics. For \bar{B} mesons produced at the $\Upsilon(4S)$ resonance, decays via the quark level process $b \rightarrow cl\bar{\nu}_\ell$ have a maximum lepton energy of 2.4 GeV/c, while the leptons from a $b \rightarrow ul\bar{\nu}_\ell$ process may have energies up to 2.6 GeV/c. Consequently, these inclusive decay processes can be unravelled in the endpoint region of the lepton spectrum.

As previously mentioned, the physics of this endpoint region has been the subject of intense discussion [56]. The ISGW papers met with strong criticism by many who argued that its treatment of the endpoint region was inconsistent with the parton model. This issue has recently been clarified in favor of ISGW by rigorous $1/m_Q$ expansions of the inclusive rate. The zeroth order argument was given in Ref. [57]. It is shown there how, in a $b \rightarrow ul\bar{\nu}_\ell$ transition, the zeroth order lepton spectrum is controlled by quark level kinematics. The key observation is that decays to low mass *hadronic* final states (in this approximation, the hadronic mass is just the invariant mass of the recoiling u quark and the noninteracting spectator quark) only populate the high t (low recoil) region of their Dalitz plot which therefore cuts off their electron spectrum at the quark level endpoint energy. Thus while from kinematics alone such decays might have produced electrons with energies out to the physical (*i.e.* hadronic) endpoint, they do not for dynamical reasons. Conversely, high mass hadronic final states produce electrons out to their kinematic endpoint, but the highest mass hadrons have an endpoint which exactly coincides with the quark level endpoint in zeroth order. Recent work [52,53] has demonstrated that this picture is the beginning of a rigorous $1/m_Q$ expansion of inclusive decays, and that the $1/m_Q$ corrections have exactly

the character anticipated by ISGW and Ref. [57] and continued in this work.

It has very recently been speculated that, within the $1/m_Q$ expansion, even the endpoint region is amenable to treatment *via* an operator product analysis [54]. If, as indicated by Fig. 10(a), this region is really dominated by a few resonances (mainly the ρ , a_1 , and b_1), then this analysis may not apply. Thus while for $b \rightarrow u$ decays, in contrast to $c \rightarrow s$ and $b \rightarrow c$ decays, the hadronic spectral function over most of the Dalitz plot will be well-approximated by the partonic spectral function (corresponding to strong applicability of the results of Ref. [52]), the endpoint region is only dual to the partonic spectral function in an average sense.

The experimental analysis of this data requires simultaneous fits to the $b \rightarrow c \ell \bar{\nu}_\ell$ and $b \rightarrow u \ell \bar{\nu}_\ell$ inclusive spectra combined with the measured continuum backgrounds. Consequently, it is not possible to simply convert the values determined by various experiments which have used the ISGW model to the modified version of the model presented here, since the results are dependent upon the shape as well as the integrated inclusive rate. Since our spectrum is considerably harder than that of ISGW, it seems clear that the ISGW value of $|V_{ub}/V_{cb}|$ will decrease when reanalyzed. However, the change seems unlikely to be very large. While the rate to the ρ , which is most important in the extreme endpoint, has increased by 70%, the total rate to the states we consider has only increased by 23%. Given that these rates are proportional to $|V_{ub}|^2$, the decrease in $|V_{ub}/V_{cb}|$ itself seems likely to be less than 25%.

We would like to caution against interpreting this decrease, which brings ISGW into better agreement with other models of the endpoint region [58], as leading to a more reliable value for $|V_{ub}|$ from the inclusive spectrum. In the first place, it is a mistake to use models for this region which consider only the π and ρ final states: the endpoint region is clearly going to be populated by many more states than these. This exclusion leaves only ACCMM [11] and ISGW as potentially realistic models for this region. However, we would continue to stress, in spite of the real improvements of ISGW2, that our theoretical errors here are of order $\pm 50\%$. The recent clarification [53-55] of the status of the ACCMM calculation [11] in this region suggests that it should be assigned a very substantial theoretical error as well.

VII. CONCLUSIONS

We would argue that ISGW was already a good model for heavy meson semileptonic decay, and that with the improvements added here ISGW2 is an even better model for this sector. ISGW2 behaves correctly in the Heavy Quark Symmetry and Shifman-Voloshin limits, including lowest order corrections to these limits. In taking into account the leading corrections to the Heavy Quark Symmetry limit, ISGW2 adds physics to ISGW which corresponds to that demanded by Heavy Quark Effective Theory. These corrections are implemented with a well-known, and well-tuned, model of quark dynamics.

In order to extend the range of validity of the model and to include all relevant physics, ISGW2 also adds to ISGW other effects. These extensions have improved our agreement with the experimental data. For example, the mesonic decay rate for $P \rightarrow V \ell \bar{\nu}_\ell$, where P and V are pseudoscalar and vector mesons, respectively, is sensitive to the S-wave axial current form factor. This form factor probably receives sizable relativistic corrections (of order 10%) which we have attempted to take into account. The motivation for such extensions comes not only from first principles: in this case, such a correction is needed in the quark model to understand g_A in neutron beta decay.

Given these points, the extraction of $|V_{cb}|$ from the measurements of $\Gamma(\bar{B} \rightarrow D e \bar{\nu}_e)$, and $\Gamma(\bar{B} \rightarrow D^* e \bar{\nu}_e)$ should be reliable. Ultimately, a precise determination of $|V_{cb}|$ will come from a careful consideration of the heavy quark limit in which models like this one have been used to estimate $1/m_q$ and $1/m_Q$ corrections.

The determination of $|V_{ub}|$ is important for understanding CP violation in the standard model, since it is vital for determining the area of the “unitarity triangle” to which standard model CP violation is proportional. In most decays considered in this paper the model dependence of our results is modest. The $b \rightarrow u e \bar{\nu}_e$ decays are, however, an exception. The large available recoil, the relativistic nature of the π and ρ , and the fact that such decays are far from any symmetry limits leave these predictions very exposed to uncertainties. We estimate that the theoretical uncertainties within our model for extracting $|V_{ub}/V_{cb}|$ from

the inclusive endpoint spectrum are at the 50% level. The uncertainties associated with individual exclusive channels are even larger: we would estimate them to be almost a factor of two for $\bar{B} \rightarrow \pi \ell \bar{\nu}_\ell$ (where our model uncertainties are compounded by the uncertain effects of the nearby \bar{B}^* pole [46]) and 50% for $\bar{B} \rightarrow \rho \ell \bar{\nu}_\ell$ and $\bar{B} \rightarrow \omega \ell \bar{\nu}_\ell$. Fortunately, the determination of $|V_{ub}|$ can be greatly improved by combining the observation of exclusive \bar{B} decays with their analogous D decays since such measurements can be related by Heavy Quark Symmetry. Here, once again, a model like ISGW2 has an important role to play, since it can assess the size of symmetry-breaking effects in this procedure. As we showed in Section V, our model predicts that this technique should allow the extraction of $|V_{ub}|$ with a theoretical error of about 10%.

ACKNOWLEDGEMENTS

In the first instance we would like to thank our coauthors in ISGW, Benjamin Grinstein and Mark Wise, for their encouragement in producing this update to ISGW, as well as for innumerable discussions along the way. We are also grateful to many of our experimental colleagues for their interest in this work and for their many helpful comments; we would especially like to acknowledge conversations with Marina Artuso, Arne Freyberger, Douglas Potter, and Sheldon Stone, who significantly influenced the shape of this work.

REFERENCES

1. N. Isgur, D. Scora, B. Grinstein, and M. B. Wise, Phys. Rev. D **39**, 799 (1989).
2. B. Grinstein, M.B. Wise, and N. Isgur, Caltech Report No. CALT-68-1311, and University of Toronto Report No. UTPT-85-37, 1985 (unpublished).
3. B. Grinstein, M. B. Wise, and N. Isgur, Phys. Rev. Lett. **56**, 298 (1986).
4. N. Isgur and M.B. Wise, Phys. Lett. **B232** (1989) 113; Phys. Lett. **B237** (1990) 527. For an overview of Heavy Quark Symmetry see N. Isgur and M.B. Wise, “Heavy Quark Symmetry” in *B Decays*, ed. S. Stone (World Scientific, Singapore, 1991), p. 158, and in “*Heavy Flavors*”, ed. A.J. Buras and M. Lindner (World Scientific, Singapore, 1992), p. 234.
5. For some of the precursors to Heavy Quark Symmetry see, in addition to Refs. [1]-[3], M. B. Voloshin and M. A. Shifman, Yad. Fiz. **47**, 801 (1988); Sov. J. Nucl. Phys. **47**, 511 (1988); M. A. Shifman in *Proceedings of the 1987 International Symposium on Lepton and Photon Interactions at High Energies*, Hamburg, West Germany, 1987, edited by W. Bartel and R. Rückl, Nucl. Phys. B (Proc. Suppl.) **3**, 289 (1988); S. Nussinov and W. Wetzel, Phys. Rev. **D36**, 130 (1987); G.P. Lepage and B.A. Thacker, in *Field Theory on the Lattice*, edited by A. Billoire, Nucl. Phys. B (Proc. Suppl.) **4** (1988) 199; E. Eichten, in *Field Theory on the Lattice*, edited by A. Billoire, Nucl. Phys. B (Proc. Suppl.) **4**, (1988) 170; E. Shuryak, Phys. Lett. **B93**, 134 (1980); Nucl. Phys. **B198**, 83 (1982).
6. For an overview of Heavy Quark Effective Theory see the review cited in Ref. [4] and the references therein, especially H. Georgi, Phys. Lett. **B240** (1990) 447; E. Eichten and B. Hill, Phys. Lett. **B234** (1990) 511; M.B. Voloshin and M.A. Shifman, Sov. J. Nucl. Phys. **45** (1987) 463; H.D. Politzer and M.B. Wise, Phys. Lett. **B206** (1988) 681; Phys. Lett. **B208** (1988) 504; A.F. Falk, H. Georgi, B. Grinstein and M.B. Wise,

- Nucl. Phys. **B343**, 1 (1990); B. Grinstein, Nucl. Phys. **B339**, 253 (1990); M.B. Wise, “CP Violation” in *Particles and Fields 3: Proceedings of the Banff Summer Institute (CAP)* 1988, p. 124, edited by N. Kamal and F. Khanna, World Scientific (1989).
7. The phenomenological literature based on Heavy Quark Symmetry is too extensive for us to do more than quote some of the papers that have discussed issues related to those being addressed here. In particular, there have been a number of papers which have shared with us as one of their main goals the study of $1/m_Q$ effects using the quark model. C.O. Dib and F. Vera, Phys. Rev. **D47**, 3938 (1993) considered heavy-to-light transitions; J.F. Amundson, Phys. Rev. **D49**, 373 (1994) has considered the $\bar{B} \rightarrow D$ and $\bar{B} \rightarrow D^*$ decays. See also J.F. Amundson and J.L. Rosner, Phys. Rev. **D47**, 1951 (1993) for a model-independent discussion of the use of the $c \rightarrow s$ transition as a gauge of $1/m_Q$ effects. For related work on $1/m_Q$ effects in the QCD sum rule approach, see E. Bagan, P. Ball, V.M. Braun, and H.G. Dosch, Phys. Lett. **B278**, 457 (1992); M. Neubert, Phys. Rev. **D46**, 3914 (1993); M. Neubert, Z. Ligeti, and Y. Nir, Phys. Lett. **B301**, 101 (1993); Phys. Rev. **D47**, 5060 (1993). For a model based on the Schwinger-Dyson equation, see B. Holdom and M. Sutherland, Phys. Rev. **D47**, 5067 (1993).
8. We accordingly suggest that, when quoting the results presented here, reference be made to both this work *and* Ref. [1]. Some very preliminary results of ISGW2 have already been reported in D. Scora, “ D_s Semileptonic Decay in the Quark Model”, in *Particles and Nuclei, Proceedings of the Twelfth International Conference on Particles and Nuclei*, M.I.T., Cambridge, MA, USA, 1990, Nucl. Phys. **A527**, 743c (1991).
9. J.D. Bjorken, in Proceedings of the 4th Rencontre de Physique de la Vallée d’Aoste, La Thuile, Italy, 1990, ed. M. Greco (Editions Frontieres, Gif-sur-Yvette, France, 1990); J. D. Bjorken, *Recent Developments in Heavy Flavor Theory*, in Proceedings of the XXVth International Conference on High Energy Physics, Singapore, (World

- Scientific, Singapore, 1992); N. Isgur and M. B. Wise, Phys. Rev. D **43**, 819 (1991).
10. N. Isgur and M.B. Wise, Phys. Rev. **D42**, 2388 (1990).
 11. G. Altarelli, N. Cabibbo, G. Corbò, L. Maiani, and G. Martinelli, Nucl. Phys. B **208**, 365 (1982); N. Cabibbo, G. Corbò, and L. Maiani, Nucl. Phys. B **155**, 93 (1979).
 12. M.K. Gaillard, B.W. Lee, and J.L. Rosner, Rev. Mod. Phys. **47**, 277 (1975); J. Ellis, M.K. Gaillard, and D.V. Nanopoulos, Nucl. Phys. **B100**, 313 (1975); A. Ali and E. Pietarinen, Nucl. Phys. B **154**, 519 (1979).
 13. N. Cabibbo, Phys. Rev. Lett. **10**, 531 (1963); M. Kobayashi and K. Maskawa, Prog. Theor. Phys. **49**, 652 (1973).
 14. See, e.g., E.H. Thorndike, in Proceedings of the 1985 International Symposium at High Energies, Kyoto, Japan, 1985, ed. M. Konuma and K. Takahashi (Research Institute for Fundamental Physics, Kyoto University, 1986) p. 406.
 15. M.B. Voloshin and M.A. Shifman in Ref. [5].
 16. N. Isgur, Phys. Rev. D **40**, 101 (1989).
 17. N. Isgur and M. B. Wise, Phys. Rev. D **41**, 151 (1990); R. Jaffe, Phys. Lett. B **245**, 221 (1990); R. Jaffe and P. F. Mende, Nucl. Phys. B **369**, 189 (1992); B. Grinstein and P.F. Mende, Phys. Rev.Lett. **69**, 1018 (1992).
 18. C. Bebek et al., Phys. Rev. D **17**, 1693 (1978).
 19. The status of semileptonic B decays has recently been summarized by R.J. Morrison and J.D. Richman for the Particle Data Group in p. 1602-1609 of the *Review of Particle Properties*, Phys. Rev. **D50**, 1173 (1994). For other recent reviews, see D.Z. Besson in *Lepton and Photon Interactions*, proceedings of the XVI International Symposium, Ithaca, N.Y., ed. P. Drell and D. Rubin (AIP Conf. Proc. No. 302)(AIP, New York, 1994), p. 221; S. Stone, "Semileptonic B Decays – Experimental", in *B Decays*, edited

- by S. Stone (World Scientific, Singapore, 1991), p. 210. See Refs. [20-22] for many of the individual measurements of \bar{B} decay.
20. CLEO Collaboration, R. Fulton et al., Phys. Rev. Lett. **64**, 16 (1990) and J. Bartelt *et al.*, Phys. Rev. Lett. **71**, 4111 (1993); ARGUS Collaboration, H. Albrecht et al., Phys. Lett. B **234**, 409 (1990).
 21. In addition to Ref. [19], see CLEO Collaboration, R. Fulton et al., Phys. Rev. D **43**, 651 (1991); ARGUS Collaboration, H. Albrecht et al., Phys. Lett. B **219**, 121 (1989); Phys. Lett. **B229**, 175 (1985); Z. Phys. **C57**, 523 (1993); Phys. Lett. **B324**, 249 (1994); Phys. Lett. **B275**, 175 (1992); CLEO Collaboration, D. Bortoletto et al., Phys. Rev. Lett. **63**, 1667 (1989). For a recent CLEO measurement of $\bar{B} \rightarrow D^* \ell \nu_\ell$ decay see preprint CLNS94/1285 of June 1994, to appear in Physical Review **D**.
 22. ARGUS Collaboration, H. Albrecht et al., Phys. Lett. B **255**, 297 (1991); M. Danilov, *Heavy Flavour Physics (Non-LEP)*, presented at the 15th Int. Conf. on Lepton and Photon Interactions at High Energy, Geneva (1991); The CLEO Collaboration, A. Bean *et al.*, Phys. Rev. Lett. **70**, 2681 (1993) and as reported by D. Besson in Ref. [19].
 23. The status of semileptonic D decays has recently been summarized by R.J. Morrison and J.D. Richman for the Particle Data Group in p. 1565-1572 of the *Review of Particle Properties*, Phys. Rev. **D50**, 1173 (1994). For other recent reviews, see S. Stone, "Charmed Meson Decays", in *Heavy Flavours*, edited by A.J. Buras and H. Lindner (World Scientific, Singapore, 1992), p. 334; M. Witherell in *Lepton and Photon Interactions*, proceedings of the XVI International Symposium, Ithaca, N.Y., ed. P. Drell and D. Rubin (AIP Conf. Proc. No. 302)(AIP, New York, 1994), p. 198. See Refs. [24] for many of the individual measurements of D decay.
 24. The Mark III Collaboration, J. Adler et al., Phys. Rev. Lett. **62**, 1821 (1989); CLEO Collaboration, G. Crawford et al., Phys. Rev. D **44**, 3394 (1991); Tagged Photon

- Collaboration, J.C. Anjos et al., Phys. Rev. Lett. **62**, 1587 (1989); The Mark III Collaboration, Z. Bai et al., Phys. Rev. Lett. **66**, 1011 (1991); R. Wanke, diploma thesis and private communication from H. Schroder to S. Stone, see note 51 of the review by Stone quoted in Ref. [23]; E653 Collaboration, K. Kodama et al., Phys. Rev. Lett. **66**, 1819 (1991); Tagged Photon Collaboration, J.C. Anjos et al., Phys. Rev. Lett. **67**, 1507 (1991); ARGUS Collaboration, H. Albrecht et al., Phys. Lett. B **255**, 634 (1991); E653 Collaboration, K. Kodama et al., Phys. Lett. B **274**, 246 (1992); WA82 Collaboration, M. Adamovich et al., Phys. Lett. B **268**, 142 (1991); Tagged Photon Collaboration, J.C. Anjos et al., Phys. Rev. Lett. **65**, 2630 (1990); CLEO Collaboration, M.S. Alam *et al.*, Phys. Rev. Lett. **71**, 1311 (1993).
25. D. Scora and N. Isgur, Phys. Rev. D **40**, 1491 (1989).
26. N.N. Bogoliubov, Ann. Inst. Henri Poincaré **8**, 163 (1963); A. Le Yaouanc *et al.*, Phys. Rev. **D9**, 2636 (1974); **D15**, 844 (1977) and references therein; Michael J. Ruiz, *ibid.* **D12**, 2922 (1975); A. Chodos, R.L. Jaffe, K. Johnson, and C.B. Thorn, *ibid.* **D10**, 2599 (1974); P. Ditsas, N.A. McDougall, and R.G. Moorhouse, Nucl. Phys. **B146**, 191 (1978); J.S. Kang and J. Sucher, Phys. Rev. **D18**, 2698 (1978); R.K. Bhaduri, L.E. Cohler, and Y. Nogami, Phys. Rev. Lett. **44**, 1369 (1980).
27. C. Hayne and N. Isgur, Phys. Rev. D **25**, 1944 (1982); for some more recent related work, see S. Godfrey and N. Isgur, Phys. Rev. D **32**, 189 (1985); P. J. O'Donnell and H. K. K. Tung, Phys. Rev. D **44**, 741 (1991).
28. G. Karl, private communication.
29. See N. Isgur and M.B. Wise in Ref. [9].
30. N. Isgur and M.B. Wise, Phys. Rev. Lett. **66**, 1130 (1991).
31. The matching conditions first described in Refs. [6] were performed to leading logarithmic order, valid for $m_i \ll m_j$. A.F. Falk and B. Grinstein, Phys. Lett. **B247**,

406 (1990) and Phys. Lett. **B249**, 314 (1990), extended these results to matching corrections of order m_j/m_i and to the case of matching for $m_i \simeq m_j$. The matching problem has recently been addressed in a series of papers by Neubert and collaborators, and we adopt the general approach of these papers here. See M. Neubert, Phys. Rev. **D46**, 2212 (1992); Nucl. Phys. **B371**, 149 (1992); and references therein. In the first of these papers, matching is done up to corrections of order $\alpha_s^2(\frac{m_c}{m_b} \ln \frac{m_b}{m_c})^2$. Here we simplify and retain only the leading corrections as in the second paper quoted. The error inherent in this simplification is of order 5%, which is adequate for our purposes and readily improved upon when necessary.

32. A.F. Falk, Nucl. Phys. **B378**, 79 (1992).
33. Particle Data Group, Phys. Rev. **D50**, 1173 (1994).
34. *E.g.*, the axial current can be renormalized in the “classical” way by hadronic loop diagrams. For a very interesting recent approach to such effects, see S. Weinberg, Phys. Rev. Lett. **65**, 1181 (1990); Phys. Rev. Lett. **67**, 3473 (1991).
35. See S. Godfrey and N. Isgur in Ref. [27].
36. The CLEO Collaboration, preprint CLNS94/1266 and CLEO 94-1 (1994).
37. C.-H. Chang and Y.-Q. Chen, The production of B_c or \bar{B}_c meson associated with two heavy quark jets in Z^0 boson decay, Institute of Theoretical Physics, Academia Sinica, Beijing preprint AS-ITP-91-64.
38. E. Eichten and C. Quigg, Phys. Rev. **D49**, 5845 (1994).
39. There has been some confusion over the value of this ratio in our model. Phase space alone gives 0.80, which value has been quoted by CLEO in Phys. Rev. Lett. **65**, 1531 (1990). A typographical error in the manuscript copy of the contribution by D. Scora quoted in Ref. [8] gave a value of 1.08, which was corrected to 1.02

before publication, but still added to the confusion. This ratio is important because it is used to set the scale for all D_s decay rates using $\Gamma(D_s \rightarrow \phi e^+ \nu_e)/\Gamma(D_s \rightarrow \phi \pi)$, $\Gamma(D \rightarrow \bar{K}^* e^+ \nu_e)/\Gamma(D \rightarrow \bar{K} \pi \pi)$, and τ_{D_s}/τ_{D^+} to determine $\Gamma(D_s \rightarrow \phi \pi)$. For example, using our new prediction, the branching ratio for $\Gamma(D_s \rightarrow \phi \pi)$ presented in F. Butler *et al.*, Phys. Lett. **B324**, 255 (1994) becomes $4.3 \pm 0.3 \pm 0.3 \pm 0.6$ with a theoretical error which we estimate to be ± 0.4 .

40. See the work quoted in Ref. [7]; for related estimates of $1/m_Q$ effects using QCD Sum Rules see E. Bagan, P. Ball, V.M. Braun, and H.G. Dosch, Phys. Lett. **B278**, 457 (1992); M. Neubert, Phys. Rev. **D46**, 3914 (1993); M. Neubert, Z. Ligeti, and Y. Nir, Phys. Lett. **B301**, 101 (1993); Phys. Rev. **D47**, 5060 (1993); for a Nambu-Jona-Lasinio-like approach see B. Holdom and M. Sutherland, Phys. Rev. **D47**, 5067 (1993). For related work using lattice QCD, see the review by P.B. Mackenzie in *Lepton and Photon Interactions*, proceedings of the XVI International Symposium, Ithaca, N.Y., ed. P. Drell and D. Rubin (AIP Conf. Proc. No. 302)(AIP, New York, 1994), p.634.
41. The proof in Ref. [42] that certain predictions of Heavy Quark Symmetry are protected from first order corrections in $1/m_q$ and $1/m_Q$ (“Luke’s Theorem”) plays an important role in increasing the reliability of theory for the extraction of V_{cb} from experiment. It is very similar in physics content to the analogous theorem for extracting V_{us} from $\bar{K} \rightarrow \pi \ell \bar{\nu}_\ell$ from Ref. [47].
42. M. E. Luke, Phys. Lett. B **252**, 447 (1990).
43. H. Georgi, B. Grinstein, and M. B. Wise, Phys. Lett. B **252**, 456 (1990).
44. C. Boyd and D. Brahm, Phys. Lett. **B257**, 393 (1991).
45. M. Neubert and V. Rieckert, Nucl. Phys. **B382**, 97 (1992); A. Falk, M.E. Luke, and M. Neubert, Nucl. Phys. **B388**, 363 (1992).

46. N. Isgur and M.B. Wise, Phys. Rev. **D41**, 151 (1990); M.B. Wise, Phys. Rev. **D45**, 2188 (1992); G. Burdman and J.F. Donoghue, Phys. Lett. **B280**, 287 (1992); L. Wolfenstein, Phys. Lett. **B291**, 177 (1992); G. Burdman, Z. Ligeti, M. Neubert, and Y. Nir, Phys. Rev. **D49**, 2331 (1994); B. Grinstein and P.F. Mende, Phys. Rev. Lett. **69**, 1018 (1992) and preprint SMU-HEP/94-11 and UCSD/PTH 94-09.
47. M. Ademollo and R. Gatto, Phys. Rev. Lett. **13**, 264 (1964).
48. For an excellent review of the status of the determination of the CKM parameters, see J.L. Rosner, in *B Decays*, ed. S. Stone (World Scientific, Singapore, 1991), p. 312.
49. H. Leutwyler and M. Roos, Z. Phys. **C25**, 91 (1984).
50. The CLEO Collaboration, A. Ryd *et al.*, Proceedings of the APS/DPF Meeting, Albuquerque, August 1994; for an earlier result see S. Sanghera *et al.*, Phys. Rev. **D47**, 791 (1993). Note that these papers quote their results in terms of the form factors A_1 , V , and A_2 defined in K. Hagiwara, A. Martin, and M. Wade, Phys. Lett. B **228**, 144 (1989); M. Bauer and W. Wirbel, Z. Phys. C **42**, 671 (1989); F. J. Gilman and R. L. Singleton, Jr., Phys. Rev. D **41**, 142 (1990). These form factors are related to ours via $f = (m_{P_Q} + m_{V_q})A_1$, $g = (m_{P_Q} + m_{V_q})^{-1}V$, and $a_+ = -(m_{P_Q} + m_{V_q})^{-1}A_2$.
51. E653 Collaboration, K. Kodama *et al.*, Phys. Lett. **B316**, 455 (1993); E687 Collaboration, P.L. Frabetti *et al.*, Phys. Lett. **B313**, 253 (1993); CLEO Collaboration, P. Avery *et al.*, CNLS 94/1290, to appear in Phys. Lett. **B**. The quoted form factor ratios are based on our rough averaging of these three measurements.
52. J. Chay, H. Georgi, and B. Grinstein, Phys. Lett. **B247**, 399 (1990).
53. A.V. Manohar and M.B. Wise, Phys. Rev. **D49**, 1310 (1994); I.I. Bigi, M. Shifman, N.G. Uraltsev, and A.I. Vainshtein, Phys. Rev. Lett. **71**, 496 (1993); B. Blok, L. Koyrakh, M. Shifman, and A.I. Vainshtein, ITP Report No. NSF-ITP-93-68 (1993); T. Mannel, Nucl. Phys. **B413**, 396 (1994); I.I. Bigi, N.G. Uraltsev, and A.I. Vainshtein,

- Phys. Lett. **B293**, 430 (1992); A.F. Falk, M. Luke, and M.J. Savage, Phys. Rev. **D49**, 3367 (1994).
54. M. Neubert *et al.*, Phys. Rev. **D49**, 3392 (1994); Phys. Rev. **D49**, 4623 (1994).
55. M. Savage in Proceedings of “Intersections of Particle and Nuclear Physics”, St. Petersburg, Florida (1994).
56. See for examples of the discussion of the $b \rightarrow u$ endpoint problem C. Ramirez, J. F. Donoghue, and G. Burdman, Phys. Rev. **D41**, 1496 (1990); G. Altarelli and P. Franzini, in Conf. Proc. Vol. 15, *Present Trends, Concepts and Instruments of Particle Physics*, (Italian Phys. Soc., Bologna, 1988).
57. N. Isgur, Phys. Rev. **D47**, 2782 (1993).
58. M. Wirbel, B. Stech, and M. Bauer, Z. Phys. C **29**, 637 (1985); T. Altomari and L. Wolfenstein, Phys. Rev. Lett. **58**, 1583 (1987); T. Altomari and L. Wolfenstein, Phys. Rev. D **37**, 681 (1988); E. Golowich *et al.*, Phys. Lett. B **213**, 521 (1988); J. G. Körner and G. A. Schuler, Z. Phys. C **38**, 511 (1988); J. G. Körner and G. A. Schuler, **226**, 185 (1989); Xin-heng Guo and Tao Huang, Phys. Rev. D **43**, 2931 (1991); see also the three papers of Ref. [52].

APPENDIX A: hyperfine-corrected wavefunctions

Of the two leading order effects which break Heavy Quark Symmetry, the heavy quark kinetic energy and its hyperfine interaction, only the first was included in the constituent quark model which formed the basis of the ISGW prediction for form factors. In this Appendix we present a simple extension of their spectroscopic model which qualitatively takes hyperfine interactions into account.

The extended spectroscopic model remains a nonrelativistic constituent quark model with essentially the same Coulomb-plus-linear central potential:

$$V(r) = -\frac{4\alpha_s}{3r} + c + br \quad . \quad (91)$$

One cannot simply extend such a model by adding the non-relativistic hyperfine interaction since the Fermi spin-spin contact term, which is proportional to $\vec{S}_i \cdot \vec{S}_j \delta^3(\vec{r})$ is an illegal operator in the Schrodinger equation. The problem is that, in channels where it is attractive, this interaction is more singular than the kinetic energy so that the solutions of the Schrodinger equation collapse into $r_{ij} = 0$ and to infinitely negative energies. This problem is solved by relativistic corrections which turn this operator into an extended and nonlocal one. Here we model this behavior by taking

$$\bar{H}_{hyp}^{ij} = \left[\frac{m_i m_j}{E_i E_j}\right]^{\frac{1}{2}} \left(\frac{32\pi a \alpha_s \vec{S}_i \cdot \vec{S}_j \delta^3(\vec{r})}{9m_i m_j} \right) \left[\frac{m_i m_j}{E_i E_j}\right]^{\frac{1}{2}} \quad (92)$$

where the term in parentheses would be the ordinary Fermi contact term if the anomalous coupling coefficient a were unity, and where $E_i = (m_i^2 + p^2)^{\frac{1}{2}}$. We have examined the effects of smearing out $\delta^3(\vec{r})$ and found it to be small compared to the very strong nonlocality created by the pre- and postfactors of $\left[\frac{m_i m_j}{E_i E_j}\right]^{\frac{1}{2}}$. We have also ignored the tensor part of the hyperfine interaction as well as spin-orbit interactions. Neither can play a leading-order role in the S-waves which dominate our discussions, and both are also observed to be relatively weak even in excited states. Finally, we have made the running of α_s in ISGW slightly less crude by taking α_s for the ρ , K^* , ϕ , D^* , \bar{B} , D_s^* , \bar{B}_s^* , ψ , \bar{B}_c , and Υ families to be 0.60, 0.55,

0.55, 0.50, 0.50, 0.45, 0.40, 0.40, 0.35, and 0.30, respectively on the basis of their reduced masses. Note that, following Ref. [35] we assume α_s “freezes out” at 0.60 at low mass scales.

Also as in ISGW, we solve the Hamiltonian variationally in a basis of harmonic oscillator states truncated to include only the $1S$, $1P$ and $2S$ states. An interesting feature of this procedure, realized numerically in ISGW but thought to be an accident, is that the solution will exhibit zero $1S - 2S$ mixing. This is proved in Appendix B. As a result, we need only the diagonal matrix elements of p^2 , $1/r$, 1 , r , and $(A1)$ to solve for the wavefunctions. All but the last are trivial; for it one easily finds that the diagonal matrix elements all vanish except in the S-waves where

$$\langle n^{2s+1}S_{2s+1} | \bar{H}_{hy p} | n^{2s+1}S_{2s+1} \rangle = \left[\frac{2s(s+1) - 3}{4} \right] \left(\frac{32\pi a \alpha_s}{9m_i m_j} \right) |\bar{\psi}_{nS}(0)|^2 \quad (93)$$

with $s = 0$ or $s = 1$ the total quark-plus-antiquark spin,

$$\bar{\psi}_{nS}(0) = \frac{1}{(2\pi)^{3/2}} \int d^3p \left[\frac{m_i m_j}{E_i E_j} \right]^{\frac{1}{2}} \phi_{nS}(p) \quad (94)$$

with m_1 and m_2 the constituent quark and antiquark masses and $\phi_{nS}(p)$ the momentum space wavefunction. (Note that $\bar{\psi}_{nS}(0)$ reduces to the nonrelativistic spatial wavefunction at $\vec{r} = 0$ in the nonrelativistic limit).

On minimizing energies with respect to the gaussian wavefunction parameters β_i previously defined in ISGW and searching for a fit to the observed meson spectra, we found the results listed in Tables A1 and A2. We assume that defects like the $\rho - \pi$ splitting would improve with a larger basis space, but given the crude nature of this quasirelativistic model and our goal of a qualitative description of hyperfine effects, we do not attempt a better fit via a more complicated variant of the model. We also emphasize that full consistency would require a parallel relativistic treatment of both the spectrum and the weak matrix elements; this far more ambitious program would be very worthwhile, but it is well beyond the scope of this work.

APPENDIX B: variational solution in a 1S-2S basis

Let $\beta_S^{(0)}$ be the value of β_S which minimizes the full Hamiltonian in the harmonic oscillator ground state

$$\psi_{1S}^{(\beta_S)} = \frac{\beta_S^{3/2}}{\pi^{3/4}} e^{-\frac{1}{2}\beta_S^2 r^2}. \quad (95)$$

Thus

$$\frac{d}{d\beta_S} \int d^3r \psi_{1S}^{(\beta_S)} H(p, r) \psi_{1S}^{(\beta_S)} = 0 \quad (96)$$

for $\beta_S = \beta_S^{(0)}$. But

$$\frac{d}{d\beta_S} \psi_{1S}^{(\beta_S)} = \left(\frac{3}{2}\right)^{1/2} \beta_S^{-1} \psi_{2S}^{(\beta_S)} \quad (97)$$

since

$$\psi_{2S}^{(\beta_S)} = \left(\frac{2}{3}\right)^{1/2} \frac{\beta_S^{7/2}}{\pi^{3/4}} (r^2 - \frac{3}{2}\beta_S^{-2}) e^{-\frac{1}{2}\beta_S^2 r^2}. \quad (98)$$

Thus, if $\beta_S^{(0)}$ minimizes H,

$$\int d^3r \psi_{2S}^{(\beta_S^{(0)})} H \psi_{1S}^{(\beta_S^{(0)})} + \int d^3r \psi_{1S}^{(\beta_S^{(0)})} H \psi_{2S}^{(\beta_S^{(0)})} = 0. \quad (99)$$

But $\langle \psi_{1S}^{(\beta_S)} | H(p, r) | \psi_{2S}^{(\beta_S)} \rangle = \langle \psi_{2S}^{(\beta_S)} | H(p, r) | \psi_{1S}^{(\beta_S)} \rangle^*$ and both are real so

$$\langle \psi_{2S}^{(\beta_S^{(0)})} | H | \psi_{1S}^{(\beta_S^{(0)})} \rangle = 0 \quad (100)$$

i.e. ψ_{2S} does not mix with ψ_{1S} if it has been chosen variationally to minimize H. This argument can be extended; for example, ψ_{2P} does not mix with ψ_{1P} if it has been chosen variationally to minimize H.

APPENDIX C: form factor modifications for ISGW2

As described in the text, the formulas of Appendix B of ISGW (and of those additional formulas in Refs. [25] and [30] needed when the lepton mass cannot be neglected) require modification.

First, as discussed in Section III.C, all formulas are affected by the replacement in eq. (B1) of ISGW shown in eq. (20). In addition, the conversion from the \tilde{f}_i^{qm} to the f_i described in Section III.A introduces factors of $(\bar{m}_B/\tilde{m}_B)^{n_B(\alpha)}(\bar{m}_X/\tilde{m}_X)^{n_X(\alpha)}$ into each ISGW formula. With both of these changes effected, the factor F_n of eq. (B1) of ISGW is converted to a factor we denote by $F_n^{(\alpha)}$ since it now depends on the form factor α under consideration. The powers $n_B(\alpha)$ and $n_X(\alpha)$ required to make these conversions are given in Table C1. Note that in many instances it is a special combination (*e.g.*, $f_+ + f_-$) which has a simple mass scaling law and not the individual form factors (*e.g.*, f_+). For this reason we quote below formulas for these special combinations. To compute a particular form factor in such cases, one must apply the methods described here to those special combinations and then combine these results. Section III.A also describes how all S -wave to S -wave transition form factors must be modified by the matching conditions given in Section III.A. These corrections lead below to the appearance of the factors $R^{(\alpha)} \equiv \mathbf{C}_{ji}(1 + \tilde{\beta}^{(\alpha)}\alpha_s/\pi)$ (or, in the case of $a_+ + a_-$, to terms proportional to $\mathbf{C}_{ji}\tilde{\beta}^{(\alpha)}\alpha_s/\pi$) which are the coefficients of $\xi(w)$ in eq. (5). (In practice we use the “renormalization group improved” matching for all decays except those induced by the $s \rightarrow u$ transition for which we implement “lowest order matching”.)

In the following we employ the notation of ISGW augmented with \tilde{w} as identified by Eq. (3). As in ISGW, all formulas are given for the $b \rightarrow c$ transition but can be immediately adapted to any decay; see Ref. [1] for details including the explicit definition of each form factor. For an example, see eq. (103) below for the f form factor. The new formulas are:

1. Eqs. (B8) and (B9) are replaced by the two equations

$$f_+ + f_- = \left[2 - \frac{\tilde{m}_X}{m_q} \left(1 - \frac{m_d m_q}{2\mu_+ \tilde{m}_X} \frac{\beta_B^2}{\beta_{BX}^2} \right) \right] F_3^{(f_++f_-)} R^{(f_++f_-)} \quad (101)$$

$$f_+ - f_- = \frac{\tilde{m}_B}{m_q} \left(1 - \frac{m_d m_q}{2\mu_+ \tilde{m}_X} \frac{\beta_B^2}{\beta_{BX}^2} \right) F_3^{(f_+ - f_-)} R^{(f_+ - f_-)} \quad (102)$$

which determine both f_+ and f_- .

2. Eq. (B15) becomes

$$f = C_f \tilde{m}_B \left[(1 + \tilde{w}) + \frac{m_d(\tilde{w} - 1)}{2\mu_+} \right] F_3^{(f)} R^{(f)}. \quad (103)$$

The $(1 + \tilde{w})$ and $(\tilde{w} - 1)$ terms come from the constraints of Heavy Quark Symmetry in leading [4] and next-to-leading order [42-44], respectively, in the $1/m_Q$ expansion.

C_f is from Eq. (7), and $F_3^{(f)}$ is the modified factor F_3 described above, namely

$$F_3^{(f)} = (\bar{m}_X/\tilde{m}_X)^{\frac{1}{2}} (\bar{m}_B/\tilde{m}_B)^{\frac{1}{2}} \times (\tilde{m}_X/\tilde{m}_B)^{\frac{1}{2}} \left(\frac{\beta_X \beta_B}{\beta_{BX}^2} \right)^{\frac{3}{2}} \left[1 + \frac{1}{12} r_{XB}^2 (t_m - t) \right]^{-2}. \quad (104)$$

3. Eq. (B16) for g becomes

$$g = \frac{1}{2} \left[\frac{1}{m_q} - \frac{m_d \beta_B^2}{2\mu_- \tilde{m}_X \beta_{BX}^2} \right] F_3^{(g)} R^{(g)} \quad (105)$$

4. Eq. (B17) for a_+ is replaced by the two equations

$$a_+ + a_- = \mathbf{C}_{ji} \left[\frac{m_d}{(1 + \tilde{w}) m_q m_b} \frac{\beta_X^2}{\beta_{BX}^2} \left(1 - \frac{m_d}{2\tilde{m}_B} \frac{\beta_X^2}{\beta_{BX}^2} \right) + \tilde{\beta}^{(a_+ + a_-)} \frac{\alpha_s}{\pi} \tilde{m}_B \right] F_3^{(a_+ + a_-)} \quad (106)$$

$$a_+ - a_- = - \frac{1}{\tilde{m}_X} \left[\frac{\tilde{m}_B}{m_b} - \frac{m_d}{2\mu_+} \frac{\beta_X^2}{\beta_{BX}^2} + \frac{\tilde{w} m_d \tilde{m}_B}{(\tilde{w} + 1) m_q m_b} \frac{\beta_X^2}{\beta_{BX}^2} \left(1 - \frac{m_d}{2\tilde{m}_B} \frac{\beta_X^2}{\beta_{BX}^2} \right) \right] F_3^{(a_+ - a_-)} R^{(a_+ - a_-)}. \quad (107)$$

These formulas follow from ISGW and Ref. [25] with \tilde{w} -dependence dictated by the constraints of Heavy Quark Symmetry in order $1/m_Q$ [42-44]. They determine both a_+ and a_- .

5. Eq. (B23) for h becomes

$$h = \frac{m_d}{2\sqrt{2}\tilde{m}_B\beta_B} \left[\frac{1}{m_q} - \frac{m_d\beta_B^2}{2\mu_-\tilde{m}_X\beta_{BX}^2} \right] F_5^{(h)} . \quad (108)$$

6. Eq. (B24) for k becomes

$$k = \frac{m_d}{\sqrt{2}\beta_B} (1 + \tilde{w}) F_5^{(k)} . \quad (109)$$

7. Eq. (B25) for b_+ is replaced by the two equations

$$b_+ + b_- = \frac{m_d^2}{4\sqrt{2}m_q m_b \tilde{m}_B \beta_B} \frac{\beta_X^2}{\beta_{BX}^2} \left(1 - \frac{m_d}{2\tilde{m}_B} \frac{\beta_X^2}{\beta_{BX}^2} \right) F_5^{(b_++b_-)} \quad (110)$$

$$b_+ - b_- = - \frac{m_d}{\sqrt{2}m_b \tilde{m}_X \beta_B} \left[1 - \frac{m_d m_b}{2\mu_+ \tilde{m}_B} \frac{\beta_X^2}{\beta_{BX}^2} \right. \\ \left. + \frac{m_d}{4m_q} \frac{\beta_X^2}{\beta_{BX}^2} \left(1 - \frac{m_d}{2\tilde{m}_B} \frac{\beta_X^2}{\beta_{BX}^2} \right) \right] F_5^{(b_+-b_-)} \quad (111)$$

which determine both b_+ and b_- .

8. Eq. (B31) for q becomes

$$q = - \frac{m_d}{2\tilde{m}_X\beta_B} \left(\frac{5 + \tilde{w}}{6} \right) F_5^{(q)} . \quad (112)$$

See also eqs. (125) and (129) below.

See ref. [23] of ref. [29] for an explanation of the sign change.

9. Eq. (B32) becomes

$$\ell = -\tilde{m}_B\beta_B \left[\frac{1}{\mu_-} + \frac{m_d\tilde{m}_X(\tilde{w} - 1)}{\beta_B^2} \left(\frac{5 + \tilde{w}}{6m_q} - \frac{1}{2\mu_-} \frac{m_d}{\tilde{m}_X} \frac{\beta_B^2}{\beta_{BX}^2} \right) \right] F_5^{(\ell)} \quad (113)$$

See also eqs. (122) and (126) below.

10. Eq. (B33) for c_+ is replaced by the two equations

$$c_+ + c_- = -\frac{m_d \tilde{m}_X}{2m_q \tilde{m}_B \beta_B} \left(1 - \frac{m_d m_q}{2\tilde{m}_X \mu_-} \frac{\beta_B^2}{\beta_{BX}^2} \right) F_5^{(c_+ + c_-)} \quad (114)$$

$$c_+ - c_- = -\frac{m_d \tilde{m}_X}{2m_q \tilde{m}_B \beta_B} \left(\frac{\tilde{w} + 2}{3} - \frac{m_d m_q}{2\tilde{m}_X \mu_-} \frac{\beta_B^2}{\beta_{BX}^2} \right) F_5^{(c_+ - c_-)} \quad (115)$$

which determine both c_+ and c_- . See also eqs. (123), (124), (127), and (128) below.

11. Eq. (B37) for u_+ is replaced by the two equations

$$u_+ + u_- = -\sqrt{\frac{2}{3}} \frac{m_d}{\beta_B} F_5^{(u_+ + u_-)} \quad (116)$$

$$u_+ - u_- = \sqrt{\frac{2}{3}} \frac{m_d \tilde{m}_B}{\beta_B \tilde{m}_X} F_5^{(u_+ - u_-)} \quad (117)$$

which determine both u_+ and u_- .

12. Eq. (B43) for v becomes

$$v = \left[\frac{\tilde{m}_B \beta_B}{4\sqrt{2} m_b m_q \tilde{m}_X} + \frac{(\tilde{w} - 1)}{6\sqrt{2}} \frac{m_d}{\tilde{m}_X \beta_B} \right] F_5^{(v)} \quad (118)$$

See also eqs. (125) and (129) below.

13. Eq. (B44) for r becomes

$$r = \frac{\tilde{m}_B \beta_B}{\sqrt{2}} \left[\frac{1}{\mu_+} + \frac{m_d \tilde{m}_X}{3m_q \beta_B^2} (\tilde{w} - 1)^2 \right] F_5^{(r)} \quad (119)$$

See also eqs. (122) and (126) below.

14. Eq. (B45) for s_+ is replaced by the two equations

$$s_+ + s_- = \frac{m_d}{\sqrt{2} \tilde{m}_B \beta_B} \left(1 - \frac{m_d}{m_q} + \frac{m_d}{2\mu_+} \frac{\beta_B^2}{\beta_{BX}^2} \right) F_5^{(s_+ + s_-)} \quad (120)$$

$$s_+ - s_- = \frac{m_d}{\sqrt{2}m_q\beta_B} \left(\frac{4 - \tilde{w}}{3} - \frac{m_d m_q}{2\tilde{m}_X \mu_+} \frac{\beta_B^2}{\beta_{BX}^2} \right) F_5^{(s_+ - s_-)} \quad (121)$$

which determine both s_+ and s_- . See also eqs. (123), (124), (127), and (128) below.

15. Eq. (B49) for f'_+ is replaced by the two equations

$$f'_+ + f'_- = \sqrt{\frac{3}{2}} \left[\left(1 - \frac{m_d}{m_q}\right)U - \frac{m_d}{m_q}V \right] F_3^{(f'_+ + f'_-)} \quad (122)$$

$$f'_+ - f'_- = \sqrt{\frac{3}{2}} \frac{\tilde{m}_B}{m_q} \left[U + \frac{m_d}{\tilde{m}_X}V \right] F_3^{(f'_+ - f'_-)} \quad (123)$$

where

$$U = \frac{\beta_B^2 - \beta_X^2}{2\beta_{BX}^2} + \frac{\beta_B^2 \tau}{3\beta_{BX}^2} \quad (124)$$

$$V = \frac{\beta_B^2}{6\beta_{BX}^2} \left(1 + \frac{m_q}{m_b}\right) \left[7 - \frac{\beta_B^2}{\beta_{BX}^2} (5 + \tau) \right] . \quad (125)$$

and where

$$\tau \equiv \frac{m_d^2 \beta_X^2 (\tilde{w} - 1)}{\beta_B^2 \beta_{BX}^2} . \quad (126)$$

These equations determine both f'_+ and f'_- .

16. Eq. (B55) for f' becomes

$$f' = C_{f'} \sqrt{\frac{3}{2}} \tilde{m}_B (1 + \tilde{w}) U F_3^{(f')} \quad (127)$$

where U is given above.

17. Eq. (B16) for g' becomes

$$g' = \frac{1}{2} \sqrt{\frac{3}{2}} \left[\left(\frac{1}{m_q} - \frac{m_d \beta_B^2}{2\mu_- \tilde{m}_X \beta_{BX}^2} \right) U + \frac{m_d \beta_B^2 \beta_X^2}{3\mu_- \tilde{m}_X \beta_{BX}^4} \right] F_3^{(g')} \quad (128)$$

where once again U is given above.

18. Eq. (B17) for a'_+ is replaced by the two equations

$$a'_+ + a'_- = -\sqrt{\frac{2}{3}} \frac{\beta_B^2}{m_q m_b \beta_{BX}^2} \left\{ \frac{7m_d^2 \beta_X^4}{8\tilde{m}_B \beta_{BX}^4} \left[1 + \frac{1}{7}\tau\right] - \frac{5m_d \beta_X^2}{4\beta_{BX}^2} \left[1 + \frac{1}{5}\tau\right] - \frac{3m_d^2 \beta_X^4}{8\tilde{m}_B \beta_B^2 \beta_{BX}^2} + \frac{3m_d \beta_X^2}{4\beta_B^2} \right\} F_3^{(a'_+ + a'_-)} \quad (129)$$

$$a'_+ - a'_- = \sqrt{\frac{2}{3}} \frac{3\tilde{m}_B}{2m_b \tilde{m}_X} \left\{ 1 - \frac{\beta_B^2}{\beta_{BX}^2} \left[1 + \frac{1}{7}\tau\right] - \frac{m_d \beta_X^2}{2\tilde{m}_B \beta_{BX}^2} \left(1 - \frac{5\beta_B^2}{3\beta_{BX}^2} \left[1 + \frac{1}{5}\tau\right]\right) - \frac{7m_d^2 \beta_B^2 \beta_X^2}{12m_q \tilde{m}_B \beta_{BX}^4} \left(1 - \frac{\beta_X^2}{\beta_{BX}^2} + \frac{\beta_B^2 \tau}{7\beta_{BX}^2}\right) \right\} F_3^{(a'_+ - a'_-)} . \quad (130)$$

These formulas determine both a'_+ and a'_- .

For transitions to excited P-wave heavy quark systems, heavy quark symmetry tells us that the $L - S$ coupled states 3P_1 and 1P_1 which are appropriate to the light $I = 1$ and $I = 0$ sectors and to states of definite C parity should be replaced by the $j - j$ coupled states with $s_\ell^{\pi_\ell} = \frac{3}{2}^+$ and $\frac{1}{2}^+$. If we define form factors $\ell_{\frac{3}{2}, c_{+\frac{3}{2}}, c_{-\frac{3}{2}},$ and $q_{\frac{3}{2}}$ to be the exact analogs of $\ell, c_+, c_-,$ and q of equations (B26) and (B27) of ISGW but for the $s_\ell^{\pi_\ell} = \frac{3}{2}^+$ state with $J^P = 1^+,$ and a parallel set $\ell_{\frac{1}{2}}, c_{+\frac{1}{2}}, c_{-\frac{1}{2}},$ and $q_{\frac{1}{2}}$ for the $s_\ell^{\pi_\ell} = \frac{1}{2}^+$ state with $J^P = 1^+,$ then

$$\ell_{\frac{3}{2}} = -\frac{2\tilde{m}_B \beta_B}{\sqrt{3}} \left\{ \frac{1}{m_q} + \frac{\tilde{m}_X m_d (\tilde{w} - 1)}{2\beta_B^2} \left(\frac{\tilde{w} + 1}{2m_q} - \frac{m_d \beta_B^2}{2\mu_- \tilde{m}_X \beta_{BX}^2} \right) \right\} F_5^{(\ell_{\frac{3}{2}})} \quad (131)$$

$$c_{+\frac{3}{2}} + c_{-\frac{3}{2}} = -\frac{\sqrt{3}m_d}{2\beta_B \tilde{m}_B} \left[1 - \frac{m_d}{3m_q} - \frac{m_d \beta_B^2}{3\beta_{BX}^2} \left(\frac{1}{2\mu_-} - \frac{1}{\mu_+} \right) \right] F_5^{(c_{+\frac{3}{2}} + c_{-\frac{3}{2}})} \quad (132)$$

$$c_{+\frac{3}{2}} - c_{-\frac{3}{2}} = -\frac{m_d}{2\sqrt{3}\beta_B\tilde{m}_X} \left[\frac{(2-\tilde{w})\tilde{m}_X}{m_q} + \frac{m_d\beta_B^2}{\beta_{BX}^2} \left(\frac{1}{2\mu_-} - \frac{1}{\mu_+} \right) \right] F_5^{(c_{+\frac{3}{2}}-c_{-\frac{3}{2}})} \quad (133)$$

$$q_{\frac{3}{2}} = -\frac{1}{2\sqrt{3}} \left\{ \frac{1+\tilde{w}}{2} + \frac{\beta_B^2\tilde{m}_B}{2m_d m_q m_b} \right\} \frac{m_d}{\beta_b\tilde{m}_X} F_5^{(q_{\frac{3}{2}})} \quad (134)$$

and

$$\ell_{\frac{1}{2}} = \sqrt{\frac{2}{3}}\tilde{m}_B\beta_B \left\{ \frac{1}{2m_q} - \frac{3}{2m_b} + \frac{m_d\tilde{m}_X(\tilde{w}-1)}{\beta_B^2} \left[\frac{1}{m_q} - \frac{m_d\beta_B^2}{2\mu_-\tilde{m}_X\beta_{BX}^2} \right] \right\} F_5^{(\ell_{\frac{1}{2}})} \quad (135)$$

$$c_{+\frac{1}{2}} + c_{-\frac{1}{2}} = \frac{m_d^2\beta_X^2}{\sqrt{6}\tilde{m}_B m_q \beta_B \beta_{BX}^2} F_5^{(c_{+\frac{1}{2}}+c_{-\frac{1}{2}})} \quad (136)$$

$$c_{+\frac{1}{2}} - c_{-\frac{1}{2}} = -\sqrt{\frac{2}{3}} \frac{m_d}{\tilde{m}_X\beta_B} \left[1 + \frac{m_d\beta_X^2}{2m_q\beta_{BX}^2} \right] F_5^{(c_{+\frac{1}{2}}-c_{-\frac{1}{2}})} \quad (137)$$

$$q_{\frac{1}{2}} = \sqrt{\frac{1}{6}} \left\{ 1 - \frac{\beta_B^2\tilde{m}_B}{4m_d m_q m_b} \right\} \frac{m_d}{\beta_B\tilde{m}_X} F_5^{(q_{\frac{1}{2}})} \quad (138)$$

We use these latter formulas for decays to all heavy-light final states, including the kaons. Of course, to the extent that the $s_\ell^{\pi\ell} = \frac{3}{2}^+$ and $\frac{1}{2}^+$ multiplets are degenerate there formulas will give total rates to the two 1^+ states that are identical to the 3P_1 and 1P_1 formulas. However, the latter are needed to predict the rates to individual states, e.g., the rate for $\bar{B} \rightarrow D_1^{(\frac{3}{2})} \ell \bar{\nu}_\ell$.

Table I. Relativistic corrections to the f form factor

decay	C_f for 1S	C_f for 2S
$D \rightarrow \rho, \omega$	0.889	0.740
$D \rightarrow K^*$	0.928	0.782
$D_s \rightarrow K^*$	0.873	0.739
$D_s \rightarrow \phi$	0.911	0.773
$\bar{B} \rightarrow \rho, \omega$	0.905	0.776
$\bar{B} \rightarrow D^*$	0.989	0.929
$\bar{B}_s \rightarrow K^*$	0.892	0.781
$\bar{B}_s \rightarrow D_s^*$	0.984	0.924
$\bar{B}_c \rightarrow \bar{D}^*$	0.868	0.779
$\bar{B}_c \rightarrow \psi$	0.967	0.899

Table II. Exclusive partial widths for the $b \rightarrow c$ semileptonic decays, $\bar{B} \rightarrow X_{c\bar{d}} e \bar{\nu}_e$, $\bar{B}_s \rightarrow X_{c\bar{s}} e \bar{\nu}_e$ and $\bar{B}_c \rightarrow X_{c\bar{c}} e \bar{\nu}_e$, in units of $10^{13} |V_{bc}|^2 \text{sec}^{-1}$. The Heavy Quark Symmetry notation $n^{s\ell} L_J$ is used for the final states with unequal mass quarks ^{b)}. Also included are the physical meson masses used (in GeV), taken from Ref. [33] if possible; properties of unobserved or controversial states (given in parentheses) are taken from Ref. [35]. The masses of the decaying particles (in GeV) are 5.28, 5.38^{d)}, and (6.27).

X	$\bar{B}_d \rightarrow X_{c\bar{d}} e \bar{\nu}_e$		$\bar{B}_s \rightarrow X_{c\bar{s}} e \bar{\nu}_e$		$\bar{B}_c \rightarrow X_{c\bar{c}} e \bar{\nu}_e$	
	mass	partial width	mass	partial width	mass	partial width
$1^{\frac{1}{2}} S_0$	1.87	1.42	1.97	1.31	2.98	0.99
$1^{\frac{1}{2}} S_1$	2.01	2.81	2.11	2.49	3.10	1.57
$1^{\frac{3}{2}} P_2$	2.46	0.10	2.57 ^{c)}	0.14	3.56	0.12
$1^{\frac{3}{2}} P_1$	2.42	0.20	(2.54)	0.25	3.52 ^{b)}	0.21
$1^{\frac{1}{2}} P_1$	(2.49)	0.04	(2.57)	0.05	3.51 ^{b)}	0.08
$1^{\frac{1}{2}} P_0$	(2.40)	0.03	(2.48)	0.04	3.42	0.04
$2^{\frac{1}{2}} S_0$	(2.58)	0.00	(2.67)	0.01	(3.62)	0.07
$2^{\frac{1}{2}} S_1$	(2.64)	0.06	(2.73)	0.13	3.69	0.29
total		4.66		4.41		3.36

^{a)} The Γ_L/Γ_T values for these decays are 1.08, 1.03, and 0.88, respectively.

^{b)} We list $\bar{B}_c \rightarrow 1^1 P_1$ (*i.e.*, χ_{c1}) under $1^{\frac{3}{2}} P_1$ and $\bar{B}_c \rightarrow 1^3 P_1$ (*i.e.*, h_{c1}) under $1^{\frac{1}{2}} P_1$.

^{c)} See Ref. [36].

^{d)} See Ref. [37].

Table III. Exclusive partial widths for the $c \rightarrow s$ semileptonic decays, $D \rightarrow X_{s\bar{u}} e^+ \nu_e$, $D_s \rightarrow X_{s\bar{s}} e^+ \nu_e$ and $B_c \rightarrow X_{s\bar{b}} e^+ \nu_e$, in units of $10^{10} |V_{cs}|^2 \text{sec}^{-1}$. The Heavy Quark Symmetry notation $n^{s\ell} L_J$ is used for the final states with unequal mass quarks ^{c)}. Also included are the physical meson masses used (in GeV), taken from Ref.[33] if possible; properties of unobserved or controversial states (given in parentheses) are taken from Ref.[35]. The masses of the decaying particles (in GeV) are 1.87, 1.97, and (6.27), respectively.

X	$D \rightarrow X_{s\bar{u}} e^+ \nu_e$		$D_s \rightarrow X_{s\bar{s}} e^+ \nu_e$		$B_c \rightarrow X_{s\bar{b}} e^+ \nu_e$	
	mass	partial width	mass	partial width	mass	partial width
$1\frac{1}{2}S_0$	0.49	10.5	0.55 ^{b)}	3.7	5.38 ^{d)}	2.2
			0.96 ^{b)}	3.2		
$1\frac{1}{2}S_1^a)$	0.89	5.7	1.02	4.8	(5.45)	2.7
$1\frac{3}{2}P_2$	1.43	0.00	1.53	0.00	(5.88)	0.00
$1\frac{3}{2}P_1$	1.27	0.34	1.38 ^{c)}	0.27	(5.88)	0.06
$1\frac{1}{2}P_1$	1.40	0.00	1.51 ^{c)}	0.03	(5.88)	0.00
$1\frac{1}{2}P_0$	1.43	0.00	1.52	0.00	(5.88)	0.00
$2\frac{1}{2}S_0$	(1.45)	0.00	(1.63)	0.00	(5.98)	0.01
$2\frac{1}{2}S_1$	(1.58)	0.00	(1.69)	0.01	(6.01)	0.01
total		16.6		12.1		5.0

^{a)} The Γ_L/Γ_T values for these decays are 0.94, 0.96, and 1.03, respectively.

^{b)} We use the approximation of ideal mixing in $I = 0$ states in every sector except the ground state pseudoscalars where we assume an $\eta - \eta'$ mixing angle of -20° . If this mixing angle were changed to -10° , then the entries in the Table to η and η' would change to 5.6 and 2.4; note that while the individual rates change substantially, the total rate to these two states would only increase by about 16%.

^{c)} For $D_s \rightarrow X_{s\bar{s}}$ we list the rate to the 1^1P_1 under $1\frac{3}{2}P_1$ and that for the 1^3P_1 state under $1\frac{1}{2}P_1$.

^{d)} See Ref. [37].

Table IV. Exclusive partial widths for the $c \rightarrow d$ semileptonic decays $D^0 \rightarrow X_{d\bar{u}} e^+ \nu_e$ and $D_s \rightarrow X_{d\bar{s}} e^+ \nu_e$, in units of $10^{10} |V_{cd}|^2 \text{ sec}^{-1}$. Also included are the physical meson masses used (in GeV), taken from Ref. [33] if possible; properties of unobserved or controversial states (given in parentheses) are taken from Ref. [35]. The masses of the decaying particles (in GeV) are 1.87 and 1.97, respectively.

X	$D^0 \rightarrow X_{d\bar{u}} e^+ \nu_e$		$D_s^+ \rightarrow X_{d\bar{s}} e^+ \nu_e$	
	mass	partial width	mass	partial width
$1^1 S_0$	0.14	9.8	0.50	8.9
$1^3 S_1$ ^{a)}	0.77	4.9	0.89	4.4
$1^3 P_2$	1.32	0.01	1.43	0.01
$1^1 P_1$	1.23	0.52	1.27 ^{b)}	1.5
$1^3 P_1$	1.26	0.32	1.40 ^{b)}	0.01
$1^3 P_0$	1.30	0.00	1.43	0.00
$2^1 S_0$	1.30	0.02	(1.45)	0.04
$2^3 S_1$	(1.45)	0.03	(1.58)	0.03
total		15.6		14.9

^{a)} The Γ_L/Γ_T values for these decays are 0.67 and 0.76, respectively.

^{b)} We list the rate to the mainly $1^{\frac{3}{2}} P_1$ state under $1^1 P_1$ and that for the mainly $1^{\frac{1}{2}} P_1$ under $1^3 P_1$ state.

Table V. Exclusive partial widths for the $c \rightarrow d$ semileptonic decay $D^+ \rightarrow X_{d\bar{d}} e^+ \nu_e$ in units of $10^{10} |V_{cd}|^2 \text{sec}^{-1}$, separated into $I = 1$ and $I = 0$ contributions. Also included are the physical meson masses used (in GeV), taken from Ref. [33] if possible; properties of unobserved or controversial states (given in parentheses) are taken from Ref. [35]. The mass of the decaying particle is 1.87 GeV.

X	$D^+ \rightarrow X_{d\bar{d}} e^+ \nu_e$ $I = 1$		$D^+ \rightarrow X_{d\bar{d}} e^+ \nu_e$ $I = 0$	
	mass	partial width	mass	partial width
$1^1 S_0$	0.14	4.9	0.55 ^{b)}	3.0
			0.96 ^{b)}	0.6
$1^3 S_1$ ^{a)}	0.77	2.5	0.78	2.4
$1^3 P_2$	1.32	0.00	1.27	0.00
$1^1 P_1$	1.23	0.26	1.17	0.39
$1^3 P_1$	1.26	0.16	1.28	0.13
$1^3 P_0$	1.30	0.00	1.30	0.00
$2^1 S_0$	1.30	0.01	(1.44)	0.00
$2^3 S_1$	(1.45)	0.02	(1.46)	0.01
total		7.8		6.5

^{a)} The Γ_L/Γ_T values for these decays are 0.67 and 0.68, respectively.

^{b)} We use the approximation of ideal mixing in $I = 0$ states in every sector except the ground state pseudoscalars where we assume an $\eta - \eta'$ mixing angle of -20° . If this mixing angle were changed to -10° , then the entries in the Table to η and η' would change to 2.2 and 0.9; note that while the individual rates change substantially, the total rate to these two states would only decrease by about 14%.

Table VI. Exclusive partial widths for the $b \rightarrow u$ semileptonic decays with a light spectator, $\bar{B}^0 \rightarrow X_{u\bar{d}} e \bar{\nu}_e$, and $B^- \rightarrow X_{u\bar{u}} e \bar{\nu}_e$, in units of $10^{13} |V_{bu}|^2 \text{sec}^{-1}$. Also included are the physical meson masses used (in GeV), taken from Ref. [33] if possible; properties of unobserved or controversial states (given in parentheses) are taken from Ref. [35]. (The masses for the $I = 1$ final states in $B^- \rightarrow X_{u\bar{u}} e \bar{\nu}_e$ are the same as those for $\bar{B}^0 \rightarrow X_{u\bar{d}} e \bar{\nu}_e$.) The mass of the decaying particle is 5.28 GeV.

X	$\bar{B} \rightarrow X_{u\bar{d}} e \bar{\nu}_e$		$B^- \rightarrow X_{u\bar{u}} e \bar{\nu}_e$			
	mass	partial width	I = 1		I = 0	
	mass	partial width	mass	partial width	mass	partial width
1^1S_0	0.14	0.96	0.14	0.48	0.55 ^{b)}	0.45
					0.96 ^{b)}	0.28
1^3S_1 ^{a)}	0.77	1.42	0.77	0.71	0.78	0.71
1^3P_2	1.32	0.33	1.32	0.16	1.27	0.18
1^1P_1	1.23	1.09	1.23	0.54	1.17	0.57
1^3P_1	1.26	0.87	1.26	0.43	1.28	0.41
1^3P_0	1.30	0.05	1.30	0.02	1.30	0.03
2^1S_0	1.30	0.17	1.30	0.08	(1.44)	0.08
2^3S_1	(1.45)	0.41	(1.45)	0.20	(1.46)	0.20
partial total		5.3		2.6		2.9

^{a)} The Γ_L/Γ_T values for these decays are 0.30, 0.30, and 0.30 respectively.

^{b)} We use the approximation of ideal mixing in $I = 0$ states in every sector except the ground state pseudoscalars where we assume an $\eta - \eta'$ mixing angle of -20° . If this mixing angle were changed to -10° , then the entries in the Table to η and η' would change to 0.34 and 0.41; note that while the individual rates change substantially, the total rate to these two states would only increase by about 3%.

Table VII. Exclusive partial widths for the $b \rightarrow u$ semileptonic decays with a heavy spectator, $\bar{B}_s \rightarrow X_{u\bar{s}} e \bar{\nu}_e$, and $\bar{B}_c \rightarrow X_{u\bar{c}} e \bar{\nu}_e$, in units of $10^{13} |V_{bu}|^2 \text{sec}^{-1}$. The Heavy Quark Symmetry notation $n^{s\ell} L_J$ is used for the final states with unequal mass quarks. Also included are the physical meson masses used (in GeV), taken from Ref. [33] if possible; properties of unobserved or controversial states (given in parentheses) are taken from Ref. [35]. The masses of the decaying particles (in GeV) are 5.38^b and (6.27) , respectively..

X	$\bar{B}_s \rightarrow X_{u\bar{s}} e \bar{\nu}_e$		$\bar{B}_c \rightarrow X_{u\bar{c}} e \bar{\nu}_e$	
	mass	partial width	mass	partial width
$1\frac{1}{2}S_0$	0.49	0.85	1.87	0.30
$1\frac{1}{2}S_1$ ^{a)}	0.89	1.14	2.01	0.62
$1\frac{3}{2}P_2$	1.43	0.28	2.46	0.06
$1\frac{3}{2}P_1$	1.27	1.72	2.42	0.62
$1\frac{1}{2}P_1$	1.40	0.08	(2.49)	0.04
$1\frac{1}{2}P_0$	1.43	0.04	(2.40)	0.01
$2\frac{1}{2}S_0$	(1.45)	0.45	(2.58)	0.46
$2\frac{1}{2}S_1$	(1.58)	0.54	(2.64)	0.40
partial total		5.1		2.5

^{a)} The Γ_L/Γ_T values for these decays are 0.45 and 0.61, respectively.

^{b)} see Ref. [37]

Table VIII. Comparison at zero recoil of the ISGW2 meson form factors without perturbative matching corrections to those of leading order Heavy Quark Symmetry and Heavy Quark Symmetry including the $\mathcal{O}(1/m_Q)$ corrections predicted by ISGW2. Note that these ISGW2 form factors *cannot be directly compared to experiment*: they are just the \tilde{f}_α^{qm} scaled by factors of $(\bar{m}_B/m_B)^{n_B(\alpha)}(\bar{m}_X/m_X)^{n_X(\alpha)}$ with the exponents of Table C1. The form factors are those for mesons corresponding to a light (\bar{u} or \bar{d}) spectator.

		\tilde{f}_+	\tilde{f}_-	\tilde{g}	\tilde{f}	$(\tilde{a}_+ + \tilde{a}_-)$	$(\tilde{a}_+ - \tilde{a}_-)$
ISGW2-no matching	$b \rightarrow ce\bar{\nu}_e$	1.00	-0.03	1.11	0.97	-0.08	1.04
ISGW2-no matching	$c \rightarrow se^+\nu_e$	0.98	-0.00	1.28	0.84	-0.23	1.18
HQS	$b \rightarrow ce\bar{\nu}_e$	1	0	1	1	0	1
HQS	$c \rightarrow se\bar{\nu}_e$	1	0	1	1	0	1
HQS+ $\mathcal{O}(\frac{1}{m_Q})$	$b \rightarrow ce\bar{\nu}_e$	1	-0.06	1.12	1	-0.09	1.03
HQS+ $\mathcal{O}(\frac{1}{m_Q})$	$c \rightarrow se^+\nu_e$	1	-0.21	1.39	1	-0.30	1.09

Table IX. Predictions for the six form factors for $\bar{B} \rightarrow D\ell\bar{\nu}_\ell$ and $\bar{B} \rightarrow D^*\ell\bar{\nu}_\ell$. The HQET column shows the effect of QCD radiative corrections *alone* to the HQS symmetry limit column.

	ISGW2	ISGW	HQS	HQET
$\tilde{f}_+(t_m)$	1.00	1.01	1	1.00
$\tilde{f}_-(t_m)$	-0.09	-0.05	0	-0.02
$\tilde{g}(t_m)$	1.17	1.12	1	1.06
$\tilde{f}(t_m)$	0.91	1.00	1	0.93
$2\tilde{a}_+(t_m)$	0.83	0.95	1	0.88
$2\tilde{a}_-(t_m)$	-1.19	-1.11	-1	-1.08

Table X. Comparison of the form factors for $D \rightarrow \bar{K} e^+ \nu_e$ and $D \rightarrow \bar{K}^* e^+ \nu_e$ with experiment. We have used the t dependence assumed in the fits to data to extrapolate the experimental form factors to $t = t_m$ from $t = 0$.

	experiment [23]	ISGW2	ISGW
$f_+(t_m)$	1.42 ± 0.25	1.23	1.16
$f(t_m)$ (GeV)	2.21 ± 0.19	1.92	2.76
$g(t_m)$ (GeV $^{-1}$)	0.55 ± 0.08	0.55	0.47
$a_+(t_m)$ (GeV $^{-1}$)	-0.21 ± 0.04	-0.34	-0.37

Table A1. quark model parameters

parameter	ISGW2	ISGW
b	0.18 GeV ²	0.18 GeV ²
c	-0.81 GeV	-0.84 GeV
α_s	0.60 \rightarrow 0.30 (see text)	0.50 \rightarrow 0.30 (see ISGW)
$m_u = m_d$	0.33 GeV	0.33 GeV
m_s	0.55 GeV	0.55 GeV
m_c	1.82 GeV	1.82 GeV
m_b	5.20 GeV	5.12 GeV
a	2.8	not applicable

Table A2. the masses and β values in GeV for variational solutions of the hyperfine-corrected Coulomb plus linear problem in the $1S$, $1P$, $2S$ basis

meson flavor:	$u\bar{d}$	$u\bar{s}$	$s\bar{s}$	$c\bar{u}$	$c\bar{s}$	$u\bar{b}$	$s\bar{b}$	$c\bar{c}$	$b\bar{c}$	
1^1S_0	m	0.35	0.55	0.62	1.86	1.94	5.27	5.33	2.95	6.33
	β	0.41	0.44	0.53	0.45	0.56	0.43	0.54	0.88	0.92
1^3S_1	m	0.74	0.87	0.97	2.01	2.10	5.33	5.40	3.13	6.42
	β	0.30	0.33	0.37	0.38	0.44	0.40	0.49	0.62	0.75
1^1P	m	1.24	1.35	1.42	2.48	2.53	5.81	5.84	3.51	6.79
	β	0.28	0.30	0.33	0.33	0.38	0.35	0.41	0.52	0.60

Table C1: The factors F_n of eq. (B1) of ISGW are to be replaced by $F_N^{(\alpha)}$ which have the modification shown in eq. (27) of Section III.C and are multiplied by the α -dependent factor $\left(\frac{\tilde{m}_B}{\tilde{m}_B}\right)^{n_B(\alpha)} \left(\frac{\tilde{m}_X}{\tilde{m}_X}\right)^{n_X(\alpha)}$ with $n_B(\alpha)$ and $n_X(\alpha)$ given here.

TABLE I.

form factors (α)	$n_B(\alpha)$	$n_X(\alpha)$
$f_+ + f_-, f'_+ + f'_-$	-1/2	+1/2
$f_+ - f_-, f'_+ - f'_-$	+1/2	-1/2
g, g'	-1/2	-1/2
f, f'	+1/2	+1/2
$a_+ + a_-, a'_+ + a'_-$	-3/2	+1/2
$a_+ - a_-, a'_+ - a'_-$	-1/2	-1/2
h	-3/2	-1/2
k	-1/2	+1/2
$b_+ + b_-$	-5/2	+1/2
$b_+ - b_-$	-3/2	-1/2
$\ell, r, \ell_{\frac{3}{2}}, \ell_{\frac{1}{2}}$	+1/2	+1/2
$c_+ + c_-, s_+ + s_-, c_{+\frac{3}{2}} + c_{-\frac{3}{2}}, c_{+\frac{1}{2}} + c_{-\frac{1}{2}}$	-3/2	+1/2
$c_+ - c_-, s_+ - s_-, c_{+\frac{3}{2}} - c_{-\frac{3}{2}}, c_{+\frac{1}{2}} - c_{-\frac{1}{2}}$	-1/2	-1/2
$q, v, q_{\frac{3}{2}}, q_{\frac{1}{2}}$	-1/2	-1/2
$u_+ + u_-$	-1/2	+1/2
$u_+ - u_-$	+1/2	-1/2

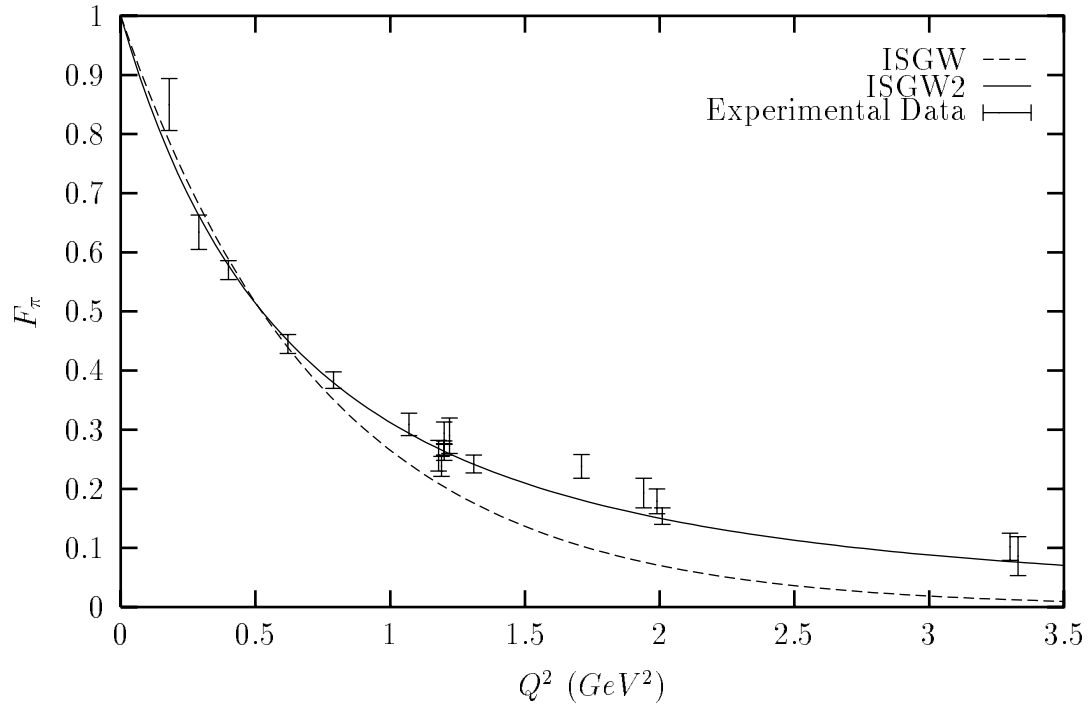


Fig. 1. Measurements of the pion form factor [18] compared to the form factors of ISGW and ISGW2.

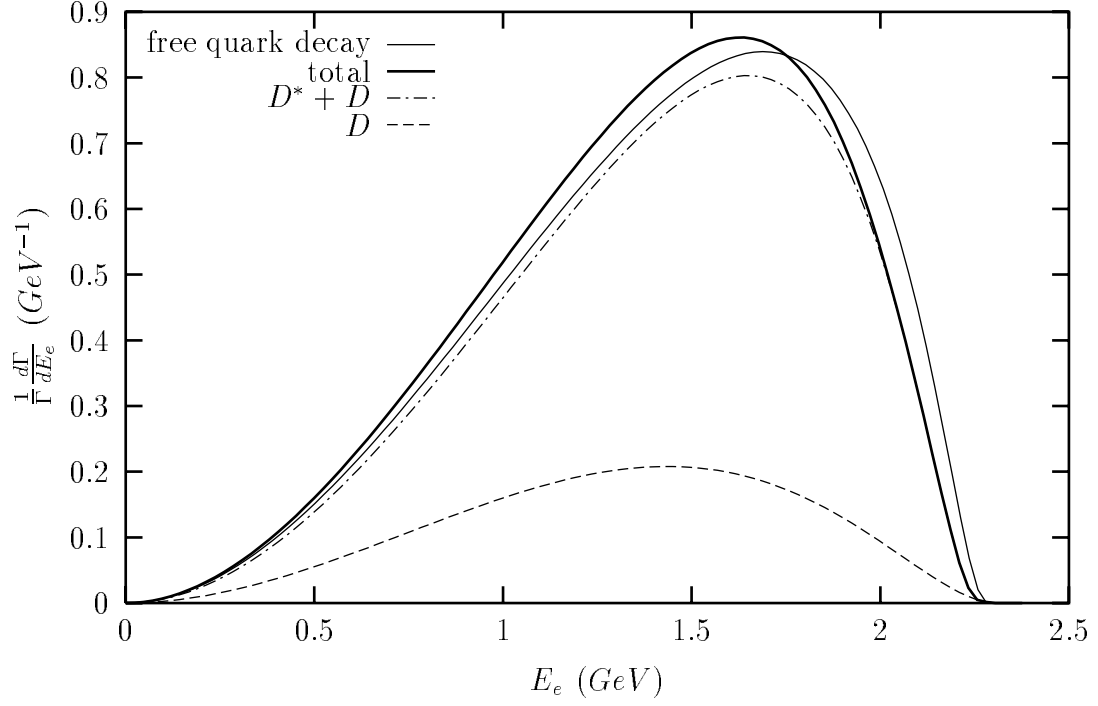


Fig. 2. $(1/\Gamma)(d\Gamma/dE_e)$ for $\bar{B} \rightarrow X_c e \bar{\nu}_e$ showing contributions of D , D^* , and the total contribution from all 1S, 1P, and 2S states; also shown is the corresponding free quark curve. Absolute rates are given in Table II, and may be compared to $\Gamma_{free} = 4.84 \times 10^{13} |V_{cb}|^2 \text{sec}^{-1}$.

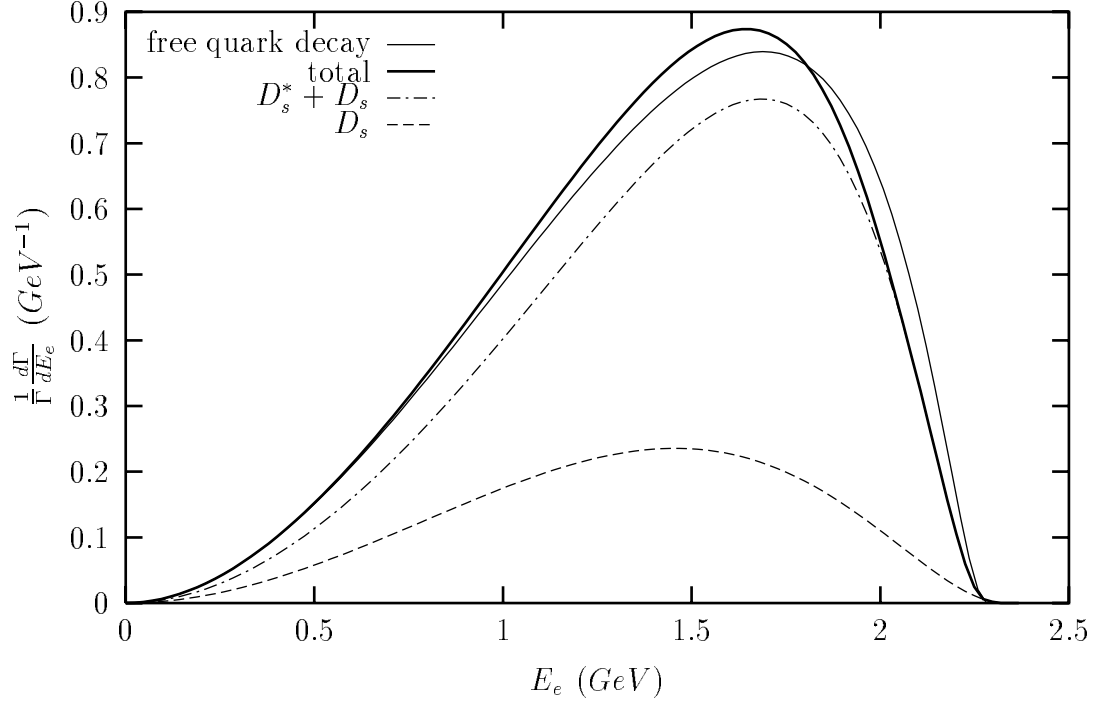


Fig. 3. $(1/\Gamma)(d\Gamma/dE_e)$ for $\bar{B}_s \rightarrow X_{c\bar{s}}e\bar{\nu}_e$ showing contributions of D_s , D_s^* , and the total contribution from all 1S, 1P, and 2S states; also shown is the corresponding free quark curve. Absolute rates are given in Table II, and may be compared to $\Gamma_{free} = 4.84 \times 10^{13} |V_{cb}|^2 \text{sec}^{-1}$.

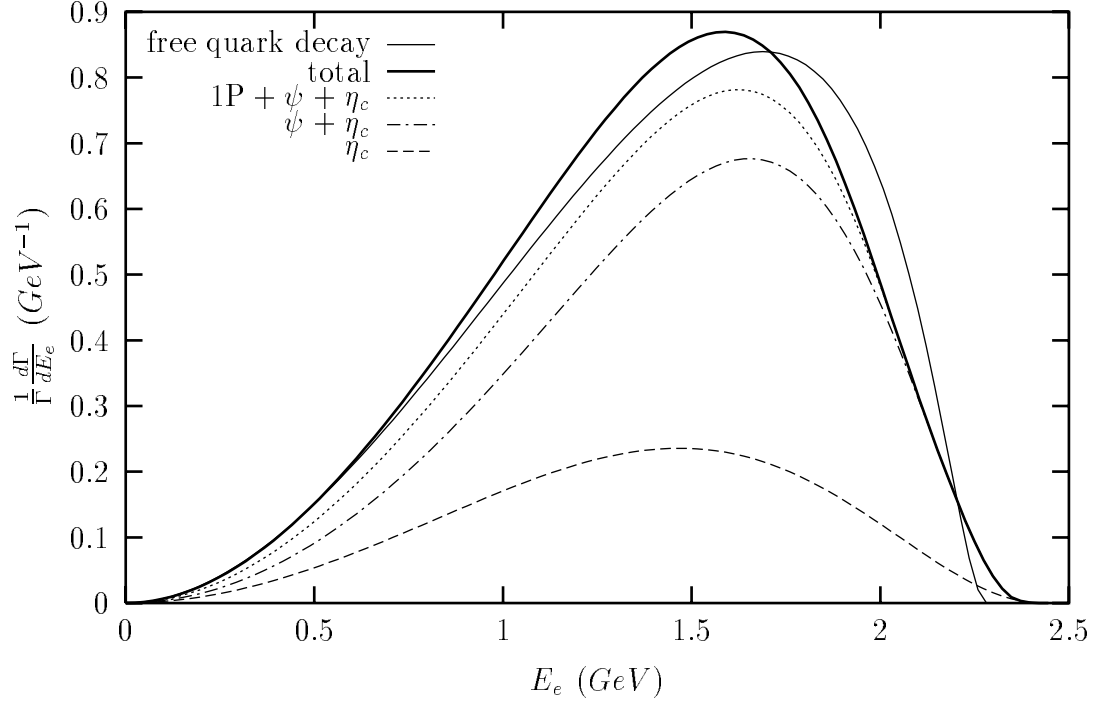


Fig. 4. $(1/\Gamma)(d\Gamma/dE_e)$ for $\bar{B}_c \rightarrow X_{c\bar{c}}e\bar{\nu}_e$ showing contributions of η_c , J/Ψ , and the total contribution from all 1S, 1P, and 2S states; also shown is the corresponding free quark curve. Absolute rates are given in Table II, and may be compared to $\Gamma_{free} = 4.84 \times 10^{13} |V_{cb}|^2 \text{sec}^{-1}$.

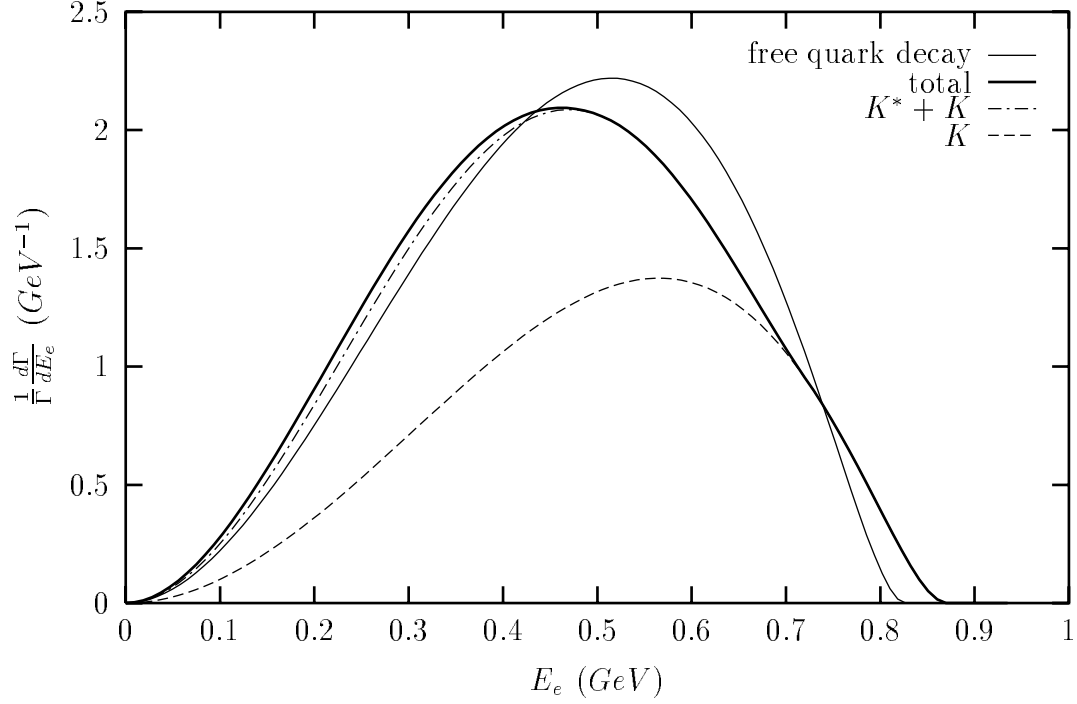


Fig. 5. $(1/\Gamma)(d\Gamma/dE_e)$ for $D \rightarrow X_{s\bar{u}} e^+ \nu_e$ showing contributions of K , K^* , and the total contribution from all 1S, 1P, and 2S states; also shown is the corresponding free quark curve. Absolute rates are given in Table III, and may be compared to $\Gamma_{free} = 0.34 \times 10^{12} |V_{cs}|^2 \text{ sec}^{-1}$.

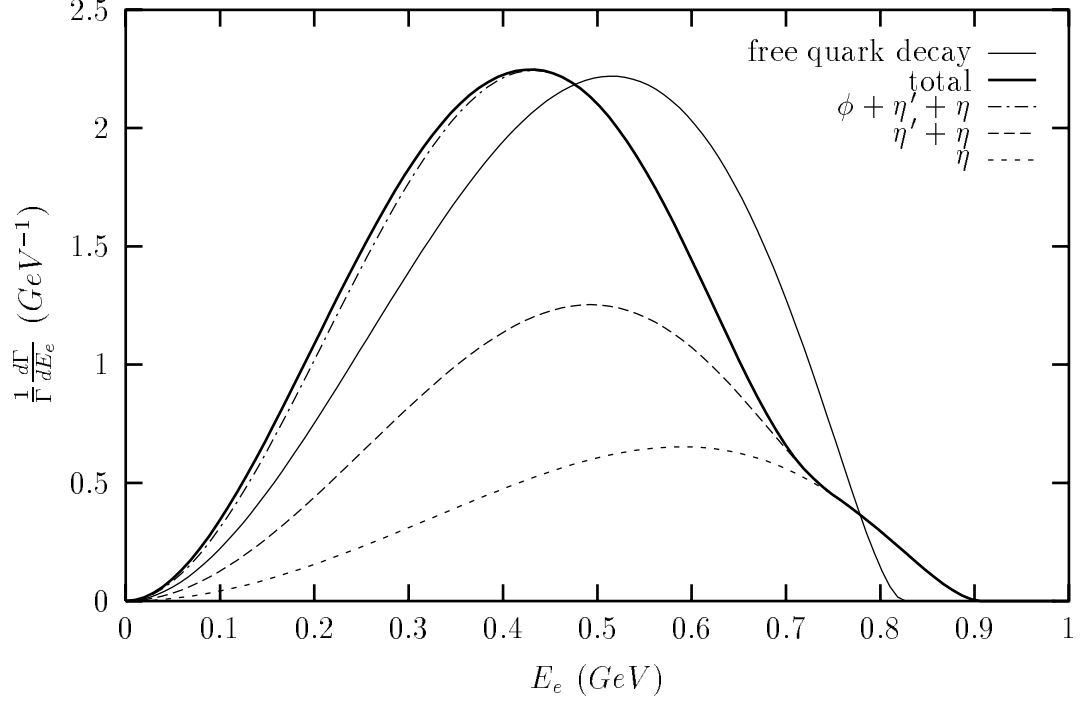


Fig. 6. $(1/\Gamma)(d\Gamma/dE_e)$ for $D \rightarrow X_{s\bar{s}}e^+\nu_e$ showing contributions of η , η' , J/Ψ , and the total contribution from all 1S, 1P, and 2S states; also shown is the corresponding free quark curve. Absolute rates are given in Table III, and may be compared to $\Gamma_{free} = 0.34 \times 10^{12} |V_{cs}|^2 \text{sec}^{-1}$.

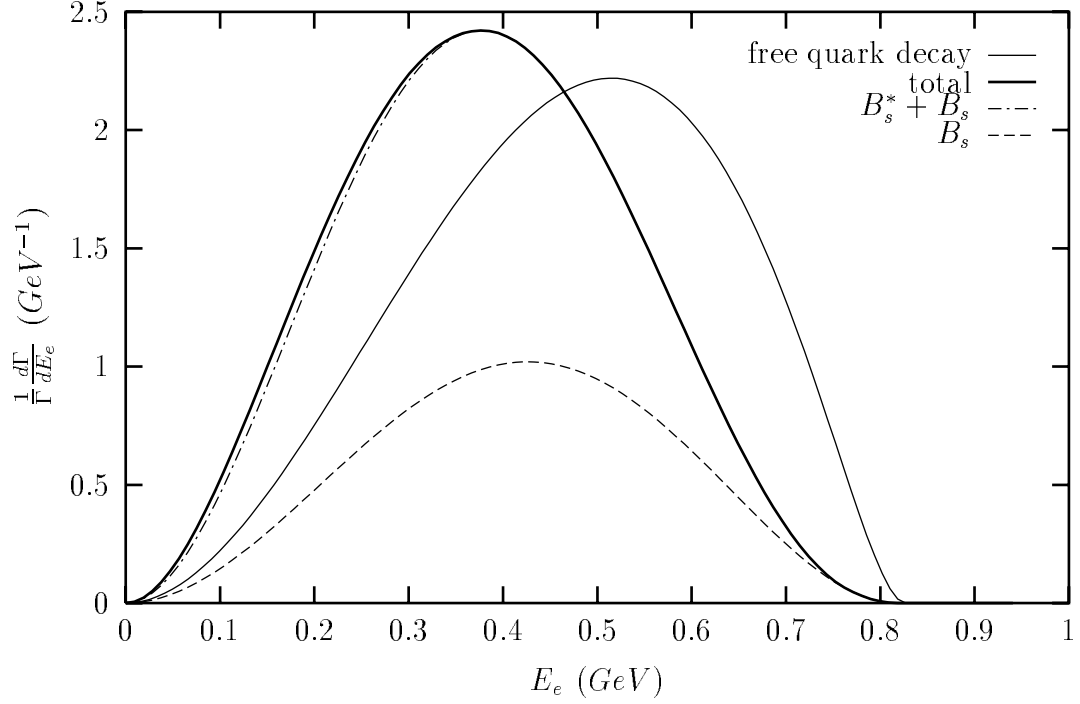


Fig. 7. $(1/\Gamma)(d\Gamma/dE_e)$ for $B \rightarrow X_{s\bar{b}}e^+\nu_e$ showing contributions of B_s , B_s^* , and the total contribution from all 1S, 1P, and 2S states; also shown is the corresponding free quark curve. Absolute rates are given in Table III, and may be compared to $\Gamma_{free} = 0.34 \times 10^{12} |V_{cs}|^2 \text{ sec}^{-1}$.

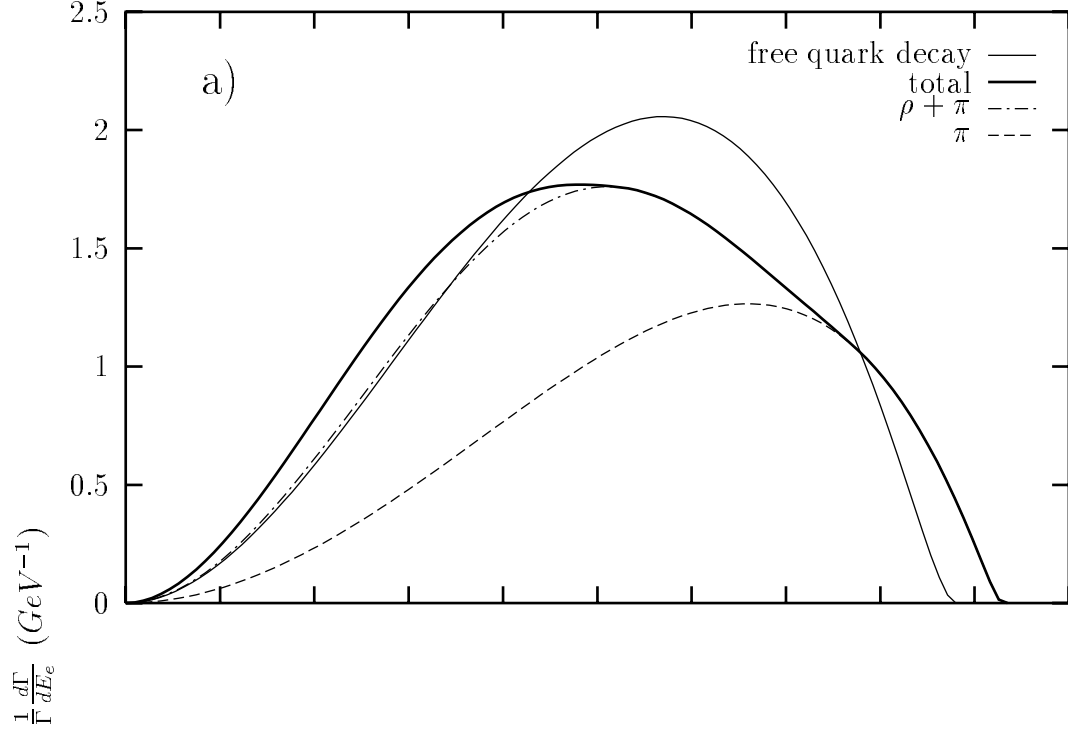


Fig. 8a. $(1/\Gamma)(d\Gamma/dE_e)$ for $D^0 \rightarrow X_{d\bar{u}}e^+\nu_e$ showing contributions of π , ρ , and the total contribution from all 1S, 1P, and 2S states. Absolute rates are given in Table IV.

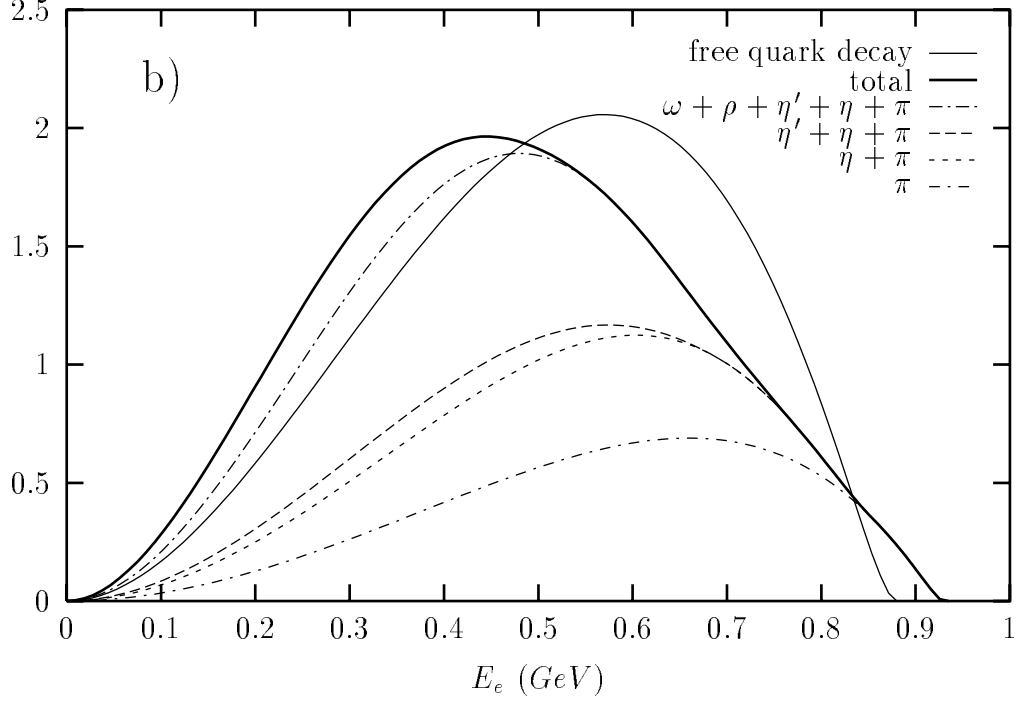


Fig. 8b. $(1/\Gamma)(d\Gamma/dE_e)$ for $D^+ \rightarrow X_{d\bar{d}}e^+\nu_e$ showing contributions from π^0 , η , η' , ρ and ω , and the total including 1P and 2S states. Absolute rates are given in Table V. The free quark decay curve is shown on both plots and has an absolute rate of $\Gamma_{\text{free}} = 0.51 \times 10^{12} |V_{cd}|^2 \text{sec}^{-1}$.

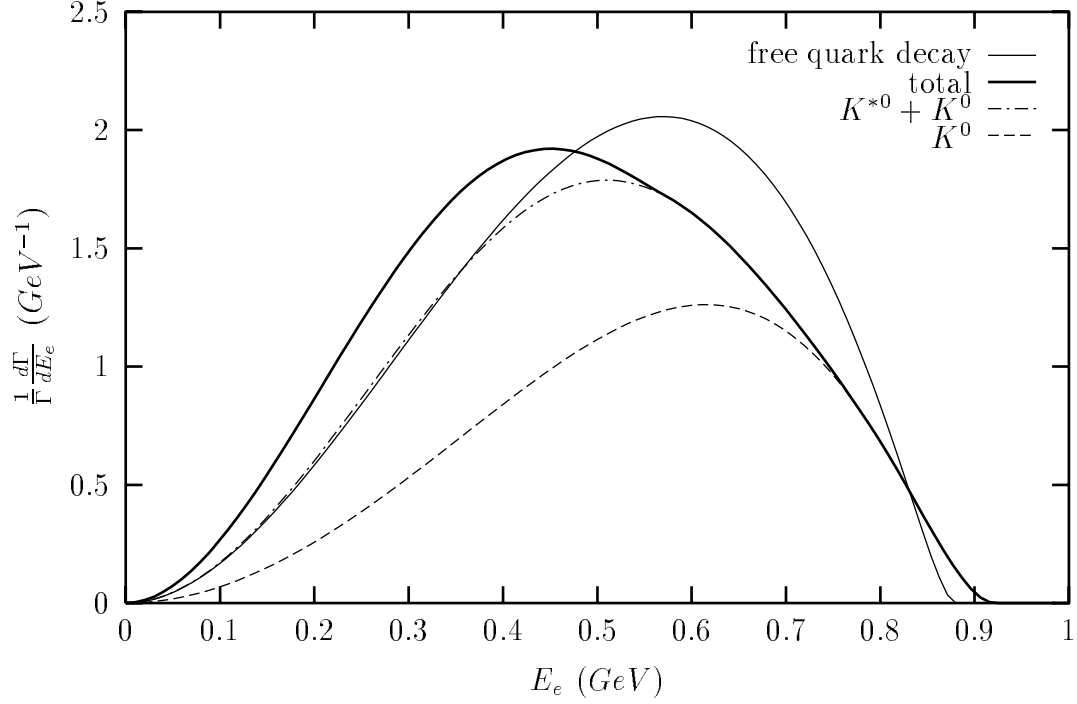


Fig. 9. $(1/\Gamma)(d\Gamma/dE_e)$ for $D_s \rightarrow X_{d\bar{s}}e^+\nu_e$ showing contributions of K^0 , K^{*0} , and the total contribution from all 1S, 1P, and 2S states; also shown is the corresponding free quark curve. Absolute rates are given in Table IV, and may be compared to $\Gamma_{\text{free}} = 0.51 \times 10^{12} |V_{cd}|^2 \text{sec}^{-1}$.

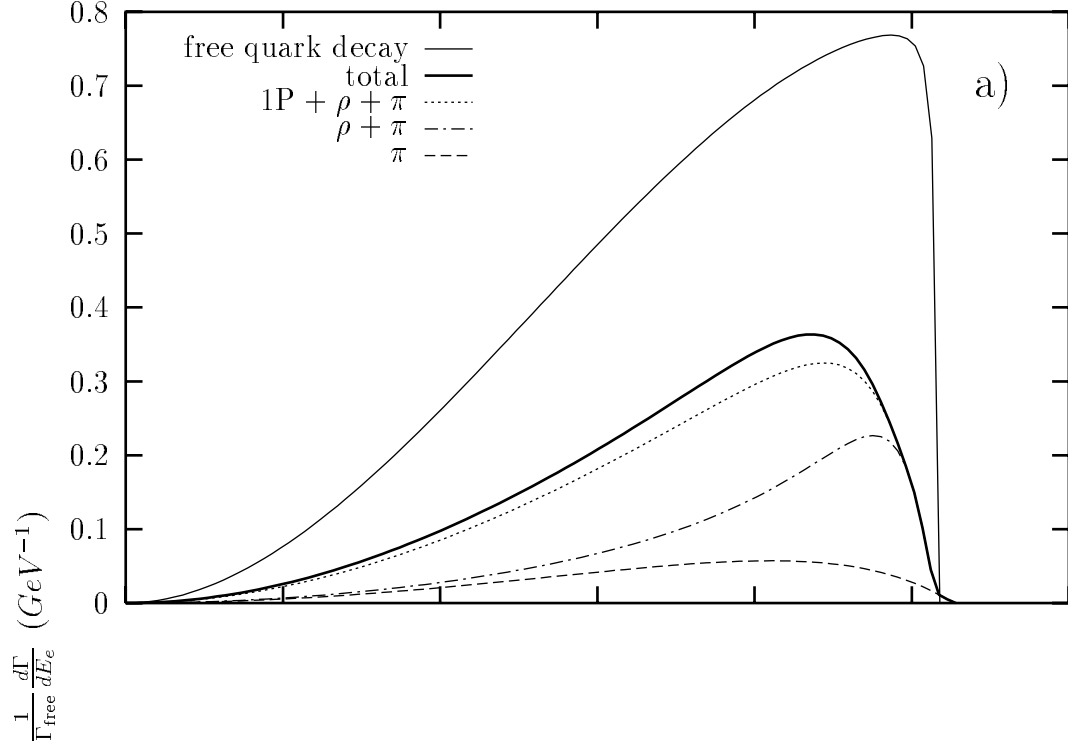


Fig. 10a. $(1/\Gamma_{\text{free}})(d\Gamma/dE_e)$ for $\bar{B}^0 \rightarrow X_{u\bar{d}}e\bar{\nu}_e$ showing contributions of π , ρ , the $1P$ states, and the $2S$ states π' and ρ' .

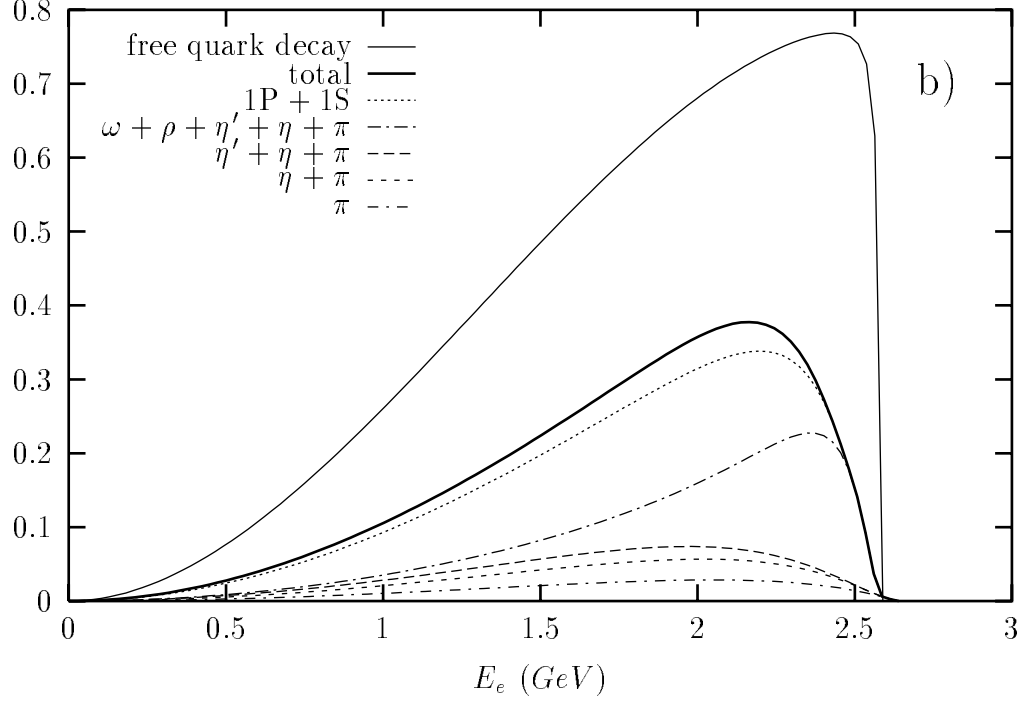


Fig. 10b. $(1/\Gamma_{\text{free}})(d\Gamma/dE_e)$ for $\bar{B}^- \rightarrow X_{u\bar{u}} e \bar{\nu}_e$ showing contributions of π^0 , η , η' , ρ^0 , ω , and the $1P$ and $2S$ states. The corresponding free quark curve is shown for both graphs corresponding to $\Gamma_{\text{free}} = 1.15 \times 10^{14} |V_{bu}|^2 \text{sec}^{-1}$. The partial widths are given in Table VI. Note that the curves shown are all normalized to Γ_{free} since our partial sum over exclusive channels does not exhaust the semileptonic rate.

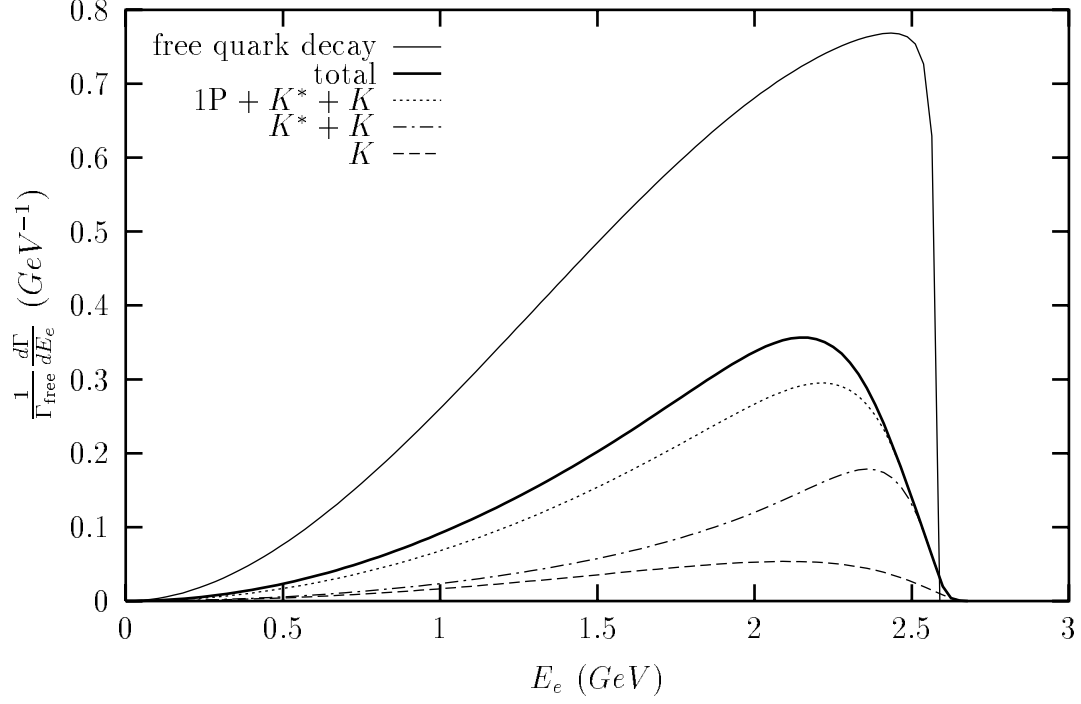
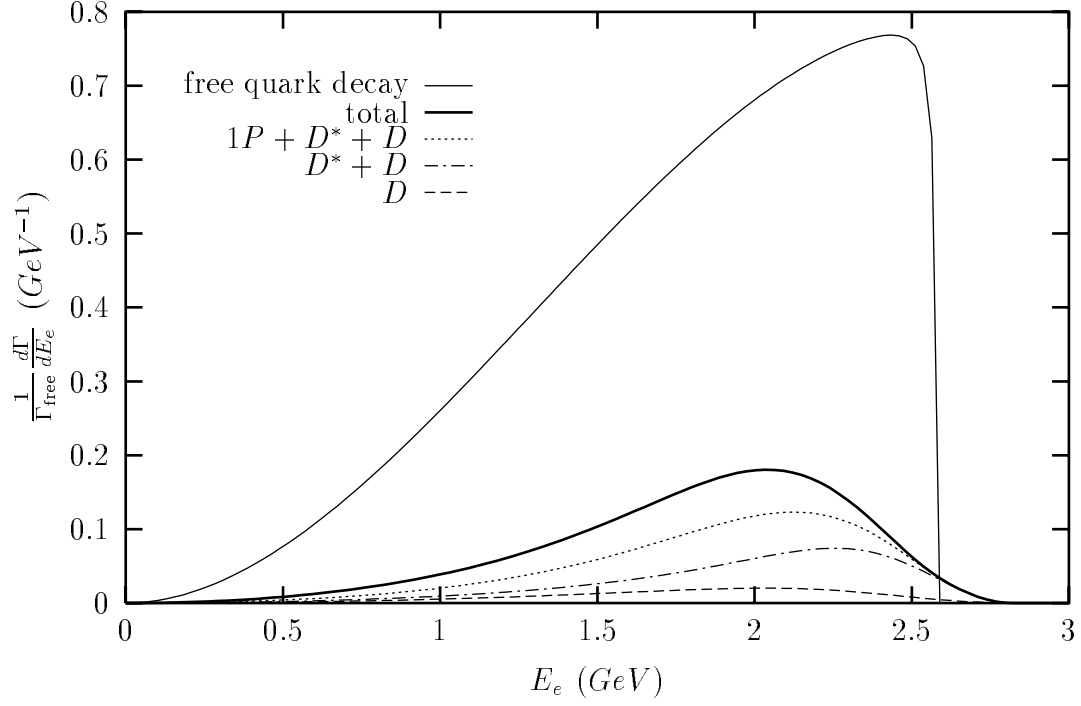


Fig. 11. $(1/\Gamma_{\text{free}})(d\Gamma/dE_e)$ for $\bar{B}_s \rightarrow X_{u\bar{s}}e\bar{\nu}_e$ showing contributions of K , K^* , the $1P$ states, and the $2S$ states; also shown is the corresponding free quark curve. Absolute rates are given in Table VII, and may be compared to $\Gamma_{\text{free}} = 1.15 \times 10^{14} |V_{bu}|^2 \text{sec}^{-1}$.



hfill

Fig. 12. $(1/\Gamma_{\text{free}})(d\Gamma/dE_e)$ for $\bar{B}_c \rightarrow X_{u\bar{c}}\epsilon\bar{\nu}_e$ showing contributions of D , D^* , the $1P$ states, and the $2S$ states; also shown is the corresponding free quark curve. Absolute rates are given in Table VII, and may be compared to $\Gamma_{\text{free}} = 1.15 \times 10^{14} |V_{bu}|^2 \text{sec}^{-1}$.